博士論文番号：1481209

(Doctoral student number)

Studies on molecular functions of Arabidopsis DOF transcription factors regulating vascular cell differentiation

Vasagi Ramachandran

Nara Institute of Science and Technology

Graduate School of Biological Sciences

Laboratory of Plant Metabolic Regulation

Supervisor: Professor Dr. Taku Demura

2017/08/08

ABSTRACT

Vascular system is one of critical tissues for vascular plants to transport low-molecular compounds, such as water, minerals, and the photosynthetic product, sucrose. For vascular cell differentiation, cell wall modification and programmed cell death are known to be important molecular events. In the case of xylem cells, which function in water conduction and supporting, thick lignified cell walls, called secondary cell walls (SCWs) are generated. Typical SCWs of xylem are composed of biopolymers, such as cellulose, hemicellulose, and lignin. SCWs provide stiffness and strength as well as waterproofness to plant cells, and thus the regulation of SCW biosynthesis is a vital issue for vascular plants.

Molecular genetics studies have revealed a set of key transcription factors for the process of vascular cell differentiation in *Arabidopsis thaliana*, and plant specific Dof (DNA binding with one finger) transcription factors have shown to be involved in development of vascular tissues and/or vascular cell differentiation. Previous screening of Arabidopsis transgenic lines overexpressing xylem vessel element differentiation-related genes in our laboratory identified two Dof genes, named *VASCULAR-RELATED DOF1* (*VDOF1*) and *VDOF2*, as novel factors to increase glucose yields from stem samples by enzymatic saccharification treatment, suggesting that VDOF1 and VDOF2 regulate SCW properties associated with saccharification efficiency. However, no information on physiological function of VDOF1 and VDOF2 have been reported yet. Therefore, I focus on molecular functional analysis of these VDOF transcription factors, to reveal their roles in regulating vascular cell differentiation.

Transient expression analysis of VDOF genes fused to yeast GAL4 DNA binding domain sequences suggested that VDOF2 would have an activity of transcription repressor, while VDOF1 did not show any significant activity as an activator nor a repressor. Observations of VDOF-YFP translational fusion reporters driven by 35S promoters (35S *promoter-VDOF-YFP*) or by VDOF own promoter (*VDOF promoter-VDOF-YFP*) showed the nuclear

localization of both VDOF-YFP proteins, supporting the molecular functions of VDOF proteins as transcription factors.

Next, the expression pattern of VDOF genes was examined by using *VDOF promoter-VDOF-YFP*, *VDOF promoter-GUS,* and *VDOF promoter-VDOF-GUS* reporters. Througout plant developmental stages, the expression of both VDOF genes was detected in vasculature regions of all organs tested, i.e. roots, leaves, hypocotyls, inflorescence stems, and floral organs. The detailed observation of inflorescence stem of 40-day-old plants revealed that VDOF1 promoter-GUS was detected in the regions of xylem, phloem, and interfascicular fiber, while that VDOF2 promoter-GUS was predominant in the phloem and xylem parenchyma cells. These results suggested that the *VDOF* genes are involved in the vascular development, and their functions for vascular development could be partly different each other.

In order to reveal physiological roles of *VDOF* genes, I generated *VDOF1* and *VDOF2* overexpressors (*VDOF1*ox and *VDOF2*ox) as well as a double knock-out mutant *vdof1 vdof2*. Although the *vdof1 vdof2* mutant did not show apparent growth and morphological changes, the 14-day-old seedlings of *VDOF1*ox and *VDOF2*ox showed variations in the growth. However, the growth defects of *VDOF1*ox and *VDOF2*ox were recovered during subsequent growth period, resulted in comparative plant sizes compare to the wild-type at 40-day-old. Notably, the vein patterning in 7-day-old and 14-day-old cotyledons was affected in *VDOF1*ox, *VDOF2*ox and *vdof1 vdof2*; especially connectivity and cardinality of veins were significantly increased in 7-day-old and 14-day-old cotyledons of *vdof1 vdof2*, respectively, suggesting enhancement of vein formation in the *vdof1 vdof2* double mutant. Furthermore, I performed histochemical analysis of 40-day-old inflorescence stems. Phloroglucinol-HCl staining indicated that lignin deposition was enhanced in the young regions of *vdof1 vdof2* inflorescence stems, while *VDOF1*ox showed the reduction of lignin signals in the middle regions of stems. Total lignin contents quantified by thioglycolic acid analysis demonstrated that total lignin

amounts in the bottom regions of stems were significantly increased in *VDOF1*ox and *vdof1 vdof2* compared to the wild type, whereas the *VDOF2*ox stems showed a slight reduction in total lignin contents. These results suggest that VDOF1 and VDOF2 would function as negative regulators of vein formation in seedlings and lignin deposition in inflorescence stems, and that effects of overexpression on lignin biosynthesis could be different between VDOF1 and VDOF2.

Finally, to identify target genes of the VDOF1 and VDOF2 proteins, RNA-seq analysis was performed with the estradiol-inducible overexpressors of *VDOF1* and *VDOF2*. After 24 h of *VDOF1*- or *VDOF2*-induction in seedlings, 160 and 141 genes were found to be commonly upregulated and downregulated, respectively, between *VDOF1* and *VDOF2* overexpression. Gene ontology term analysis on these common target genes indicated that the genes for cell wall biosynthesis, including lignin biosynthetic genes, such as *MYB63* encoding a transcriptional activator of lignin biosynthesis pathway and *LAC7* encoding a lignin polymerization enzyme, were significantly enriched in the list of common target genes. In inflorescence stems of *VDOF1*ox, *VDOF2*ox, and *vdof1 vdof2*, the expression patterns of these lignin-related genes were changed, correlating to the observations of lignin deposition phenotype. The list also contained known transcription factors involved in cell wall modification and subsequent cell expansion, and/or cell differentiation. Thus, it could be speculated that the *VDOF* genes regulate vascular cell differentiation by modulating activities of these transcription factors.

Taken together, I concluded that VDOF1 and VDOF2 are novel regulators of vascular cell differentiation through the course of a lifetime, with shifting their transcriptional target genes: in seedlings, the *VDOF* genes negatively regulate vein formation, while at reproductive stages, the VDOF proteins target lignin biosynthesis pathway. Future utilization of these *VDOF* genes can become a new biotechnological strategy to design SCW property by lignin modification.

TABLE OF CONTENTS

LIST OF FIGURES

LIST OF TABLES

CHAPTER 1

INTRODUCTION

1.1 Plant vascular tissues

Vascular tissues in plants include the xylem, phloem, and cambium (Figure 1.1). The xylem transports water and nutrients from roots to aboveground tissues and provides mechanical support to the plant body, while the phloem transports biosynthetic products, i.e., the photosynthetic product sucrose and proteins, throughout the plant (Myburg *et al*., 2001; Ye, 2002; Shuetz *et al*., 2013). The xylem is composed of several types of cells, including tracheary elements, fibers and parenchyma cells (Schuetz *et al*., 2013). Water is conducted through tracheary elements, including tracheids in pteridophyte and gymnosperm plants and vessel elements in angiosperm plants. Xylem fibers support the plant body. These cells can be characterized based on their lignified, thick secondary cell walls (SCWs) (Myburg *et al*., 2001; Shuetz *et al*., 2013; for details, see section 1.2.1). The SCWs of tracheary elements are characterized by their specific patterns of deposition: in the case of vessel elements, protoxylem vessel elements have an annular or helical pattern of SCW thickening, while the SCWs of metaxylem vessel elements exhibit a pitted or reticulate pattern. Another characteristic of tracheary element cells is programmed cell death (PCD), which occurs during the final stage of differentiation, leading to the formation of hollow cells that function effectively in water transport (Shuetz *et al*., 2013). By contrast, xylem parenchyma cells, which lack lignified SCWs, function in the storage of carbohydrates and minerals, and aid the activities of neighboring vessel elements and fibers (Shuetz *et al*., 2013; Myburg *et al*., 2001).

The phloem is composed of conducting sieve elements (sieve tube elements and companion cells) and nonconducting cells (parenchyma cells and fibers) (Lucas *et al*., 2013). Sieve tube elements are living cells that lack a nucleus and most organelles. In angiosperms, sieve tube

elements are symplastically linked to adjacent companion cells through the plasmodesmata, which help them maintain their activity. Sieve tube elements, which are connected to each other via sieve plates on their end walls, conduct photoassimilates such as sucrose from source organs (leaves) to sink regions (Shuetz *et al*., 2013; Hoe *et al*., 2014). Phloem parenchyma cells store starch and fats, as well as resins in some plant species. In tree species, phloem parenchyma cells play important roles in defense responses against invading organisms (Franceschi *et al*., 2005). Phloem fiber cells are dead, lignified cells found in the secondary phloem. These cells help strengthen and support the plant body, as do xylem fibers (Gorshkova *et al*., 2012).

1.2 Xylem as a source of plant biomass

Not only are xylem tissues essential conductive systems for land plants, but they are also important for humans, as they represent a major source of biomass. At the molecular level, the biomass derived from xylem can be attributed to cell wall polymers that accumulate in lignified SCWs found in xylem vessels and fibers.

The primary cell wall (PCW), which is synthesized during cell growth, mainly consists of polysaccharides including cellulose, hemicellulosic polysaccharides (such as xyloglucan), and pectin. Approximately 30% of the PCW is composed of pectin, a compound with a complex structure comprising homogalacturonan, xylogalacturonan, rhamnogalacturonan I, and rhamnogalacturonan II. Crosslinking among cellulose, hemicellulose, and pectin contributes to the structural integrity of the PCW (Caffall and Mohen, 2010; Reiter, 2002; Cosgrove and Jarvis, 2012; Cosgrove, 2005). PCWs are found in all plant cells, whereas SCWs are only found in specialized types of cells after cell expansion is complete. SCWs in the xylem vessel are typically composed of the polysaccharides cellulose and hemicellulose, in addition to the phenolic polymer lignin (Schuetz *et al*., 2013; Nakano *et al*., 2015).

1.2.1 SCW polymers and their biosynthesis

1.2.1.1 Cellulose biosynthesis

Almost one-third of the total mass of a plant consists of cellulose, i.e., (1,4)- β -D-glucan (Somerville, 2006). Cellulose is the main component of both PCWs and SCWs, but several aspects of cellulose differ between these structures: 1) cellulose has a greater degree of polymerization in SCWs than in PCWs; 2) cellulose microfibrils are wider in SCWs than in PCWs; and 3) the sets of Cellulose synthase (CesA) proteins, i.e., the core enzymatic components of the cellulose synthase complex, differ between SCWs and PCWs (Cosgrove and Jarvis, 2012; Mendu *et al*., 2011). These observations suggest that the mechanisms underlying cellulose biosynthesis differ between PCWs and SCWs.

Arabidopsis thaliana (Arabidopsis) contains 10 genes encoding CesA proteins (Somerville, 2006). Among these proteins, CesA1, CesA3, and CesA6 function in PCW formation, whereas CesA4, CesA7, and CesA8 participate in SCW formation in xylem cells (Somerville, 2006). Loss-of-function mutants of SCW-type CesAs known as *irregular xylem* mutants are characterized by collapsed xylem vessel cells (*irx1*/*cesa8*, *irx3*/*cesa7* and *irx5*/*cesa4*; Taylor *et al*., 1999; Taylor *et al*., 2000; Taylor, 2003; Festucci-Buselli *et al*., 2007; Taylor, 2008). In these *irx* mutants, the two SCW-type CesAs not altered by the mutation are unstable (Taylor, 2003), suggesting that the complex formed by the three CesA proteins is normally stable, allowing it to function in SCW biosynthesis. According to the current model, the CesA complex forms in small vesicles derived from the trans-Golgi network and is delivered to the plasma membrane with the guidance of cortical microtubules (Wightman and Turner, 2010). At the plasma membrane, the CesA complex works cooperatively with several other key proteins, such as the endo-1,4-ß-glucanase-like protein KORRIGAN1 (Liebminger *et al*., 2013) and SUCROSE SYNTHASE, to generate the substrate, UDP-glucose, from sucrose (Read and Bacic, 2002; Haigler *et al*., 2001).

1.2.1.2 Lignin

Lignin, a phenolic biopolymer, is the second most abundant cell wall biopolymer on Earth (after cellulose) (Boerjan *et al*., 2003). Lignin is a critical molecular factor that helps increase the stiffness and strength of the plant cell, and provides waterproofing to the cell wall. Lignin also plays important roles in plant defense responses against pathogen attack (Boerjan *et al*., 2003; Rogers *et al*., 2005). Three types of monolignols are found in the lignin of dicot plants: coniferyl alcohol in guaiacyl (G) lignin, sinapyl alcohol in syringyl (S) lignin, and traces of *p*-coumaryl alcohol in *p*-hydroxyphenyl (H) lignin. These monolignols are transported to the cell wall where they are polymerized by laccases and/or peroxidases via oxidative coupling processes (Van Acker *et al*., 2013; Vanholme *et al*., 2010; Weng and Chapple, 2010). From a practical viewpoint, lignin represents an obstacle to isolating polysaccharides from cell walls, for instance during biofuel production; the total amount of lignin is a primary negative factor in determining the efficiency of saccharification (i.e., the hydrolysis of polysaccharides to soluble sugars). Moreover, the molecular structures of the constituent monolignols affect the chemical properties of lignin; thus, the S/G/H ratio within lignin is also of interest (Chen and Dixon, 2007; Bonawitz *et al*., 2014).

Recently, significant progress has been made towards identifying the regulatory mechanisms of the phenylpropanoid and monolignol biosynthesis pathways through molecular genetic analyses in a variety of plant species (Vanholme *et al*., 2010). For example, monolignol biosynthesis genes have been investigated in Arabidopsis (phenylalanine ammonia- lyase [PAL] 1 to PAL4; Huang *et al*., 2010), poplar (*Populus* spp.: ferulate 5-hydroxylase [F5H]; Stewart *et al*., 2009), maize (*Zea mays*: coumaroyl shikimate 3-hydroxylase [C3H] and caffeoyl CoA 3-*O*-methytransferase [CCoAOMT]; Barrière *et al*., 2004), tobacco (*Nicotiana tabacum*: CCoAOMT and caffeic acid 3-*O*-methytransferase [COMT]; Pinçon *et al*., 2001), and rice (*Oryza sativa*: cinnamyl alcohol dehydrogenase 7 [CAD7]; Li *et al*., 2009). The enzymatic

sequential processes from Phe to monolignols have been revealed in the model herbal plant Arabidopsis (Fig S1; Vanholme *et al*., 2010). Mutant analysis of genes encoding monolignol biosynthesis enzymes indicated that artificial changes in the expression of these genes can affect the amount and composition of lignin, as well as the polysaccharide contents and composition of the SCW (Van Acker *et al*., 2013). For instance, when the expression of specific enzyme genes is knocked out, such as those encoding C3H and hydroxycinnamoyl-CoA shikimate (HCT), a non-conventional bypass pathway will sometimes be activated, resulting in the production of unusually structured lignin (Bonawitz *et al*., 2014; Hoffmann *et al*., 2004). These results suggest that SCW polymers are under complex metabolic regulation.

1.3 Transcription factors regulating vascular cell development

1.3.1 Vascular stem cell formation

All vascular cells are generated from vascular stem cells known as (pro)cambial cells. Recent advances in molecular genetics using Arabidopsis have revealed many classes of transcription factors that are critical for (pro)cambium formation (Miyashima *et al*., 2013; Furuta *et al*., 2014; Rybel *et al*., 2016). The formation of (pro)cambium is initiated by auxin signaling, which is mediated by the auxin response transcription factor MONOPTEROS (MP)/AUXIN RESPONSE FACTOR5 (ARF5) (Hardtke and Berleth, 1998; Rybel *et al*., 2016; Othani *et al*., 2017). After MP/ARF5 performs its function, the basic helix-loop-helix (bHLH) type transcription factor, TARGET OF MONOPTEROS5 (TMO5), and another bHLH transcription factor, LONESOME HIGHWAY, regulate periclinal cell divisions in the (pro)cambium by functioning as a heterodimer complex that provides cell populations for vascular tissue formation during embryogenesis (Rybel *et al*., 2013; Ohashi-Ito and Bergmann, 2007; Rybel *et al*., 2016). MP/ARF5 also regulates the expression of *PIN* genes, encoding auxin efflux carriers and the homeodomain-leucine zipper (HD-Zip) III type transcription factor AtHB8. AtHB8

stabilizes *PIN1* expression to regulate the acquisition of (pro)cambial cell fate (Baima *et al*., 2001; Donner *et al*., 2009). AtHB8 also activates *ACAULIS5*, leading to the production of thermospermine, which negatively regulates xylem differentiation by downregulating *AtHB8* and other HD-ZipIII genes, as well as auxin response factor genes including *MP/ARF5* (Milhinhos *et al*., 2013; Baima *et al*., 2014). These findings suggest that the feedback regulation among auxin, MP/ARF5, and HD-Zip III genes and thermospermine is critical for (pro)cambium formation. After the initiation and establishment of the (pro)cambium, the cell population of the (pro)cambium is maintained by WUSCHEL-RELATED HOMEOBOX4 (WOX4) and its homolog WOX14, a process modulated by the CLAVATA3/ESR-RELATED (CLE)-like peptide and the leucine-rich repeat receptor-like kinase PHLOEM INTERCALATED WITH XYLEM (PXY)/TDIF RECEPTOR (TDR) (Fisher and Turner, 2007; Hirakawa *et al*., 2008; Ethchells and Turner, 2010; Etchells *et al*., 2013).

1.3.2 Phloem cell differentiation

Precursors of xylem and phloem cells are generated from (pro)cambium cells by oriented cell division (Miyashima *et al*., 2013; Furuta *et al*., 2014; Rybel *et al*., 2016); however, the processes involved in cell fate determination from the (pro)cambium to xylem or phloem precursors are largely unknown. ALTERED PHLOEM DEVELOPMENT (APL), an MYB coiled-coil transcription factor, is a critical regulator of phloem cell differentiation, as the *apl* mutant cannot produce sieve tube elements or companion cells (Bonke *et al*., 2003). It was recently shown that NAC-type transcription factors functioning downstream of APL, i.e., NAC45 and its homolog NAC86, activate the genes encoding nuclease proteins required for nuclear degradation during sieve element differentiation (Furuta *et al*., 2014). Thus, during phloem cell development, transcriptional cascades regulated by APL activate specific molecular events involved in phloem cell differentiation.

1.3.3 Xylem cell differentiation

Key regulatory factors of xylem vessel cell formation have been identified in studies employing an *in vitro* xylem vessel cell differentiation system using cultured Arabidopsis cells (Kubo *et al*., 2005). An analysis of genes upregulated during the early stages of xylem vessel cell differentiation led to the identification of *VASCULAR-RELATED NAC-DOMAIN1* (*VND1*) to *VND7*, which encode a specific group of NAC transcription factors. All of the *VND* genes are expressed in differentiating xylem vessels (Kubo *et al*., 2005; Yamaguchi *et al*., 2008), and the overexpression of *VND* genes induces ectopic differentiation of xylem vessel cells (Kubo *et al*., 2005; Endo *et al*., 2014). Conversely, the functional suppression of VND6 and VND7 via a chimeric repression domain inhibits xylem vessel cell formation in plants (Kubo *et al*., 2005; Yamaguchi *et al*., 2008). Based on these observations, VND proteins were proposed to act as the master regulators of xylem vessel cell differentiation (Kubo *et al*., 2005; Yamaguchi *et al*., 2008; Yamaguchi *et al*., 2010; Nakano *et al*., 2015).

Phylogenetic tree analysis indicated that the VND family of proteins includes two sister groups, including one comprised of three proteins: NAC SECONDARY WALL THICKENING PROMOTING FACTOR1 (NST1), NST2, and NST3/SECONDARY WALL-ASSOCIATED NAC DOMAIN PROTEIN1 (SND1) (Zhong *et al*., 2006; Mitsuda *et al*., 2007; Zhong and Ye, 2014; Nakano *et al*., 2015). The *NST* genes are expressed in xylem and interfascicular fiber cells, in addition to the anther endothecium and valve margins (Zhong *et al*., 2006; Mitsuda *et al*., 2005, 2007). Knock-out mutants of *NST* genes lack SCWs in these cells, while overexpression of these genes induces ectopic SCW deposition, indicating that NST proteins are master regulators of SCW formation in these cells (Zhong *et al*., 2006; Mitsuda *et al*., 2005, 2007). Interestingly, the specific expression of *VND* and *NST* in xylem vessels and fibers, respectively, that occurs in Arabidopsis was not observed in some plant species (Zhong *et al*., 2010, 2011; Ohtani *et al*., 2011; Yoshida *et al*., 2013). Thus, VND and NST might have

distinct functions only in a subset of species including Arabidopsis, but have common roles in xylem cell differentiation in a wide range of other plant species.

Downstream of VND and NST proteins, many MYB transcription factors function as additional key regulators of SCW formation (Zhong and Ye, 2014; Nakano *et al*., 2015). In Arabidopsis, MYB46 and MYB83 are considered to be second-layer master regulators of SCW formation (Nakano *et al*., 2015). In addition to MYB46 and MYB83, other MYB proteins, such as MYB58, MYB63, and MYB85, directly regulate lignin biosynthesis either positively or negatively (Zhou *et al*., 2009; Nakano *et al*., 2015; Zhong and Ye, 2014). Moreover, multiple types of transcription factors function in SCW formation through direct or indirect interactions with VND and NST (Nakano *et al*., 2015), suggesting that complex transcriptional networks are involved in SCW biosynthesis for functional xylem vessel cell formation.

1.4 Contributions of Dof transcription factors to vascular development

As described above, many classes of transcription factors function in vascular development. Accumulating evidence suggests that Dof transcription factors are key regulators of vascular development.

1.4.1 What are Dof transcription factors?

Dof transcription factors are a class of plant-specific transcription factors containing characteristic amino acid sequences, $CX_2CX_{21}CX_2$, named the Dof (DNA-binding with one finger) domain, which are sufficient for DNA binding activity (Yanagisawa, 2015). The Dof domain interacts with DNA sequences with a 5'-(A/T)AAAG-3' core motif (Yanagisawa and Schmidt, 1999; Hir and Bellini 2013). In addition, Dof proteins contain a nucleus localization signal sequence that efficiently directs these proteins to the nucleus (Krebs *et al*., 2010).

A single Dof gene was identified in the green unicellular alga *Chlamydomonas reinhardtii*, as were nine Dof genes in the moss *Physcomitrella patens*, eight in the fern *Selaginella moellendorffii*, eight in the gymnosperm *Pinus taeda*, 36 in Arabidopsis (Lijavetzky *et al*., 2003), 30 in rice (Gaur *et al*., 2011), 26 in barley (*Hordeum vulgare*, Moreno-Risueno *et al*., 2006), 28 in soybean (*Glycine max*, Wang *et al*., 2007), and 41 in poplar (*Populus trichocarpa*, Hir and Belini, 2013). The higher number of Dof genes in angiosperms suggests that after divergence of the angiosperm lineage, extensive duplications of Dof genes occurred, likely due to whole-genome duplication (Moreno-Risueno *et al*., 2006). Notably, many Dof genes are expressed in vascular tissues in Arabidopsis (Hir and Bellini, 2013; Gardiner *et al*., 2010; Konishi and Yanagisawa, 2007). In accordance with these observations, the importance of Dof proteins for vascular development has been reported by several groups (Guo *et al*., 2009; Gardiner *et al*., 2010; Konishi and Yanagisawa, 2007; Konishi *et al*., 2015; Kim *et al*., 2010; for the details, see next section 1.4.2). Dof proteins also function in cell cycle regulation (Skirycz *et al*., 2008; Xu *et al*., 2016), seed development and/or germination (Boccaccini *et al*., 2014; Ruiz-Medrano *et al*., 2012), secondary metabolite biosynthesis (Skirycz *et al*., 2006; Skirycz *et al*., 2007), and long-distance signaling (Gualberti *et al*., 2002; Ward *et al*., 2005).

1.4.2 Dof transcription factors regulate vascular development

Gardiner *et al*. (2010) showed that the expression regions of three Dof genes, *Dof2.1*, *Dof4.6* and *Dof5.3*, partially overlap with those of *AtHB8*, which encodes a critical factor in determining procambial cell fate, during the early stages of vascular development in leaves; *Dof2.1* and *Dof4.6* are expressed at all stages of leaf vein formation, whereas *Dof5.3* expression ceases during procambium differentiation (Gardiner *et al*., 2010; Figure 1.2). Interestingly, these Dof genes are expressed in wider domains than *AtHB8*, which is expressed within the expression regions of Dof genes. These results suggest that Dof2.1, Dof4.6, and Dof5.3

contribute to preprocambial development (Gardiner *et al*., 2010). Moreover, treatment with an auxin transport inhibitor expanded the expression regions of the Dof genes, suggesting that the expression of *Dof2.1*, *Dof4.6,* and *Dof5.3* is regulated by auxin signaling.

Another Dof gene expressed in procambial cells is *Dof5.8* (Konishi *et al*., 2015; Konishi and Yanagisawa, 2007). *Dof5.8* promoter activity was detected in provascular cells in embryos and in the leaf primordium (Konishi and Yanagisawa, 2007; Figure 1.2). MP/ARF5 was recently found to directly activate *Dof5.8* expression through binding to its promoter sequence. The functional inhibition of Dof5.8 affected root and cotyledon development, as well as vein patterning in the cotyledon (Konishi *et al*., 2015). These findings, together with the observations by Gardiner *et al*. (2010), suggest that *Dof2.1*, *Dof4.6*, *Dof5.3,* and *Dof5.8* play important roles in vascular development under the control of auxin.

The last cambium cell-related Dof gene identified was *Dof5.6*, also known as *HIGH CAMBIAL ACTIVITY2* (*HCA2*) (Guo *et al*., 2009; Figure 1.2). In general, in the vascular bundles of flower stems, interfascicular cambial cells develop from the interfascicular parenchyma cells facing the edges of fascicular cambial cells between the xylem and phloem. After periclinal asymmetric cell division of these parenchyma cells, a continuous interfascicular cambium is established through the joining of these cells (Nieminen *et al*., 2015). In the gain-of-function mutant *hca2*/*dof5.6*, the continuous ring of vascular tissues in flower stems forms early due to the early formation of interfascicular cambium (Guo *et al*., 2009). This phenotype was attributed to enhanced periclinal cell divisions of the interfascicular parenchyma cells to form the interfascicular cambium. In *hca2*/*dof5.6*, the fascicular cambium also shows enhanced periclinal cell divisions, resulting in abnormally structured vascular bundles with radial files of xylem and phloem cells (Guo *et al*., 2009). *HCA2*/*Dof5.6* is expressed in the cambium, phloem and interfascicular parenchyma cells in stems, and the *hca2*/*dof5.6* mutation causes overexpression of *HCA2*/*Dof5.6*. *AtHB8* is upregulated in *hca2*/*dof5.6*, suggesting that

HCA2/Dof5.6 is a positive regulator of this gene. A knock-down mutation of *HCA2/Dof5.6* did not have any effect on vascular development, suggesting the presence of high functional redundancy among Dof genes (Guo *et al*., 2009).

1.4.3 Dof transcription factors are involved in phenylpropanoid metabolism

Phenylpropanoids, including flavonoids and monolignols, are important secondary metabolites for plant development and environmental responses. Flavonoids are critical metabolites that protect plants against UV and visible light, and monolignols play structural roles in lignin accumulation in the SCW (Li *et al*., 1993; Roger and Campbell, 2004; Skirycz *et al*., 2007). Dof4.2 is involved in regulating phenylpropanoid-related genes (Diaz *et al*., 2002). Dof4.2 is preferentially expressed in axillary buds of the flower stalk, hypocotyls, periderm, and tapetum cells in pollen, and overexpression of *Dof4.2* induced the formation of bushy shoots (Skirycz *et al*., 2007). In transgenic plants with overexpression and RNAi-mediated silencing of *Dof4.2*, down- and upregulated expression of flavonoid biosynthetic genes, respectively, and abnormal flavonoid accumulation were detected under cold and high-light conditions, indicating that Dof4.2 is a negative regulator of flavonoid biosynthesis. Notably, lignin depositions in hypocotyl fibers were not observed in a *Dof4.2* overexpressor (Skirycz *et al*., 2007). These results suggest that in addition to regulating flavonoid biosynthesis, Dof4.2 modulates phenylpropanoid metabolism in a tissue- and stress-dependent manner (Skirycz *et al*., 2007).

1.4.4 Isolating novel factors to enhance the efficiency of enzymatic saccharification

Many studies have aimed to isolate novel genetic factors with positive or negative effects on SCW properties using various approaches. One such approach involves screening a transgenic or mutant library from Arabidopsis to isolate novel factors that enhance the efficiency of

enzymatic saccharification (Sakamoto and Mitsuda, 2015; Ohtani and Ramachandran *et al*., in preparation).

In our laboratory, an Arabidopsis overexpression library of the 108 genes that are upregulated during the early stages of xylem vessel cell differentiation (Kubo *et al*., 2005) was established. This set of genes includes genes encoding transcription factors and carbohydrate enzymes. Enzymatic saccharification analysis of seedlings and flower stem samples from these overexpressor plants led to the successful identification of several genes encoding positive regulators of saccharification efficiency. Dof 4.6 and Dof 1.8 are included in the list of positive regulators, and Dof 1.8 overexpressors showed the highest glucose yields after enzymatic saccharification among transgenic lines (Ohtani and Ramachandran *et al*., in preparation). These results suggest that Dof4.6 and Dof1.8 regulate SCW properties associated with saccharification efficiency. However, to date, no detailed information about the molecular functions of Dof4.6 and Dof1.8 is available.

1.5 Aims of this study

In my thesis study, I aimed to investigate the roles of Dof4.6 and Dof1.8 in the regulation of vascular cell differentiation in Arabidopsis. Based on the expression patterns of *Dof4.6* and *Dof1.8*, I renamed these genes *VASCULAR-RELATED DOF1* (*VDOF1*) and *VDOF2*, respectively. Overexpressors of *VDOF1* and *VDOF2*, as well as the double knock-out mutant *vdof1 vdof2*, showed abnormalities in vein patterning in seedling cotyledons, as well as lignin deposition in flower stems. In addition, transcriptome analysis using inducible *VDOF1* and *VDOF2* overexpressors identified developmental-related transcription factor and lignin biosynthesis-related genes as target genes of VDOF1 and VDOF2. These findings indicate that VDOF1 and VDOF2 are novel regulators of vascular cell differentiation.

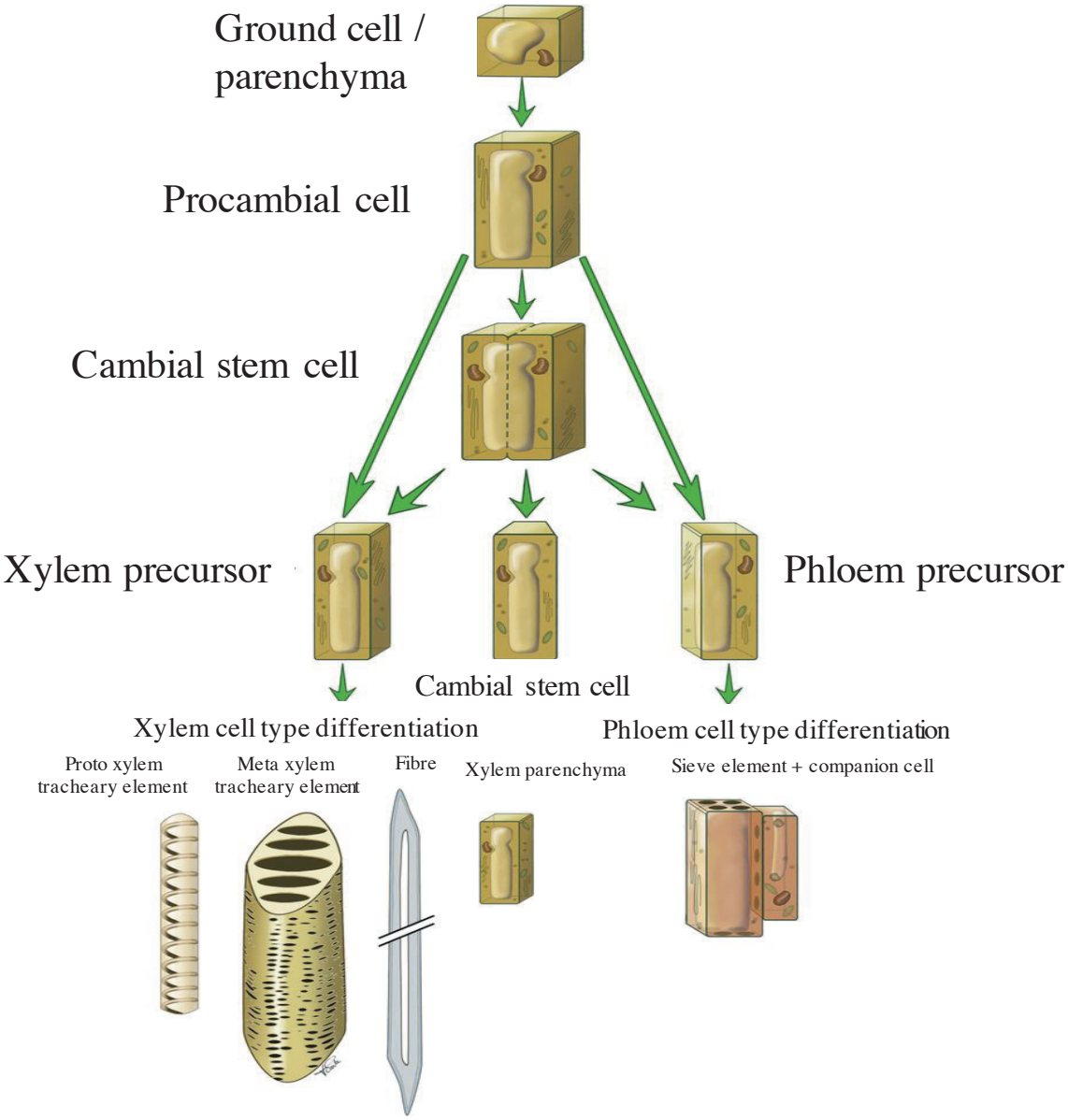

Figure 1.1 **Overview of procambial/cambial cell specification and xylem/phloem cell differentiation**. (Edited from Schuetz *et al*., 2013).

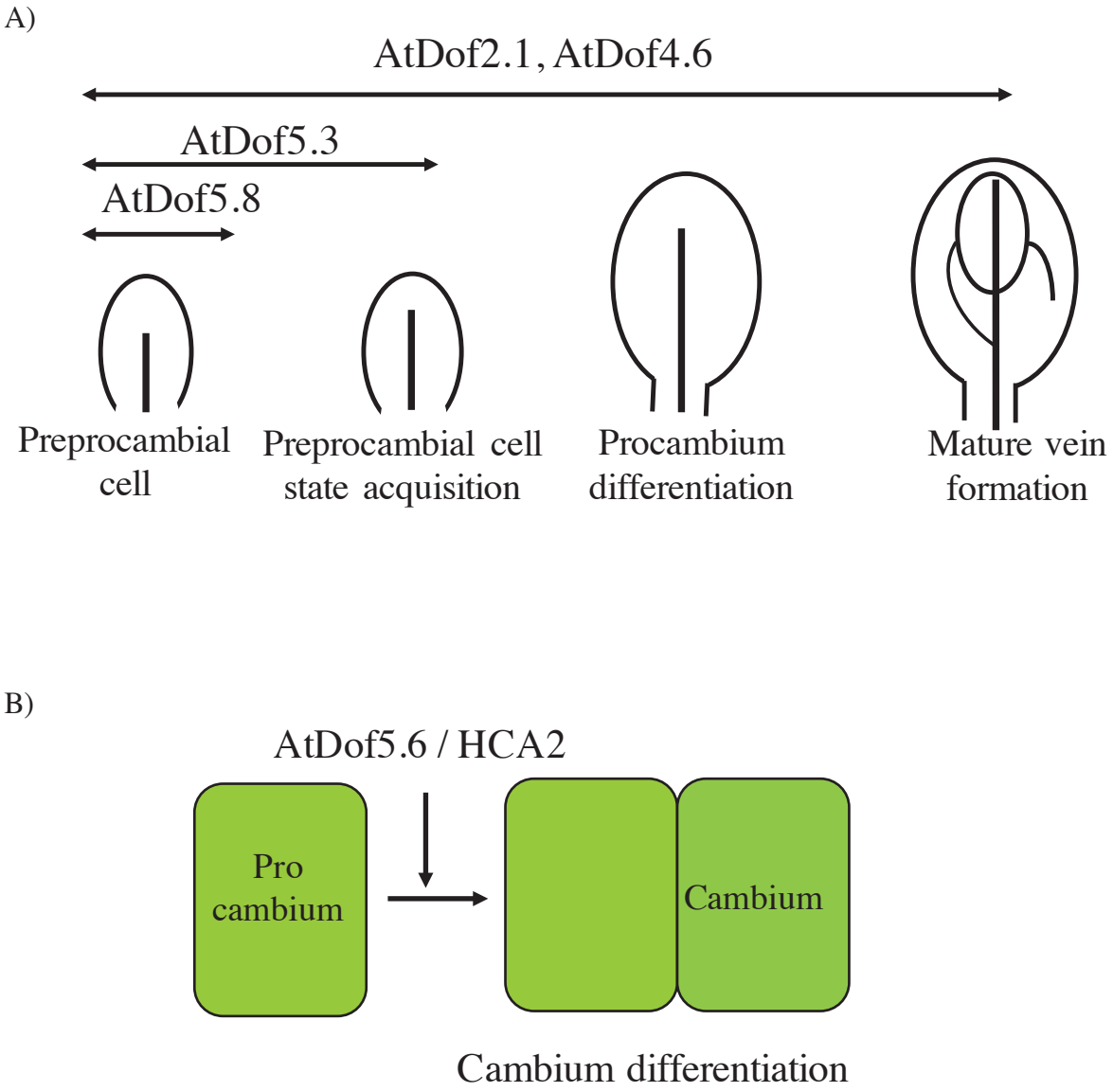

Figure 1.2 **The Dof transcription factors are involved in different steps of plant development**. (A) Pattern of expression of several Dof transcription factors at early stage of formation of the leaf vascular tissues. (B) The transcription factor AtDof5.6/HCA2 has been suggested to be involved in the transition between the procambium and the cambium. (Edited from Hir and Bellini, 2013)

CHAPTER 2

MATERIALS AND METHODS

2.1 Plant materials and growth conditions

Arabidopsis thaliana (Arabidopsis) ecotype Columbia (Col-0) was used as the wild type. T-DNA insertion lines of SALK_152104 (*vdof1*) and SALK_130584 (*vdof2*) were obtained from the Arabidopsis Biological Research Center. The *vdof1 vdof2* double mutant was established by the reciprocal crossing between *vdof1* and *vdof2*. Seeds were surface sterilized with 70% ethanol for 2 min, and incubated in Plant Preservative Mixture (PPM; Plant Cell Technology, http://www.plantcelltechnology.com/plant-preservative-mixture-ppm/) overnight at room temperature. Then, sterilized seeds were placed on germination medium (GM) containing Murashige and Skoog (MS) plant salt mixture (Wako), 0.5% (w/v) sucrose (Wako), 0.05% (w/v) MES-KOH pH 5.8 (Dojindo), MS vitamin mix (Wako), and 0.3% (w/v) gellan gum (Wako) to solidify the medium. Seeds were placed on GM plates and incubated at 4°C for 2–3 d in darkness, and then plates were transferred to a growth chamber with continuous light at 22°C. Fourteen-day-old seedlings were transferred to soil and allowed to continue growing in the growth chamber or in a greenhouse, with long-day conditions (16-h light/8-h dark) at 22°C.

2.2 Plasmid construction

Promoter sequences were obtained as approximately 2-kb upstream regions of *VDOF1* and *VDOF2*. The *VDOF* promoters (*VDOFpro*) and regions containing promoter sequences and open reading frames (ORFs) were amplified by PCR using genomic DNA as template. The coding sequences (CDSs) of *VDOF1* and *VDOF2* were amplified by PCR using cDNA as template. The amplified fragments were subcloned into the pENTR/D-TOPO vector (Invitrogen), and then the cloned fragments were integrated into the GATEWAY destination

vectors using LR Clonase (Invitrogen). To generate constitutive and estrogen-inducible overexpressors for *VDOF* genes (*VDOF1ox* and *VDOF2ox*), the CDS fragments of *VDOF1* and *VDOF2* were integrated into the binary vectors pH35GS (Kubo *et al*., 2005) and pHXGS (Endo *et al*., 2015), respectively. Reporter constructs were generated by inserting the *VDOF1* and *VDOF2* promoter fragments with or without coding sequences into pBGGUS (Kubo *et al*., 2005) to produce *VDOF1pro:GUS*, *VDOF2pro:GUS*, *VDOF1pro:VDOF1 CDS-GUS* and *VDOF2pro:VDOF2 CDS-GUS*. The regions containing *VDOF1* and *VDOF2* promoters and ORF fragments were inserted into pHGY (Yamaguchi *et al*., 2008) to produce *VDOF1-YFP* and *VDOF2-YFP*. For constitutive expression analysis of *VDOF1-YFP*, the CDSs of *VDOF1* and *VDOF2* were inserted into the pH35GY vector (Kubo *et al*., 2005) to generate *35S:VDOF1-YFP* and *35S:VDOF2-YFP*, respectively. To generate effector plasmids for the dual luciferase (LUC) transient expression assay, the CDSs of *VDOF1* and *VDOF2* were inserted into the *Sma*I/*Sal*I site of the p35S-GAL4DB plasmid (Yamaguchi *et al*., 2008). The reporter and reference plasmids containing firefly LUC and *Renilla reniformis* LUC, respectively, were prepared as described in Endo *et al*. (2015). All primers used in this study are presented in Table 2.1.

2.3 Plant transformation

The plasmid constructs were electroporated into *Agrobacterium tumefaciens* strain *GV3101:pMP90*. Agrobacteria carrying the selected constructs were transformed into Col-0 plants using the floral-dip method (Clough and Bent, 1998). Seeds of transformed plants were screened on GM plates supplemented with 20 μg mL^{-1} hygromycin or 10 μg mL^{-1} bialaphos (Bar) under continuous light at 22°C as described by Yamaguchi *et al*. (2008).

2.4 Phylogenetic tree analysis of Dof transcription factor proteins

The amino acid sequences of 36 Dof transcription factors were obtained from the NCBI (https://blast.ncbi.nlm.nih.gov/) and TAIR (https://www.arabidopsis.org) databases. The sequences were aligned using the ClustalW tool (http://www.ebi.ac.uk/Tools/msa/clustalw2/), and were determined to be conserved regions. The maximum likelihood phylogenetic tree for these aligned sequences was constructed using MEGA6 software (Tamura *et al*., 2013) with 1,000 bootstrap replications.

2.5 Dual luciferase transient expression assay

Transient expression assays were performed according to the methods of Endo *et al*. (2015). The effector, reporter, and reference plasmids were delivered into 14-day-old Arabidopsis plants by particle bombardment (Biolistic PDS-1000/He Particle Delivery System, Bio-Rad). After bombardment, plants were incubated in darkness for 18 h at 22°C. Then, leaves were excised to determine LUC activity using the Dual-Luciferase Reporter Assay System (Promega) and the Tristar LB941 Multimode Microplate Reader (Berthold).

2.6 Subcellular localization analysis of VDOF proteins

The subcellular localization of VDOF proteins was examined in 4-day-old seedlings (T_2 generation) harboring *35S:VDOF1-YFP* or *35S:VDOF2-YFP*. Seedlings were fixed overnight at 4°C in fixative solution [1.5% (v/v) formaldehyde and 0.5% (v/v) glutaraldehyde in PEMT buffer containing 50 mM PIPES, 2 mM EGTA, 2 mM $MgSO_4$, 0.05% (v/v) Triton X-100, pH 7.2] (Sugimoto *et al*., 2000). Then, the samples were washed with PEMT buffer at room temperature three times for 10 min each, followed by washing with PBS buffer three times for 10 min each at room temperature. The samples were stained with 1 mM DAPI (4′,6-diamidino-2-phenylindole) for 10 min at room temperature, and then washed with PBS buffer three times

for 10 min each (Ishida *et al*., 2009). The samples were mounted in PBS buffer before imaging. Samples were observed using an automated confocal laser-scanning microscope (FluoView FV10i-LIV, Olympus) equipped with filters for YFP (460-495 nm) and DAPI (410–585 nm). Images were processed and analyzed using ImageJ software (https://imagej.nih.gov/ij/).

The subcellular localization of VDOF proteins was also examined in 7-day-old seedlings (T_2 generation) of *VDOF1pro:VDOF1-YFP* and *VDOF1pro:VDOF2-YFP* plants. The seedlings were washed briefly in distilled water, and the roots were cut and mounted on a glass slide with a few drops of water. YFP fluorescence was observed using an automated laser-scanning confocal microscope (FluoView FV10i-LIV, Olympus) equipped with a YFP filter set (460-495 nm). Images were processed and analyzed using ImageJ software.

2.7 GUS reporter assay

The GUS reporter lines (T_2 or T_3 generation of *VDOF1pro:GUS*, *VDOF2pro:GUS*, *VDOF1pro:VDOF1 CDS-GUS* and *VDOF2pro:VDOF2 CDS-GUS*) were aseptically grown on GM plates, and 1, 2, 3, and 7-day-old seedlings were sampled for the GUS reporter assay according to the method of Pyo *et al*. (2007) with slight modifications. Samples were fixed with pre-chilled 90% (v/v) acetone overnight at –30°C, and then washed three times at room temperature with 50 mM sodium phosphate buffer (pH 7.0). Then, samples were incubated in substrate solution (1 mM 5-bromo-4-chloro-3-indolyl glucuronide, 0.5 mM potassium ferricyanide, 0.5 mM potassium ferrocyanide, and 10% Triton-X-100) for 2 to 4 h at 37°C. Samples were washed with sodium phosphate buffer and then mounted on glass slides with a few drops of clearing solution (8 g chloral hydrate, 1 mL glycerol, and 2 mL distilled water). Inflorescence stem samples were embedded in 7% (w/v) agar and sectioned into thin sections of 90–100 μm using the DTK-Zero1 microslicer (Ted Pella, Inc.). Samples were observed using a microscope equipped with Nomarski optics (BX51, Olympus), and images were

photographed with a digital camera (DP70, Olympus). More than three independent reporter lines with five technical replicates were examined.

2.8 Histochemical observations of inflorescence stems

The inflorescence stems of 40-day-old *VDOF1ox* and *VDOF2ox* plants (homozygous T_3 generation) and the *vdof1 vdof2* double mutant were cut into apical, middle, and basal samples, and fixed with freshly prepared fixative solution [ethanol:acetic acid, 9:1 (v/v)] overnight at 4°C. Then, the fixed stems were dehydrated and rehydrated with an ethanol series [30, 50, 70, 95, and 100% ethanol (v/v)] and subjected to cross-sectioning as described in Section 2.7. The sections were incubated in 20% (w/v) $CaCl_2$ as described previously by Herr (1992). The phloroglucinol-$CaCl_2$-HCl solution was prepared by adding phloroglucinol into 20% (w/v) $CaCl_2$ to make a 10:1 (w/v) phloroglucinol concentration. After the overnight incubation, concentrated hydrochloric acid was added to phloroglucinol-$CaCl_2$ solution to a final ratio of 25:4 (v/v). Sections were stained with one drop of the phloroglucinol-$CaCl_2$-HCl solution for 1–5 min. After removing the phloroglucinol-$CaCl_2$-HCl solution, the sections were mounted on glass slides in 20% (w/v) $CaCl_2$. Samples were viewed using a microscope equipped with Nomarski optics (BX51, Olympus), and images were photographed with a digital camera (DP70, Olympus).

2.9 Observations of cotyledon vein patterns

Seven-day-old and 14-day-old seedlings of *VDOF1ox* and *VDOF2ox* (homozygous T_3 generation) and the *vdof1 vdof2* double mutant were fixed in pre-chilled 90% (v/v) acetone overnight at 4°C. Samples were washed with distilled water and then mounted on glass slides with clearing solution. Samples were observed with a microscope equipped with Nomarski

optics (SZX16, Olympus) and were photographed with a digital camera (DP72, Olympus). Vein networks were analyzed according to the method of Verna *et al*. (2015).

2.10 Enzymatic saccharification analysis

Fourteen-day-old seedlings of *VDOF1ox* and *VDOF2ox* (homozygous T_3 generation) and the *vdof1 vdof2* double mutant were sampled and the roots were removed and discarded. Samples were freeze-dried for 16–18 h and then powdered with a TissueLyserII (Qiagen). The powdered samples were washed three times with 10 mL of distilled water followed by three methanol washes, and then dried in a DNA SpeedVac (Savant, Thermo) for more than 3 h. Then, 10 mg of powdered sample was incubated with 1 mL of reaction solution {1 mg/mL enzyme mixture [cellulase from *Trichoderma reesei* (Sigma-Aldrich) and cellobiase from *Aspergillus niger* (Sigma-Aldrich)] and 1 M NaOAc (pH 5.0)} in a rotating incubator at 45°C. Then, 42 μL of reaction mix was sampled at 0, 3, 6, 12, and 24 h. The enzymatic reactions were stopped in these samples by adding 41 μL of 100 mM NaOH, and then the samples were stored at 4°C until measurement (the samples were stable for at least 1week in the refrigerator). Glucose was quantified using a Glucose CII-test Kit (Wako) and a Microplate Reader (Bio-Rad) at absorbance 505 nm.

2.11 Thioglycolic acid analysis of lignin content

The inflorescence stems of 40-day-old *VDOF1ox* and *VDOF2ox* (homozygous T_3 generation) and *vdof1 vdof2* double-mutant plants were sampled for lignin content analysis. The basal 10 cm was harvested and freeze-dried. Thioglycolic acid analysis of total lignin content was performed as described previously by Suzuki *et al*. (2009). The powdered samples were extracted with water and methanol and then the obtained dried pellets were treated with 1 ml of 3 N HCl and 0.1 ml thioglycolic acid (Nacalai Tesque) for 3 h at 80^0C. The samples were

washed with water and pellets were suspended in 1 ml 1 N NaOH and shaken vertically at 80 rpm for 16 h. Next, the samples supernatants were acidified with 0.2 ml concentrated HCl for 4 h at 4^0C. The samples were centrifuged and obtained pellets were dissolved in 1 N NaOH and submitted to spectrophotometric measurement.

2.12 RNA-seq analysis of inducible *VDOF1* and *VDOF2* overexpression lines

Six-day-old seedlings of estrogen-inducible *VDOF1* and *VDOF2* overexpression lines were transferred into liquid MS medium with or without 10 μM of 17-β-estradiol for 24 h at 22°C. A total of 15 seedlings from three independent lines of estrogen-inducible overexpressors of *VDOF1* and *VDOF2* were treated with estrogen, washed briefly, and then collected for total RNA extraction using an RNeasy Mini Kit (Qiagen). RNA purity and concentration were measured using a NanoDrop 100 Spectrophotometer (Thermo Scientific, USA), and samples with an A_{260}/A_{280} ratio of 1.8–2.0 were used for further analysis. The quality of each total RNA sample was examined using an Agilent RNA 6000 Nano Kit and Agilent 2100 Bioanalyzer (Agilent Technologies, Inc.), and samples that scored a high RNA integrity number (RIN ≥ 8) were selected. RNA-seq analysis (Illumina) and construction of cDNA libraries were outsourced to Beijing Genome Institute (BGI). The Illumina HiSeq 4000 (Illumina) was used for sequencing.

The raw read data presented in fastq format contained 24–33 million reads of 49-nt in length. The Trimmomatic version 0.32 program was used with recommended settings to trim the adaptors and remove poor quality reads before mapping (Bolger *et al*., 2014). Then, the Tagdust version 2.33 program was used to filter rRNA-derived reads (Lassmann, 2015). Next, Tophat2 version 2.1.1 (Kim *et al*., 2013) was used to map RNA sequencing short reads to the Arabidopsis genome (TAIR10), which was guided by gene annotation information from Ensembl Plant Release 29 (October 2015). The following settings were used in Tophat2: "p 8,

segment length 16, segment mismatches 1, min anchor length 4, max multihits, 20x20, report secondary alignments, i 30, I 6000, min segment intron 30, max segment intron 6000, min coverage intron 30, and transcriptome index". Cuffdiff/Cufflinks version 2.2.1 (Trapnell *et al*., 2012) was used to calculate normalized expression values and identify differentially expressed genes (DEGs). The cuffdiff subcommand was used with the following settings: "p 12, c 1, u q, max bundle frags 2000000". In-house perl scripts were used to extract the data matrices of expression values, paired-end fragments per kilobase of exon model per million mapped reads (FPKM), and DEG list for each pair among the samples from selected cuffdiff output files. Genes with a q-value < 0.05 were regarded as DEGs.

2.13 Gene ontology analysis and Venn diagrams

Gene ontology (GO) enrichment was analyzed using DEG datasets derived from mock- and estradiol-treated *VDOF1ox* and *VDOF2ox* lines. The DEG data were separated into upregulated and downregulated gene sets, and then independently subjected to BiNGO analysis (Maere *et al*., 2005) using the Cytoscape version 3.3.0 plugin (http://cytoscape.org). GO terms with a Benjamini-Hochberg false discovery rate (FDR) threshold < 0.05 were considered as statistically over-represented. Venn diagrams were constructed to compare DEG sets in the *VDOF* transcriptomic data with vascular-related genes using the Venn diagram plotter (https://omics.pnl.gov/software/venn-diagram-plotter) and VENNY 2.1 (http://bioinfogp.cnb.csic.es/tools/venny/).

2.14 Quantitative and semi-quantitative RT-PCR

Total RNA was isolated using the RNeasy Mini Kit (Qiagen) with DNase 1 (Qiagen). First-strand cDNA was synthesized from 1 μg of total RNA using oligo(dT) primers and Transcriptor reverse transcriptase (Roche). For semi-quantitative RT-PCR analysis, 2 μL of 10× diluted

first-strand cDNA was used as the template, with 4 μL of 5× PCR reaction buffer, 1.2 μL of 25 mM $MgCl_2$, 0.4 μL of 10 mM dNTP, 1.0 μL of each primer (forward and reverse), 0.1 μL of Kapa Taq Extra DNA polymerase (Kapa Biosystems), and nuclease-free water to bring the reaction volume to 20 μL for each sample. The PCR products were separated on 2% (w/v) agarose gels and stained with ethidium bromide. *UBIQUITIN 10* (*UBQ10*) was used as the internal control.

Quantitative PCR analysis was performed using the first-strand cDNA as the template and a Light Cycler 480 SYBR Green 1 Master (Roche) according to the manufacturer's instructions. The reactions were incubated at 95°C for 5 min, followed by 45 cycles of 95°C for 10 s, 58°C or 60°C for 20 s, and 72°C for 20 s. Finally, the melting curve was generated by incubating the samples at 95°C for 5 s and 65°C for 1 min, and then cooling the samples at 50°C for 30 s. *UBQ10* was used as the internal control, and the expression levels of the tested gene transcripts relative to that of *UBQ10* were calculated. Three biological replicates with three technical replicates were performed. The primers used in this study are listed in Table 2.1.

Table 2.1 **List of primers used in this study**

Name	AGI No.	Forward primer sequences (5'-3')	Reverse primer sequences (5'-3')
RT-PCR			
VDOF1 promoter	AT4G24060	CACCGCACGCGCATGAGCAAAC	TGGCCACTGAGCCGTATCCAT
VDOF1 promoter CDS	AT4G24060	CACCGCACGCGCATGAGCAAAC	GCACCATGATCCTCCACTCAA
VDOF1 CDS	AT4G24060	CACCATGGATACGGCTCAGTGG	GCACCATGATCCTCCACTCAA
VDOF2 promoter	AT1G64620	CACCTCATGTCAGTAGAGGCGT	AGGCCATTTAGCAGTGTCCAT
VDOF2 promoter CDS	AT1G64620	CACCTCATGTCAGTAGAGGCGT	TTGCCATGAACCACCAGATGC
VDOF2 CDS	AT1G64620	CACCATGGACACTGCTAAATGG	TTGCCATGAACCACCAGATGC
Semi-quantitative PCR			
VDOF1	AT4G24060	GGAGAAGAAGGTGGAGAAGGTGGA	GCACCATGATCCTCCACTCAA
VDOF2	AT1G64620	CCATTTGAGAGCCTCCTCAAACTT	TTGCCATGAACCACCAGATGC
LAC7	AT3G09220	ACACACCTTCAACGTACAAAACT	TGGAAGATCCCATGCCAATGA
LAC12	AT5G05390	AATGTTTCCGGGGCCTACG	GTGTAGCTCTTTCCGGGTCG
PER4	AT1G14540	CATTGACGCGGGATTCTCCA	GAAGCTCCGGTTCCGAACAA
PER10	AT1G49570	TAAGCTCGCTGCTCTTGACG	ACTGCGAAATCCCTCGAGAA
PER15	AT2G18150	GCGACGACGACGAGAGTAA	CCTGAACGAAACAATCGTGGAA
PER24	AT2G39040	AGTGGTCGGAATGGACCCTA	ATGGACCGACCAAACTGAGC
PER 27	AT3G01190	CTTTTCCAGTCGGATGCTGC	AGCAGACCGACACGTCTTAC
PER44	AT4G26010	CTTGCTCCTTCTGCTTTGGC	GAGGGAAGCATCACAACCCC
PER52	AT5G05340	GACACGTCAACGAACTTGCC	CGGACGATGGAGTCAGTAGAG
PER53	AT5G06720	AAAACGGTAGCGCATCAACG	GAGTCTGGTTACTTGCGAACG
PER57	AT5G17820	TGGACCCCGCTTTGGTTAC	CCACAATCCCACGAGTCTGT
CCR	AT1G80820	CGGCGGCTACATTGCTTCTT	GTGGCACAGAGAGCTTCGTA
CAD5	AT4G34230	GGAATCTGCCACACCGATCT	GCTACAACCTCCGCAACATC
UBQ10	AT4G05320	AACTTTGGTGGTTTGTGTTTTGG	TCGACTTGTCATTAGAAAGAAAGAGATAA

Quantitative RT-PCR			
CAD5	AT4G34230	GGAATCTGCCACACCGATCT	GCTACAACCTCCGCAACATC
LAC7	AT3G09220	ACACACCTTCAACGTACAAAACT	TGGAAGATCCCATGCCAATGA
LAC12	AT5G05390	AATGTTTCCGGGGCCTACG	GTGTAGCTCTTTCCGGGTCG
PER 27	AT3G01190	CTTTTCCAGTCGGATGCTGC	AGCAGACCGACACGTCTTAC
PER53	AT5G06720	AAAACGGTAGCGCATCAACG	GAGTCTGGTTACTTGCGAACG
MYB63	AT1G79180	AACTGGAGATCTCTCCCCAAA	TTCCCATAGTTGTGGTGAAGC

CHAPTER 3

RESULTS

3.1 Structure and molecular characteristics of Dof transcription factors

3.1 Structure of Dof transcription factors

Arabidopsis has 36 Dof transcription factor (TF) genes. To visualize the sequence characteristics of these Dof TF genes, I aligned their encoded amino acid sequences using ClustalW software. The alignment revealed that the amino acid sequence of the Dof domain, consisting of a Cysteine (C_2C_2)-type zinc finger (Yanagisawa, 2002), is highly conserved among Arabidopsis Dof TFs (Figure 3.1). In addition, I used MEGA6 software to construct a Maximum-Likelihood phylogenetic tree based on the Dof domains of 36 Dof TFs (Figure 3.2). Bootstrapping values are indicated in the branches of the phylogenetic tree as a percentage for values over 60. Based on the nomenclature described in Yanagisawa (2015) and the TAIR database, when available, the abbreviated names of the Dof genes are shown together with their nomenclature. Dof4.6/VDOF1 and Dof1.8/VDOF2, which were the focus of this study, as described in the Introduction (Chapter 1), are highly similar, especially in the N-terminal regions, including the Dof domain (Figure 3.1–3.3), while the C-terminal regions corresponding to the activation domains are rather variable, suggesting that VDOF1 and VDOF2 might have the same or similar targets, but play different transcriptional regulatory roles for these targets.

3.1.2 VDOF proteins as transcription factors

To determine whether VDOF1 and VDOF2 have transcriptional activator domains activities or transcriptional repressor domains activities, I carried out transient expression assays with true leaves of 14-day-old Arabidopsis seedlings via particle bombardment (Figure 3.4). The effector constructs, expressing the GAL4-binding domain (BD) fused with VDOF1 and VDOF2 driven

by the CaMV 35S promoter, were delivered into Arabidopsis leaves with a reporter construct containing firefly luciferase (LUC) linked to the GAL4-binding site (Figure 3.4). No increase in LUC activity was detected using these effectors compared with the control construct (containing a multicloning site [MCS] instead of VDOF1 or VDOF2), whereas there was a ~30-fold increase in LUC activity using a positive control construct with the activation domain of the herpes virus VP16 protein (VP16), suggesting that neither VDOF1 nor VDOF2 has a transcriptional activator domain. These results prompted me to investigate whether VDOF1 and VDOF2 have transcriptional repressor domains. A reported construct expressing LUC under the control of the 35S promoter fused with the GAL4-binding site, which has increased basal LUC activity (Mitsuda *et al*., 2005), was delivered to Arabidopsis leaves with the effector constructs, resulting in reduced (~50%) LUC activity using the GAL4-BD-VDOF2 construct compared with the control MCS construct. This reduction (~50%) using the GAL4-BD-VDOF2 construct was much weaker than that (>90%) observed using the positive control (GAL4-BD fused to the strong repression domain, SRDX) (Hiratsu *et al*., 2002). These results suggest that VDOF2 has transcriptional repressor domain. Further analysis is needed to determine if VDOF1 also has a transcriptional repressor domain.

Next, I analyzed the subcellular localization of VDOF1 and VDOF2. I introduced the coding sequences of *VDOF1* and *VDOF2* fused with the *YFP* coding sequence driven by the 35S promoter into Arabidopsis and observed the root cells of 4-day-old transgenic Arabidopsis seedlings after counter-staining with DAPI (Figure 3.5). YFP signals overlapped with DAPI signals in both the *VDOF1*- and *VDOF2-YFP* transgenic seedlings, indicating that VDOF1 and VDOF2 localize to the nucleus.

3.2 Transcription factors VDOF1 and VDOF2 are involved in vascular cell differentiation

3.2.1 Expression analysis of YFP-fused VDOF proteins driven by their own promoters

To investigate the expression patterns of *VDOF1* and *VDOF2*, I fused the coding sequences of *VDOF1* and *VDOF2* with *YFP*, driven by their own promoters (2 kb and 1 kb, respectively), and introduced the constructs into Arabidopsis plants to generate transgenic plants expressing these chimeric genes. Observation of roots of 7-day-old transgenic seedlings under an automated confocal laser-scanning microscope (Figure 3.6) revealed that both VDOF1-YFP and VDOF2-YFP signals were preferentially expressed along the vascular cells of roots. However, the fluorescent signal patterns differed; for instance, at the root tips, VDOF1-YFP signals were detected throughout the vascular cells, including meristematic procambium cells, whereas VDOF2-YFP signals were specifically expressed only in the outer cells of the vascular regions.

3.2.2 Expression analysis of *VDOF1*-GUS and *VDOF2* -GUS

To further examine the expression patterns of *VDOF1* and *VDOF2*, I investigated the expression of the promoters of these genes fused to the β-glucuronidase (*GUS*) reporter gene by generating transgenic plants expressing the constructs containing the 2- and 1-kb promoters of *VDOF1* and *VDOF2*, respectively, fused with *GUS*, with or without their coding sequences (between the promoter and *GUS*) into Arabidopsis plants. Transgenic seedlings carrying either promoter-GUS construct, regardless of age (1, 2, and 3 days after germination [DAG]), showed GUS staining throughout the vasculature, with strong staining in the shoot apical meristem (SAM). Weaker GUS staining was detected in plants harboring the promoter-VDOF coding sequence-GUS constructs than in plants harboring the promoter-GUS constructs (Figure 3.7), suggesting possible post-translational regulation of *VDOF* gene expression. Notably, only some

seedlings showed dotted staining along the vasculature (Figure 3.7), suggesting that VDOF proteins are targeted to the nucleus in a developmental stage-specific manner.

I also investigated the expression patterns of *VDOF1* and *VDOF2* in transgenic Arabidopsis plants carrying the *VDOF* promoter-GUS constructs (Figures 3.8–3.10). In 7 DAG seedlings, GUS staining in plants harboring the *VDOF1* promoter-*GUS* was observed throughout the vasculature, with prominent staining in the SAM (Figure 3.8 A–E). Root cross-sections of 7 DAG seedlings showed staining in the vasculature and in the surrounding pericycle (Figure 3.8 D). Detailed observation of cotyledons and true leaves indicated that GUS staining in plants harboring the *VDOF1* promoter-GUS construct was restricted to leaf veins, while GUS staining in true leaves was somehow dependent on the developmental stage of the vascular tissues or leaves: GUS staining appeared in a gradient, from weaker staining in the tip to stronger staining at the base (Figure 3.8 F). A similar staining pattern was observed in 7 DAG seedlings carrying the *VDOF2* promoter-GUS constructs, with some exceptions (Figures 3.9 A–F). The GUS staining pattern in the root tips of plants harboring the *VDOF2* promoter-GUS often appeared U-shaped (Figure 3.9 B), as observed in the roots of seedlings harboring the *VDOF2* promoter-*VDOF2* coding sequence-*YFP* (Figure 3.6 E–H); this pattern was not detected in the roots of plants harboring the *VDOF1* promoter-*GUS* (Figure 3.8 B). In addition, the GUS staining pattern in the tips of shoot lateral roots (Figure 3.8 C and 3.9 C) of plants harboring *VDOF2* promoter-*GUS* was narrower than that of plants harboring *VDOF1* promoter-*GUS*. These observations suggest that *VDOF2* is predominantly expressed at the phloem poles of root tips.

The expression patterns of *VDOF1* and *VDOF2* differed: unclear but preferential GUS staining was found in anthers of 40-day-old plants harboring *VDOF1* promoter-*GUS* (Figure 3.8 G), while relatively strong staining was found in the middle of the anther and in the vasculature of anther stalks in plants expressing *VDOF2* promoter-*GUS* (Figure 3.9 G).

I examined the expression of *VDOF1* and *VDOF2* in cross-sections of inflorescence stems of 40-day-old transgenic plants expressing *VDOF* promoter-*GUS* (Figure 3.10). Both *VDOF1*- and *VDOF2* promoter-*GUS*-expressing plants showed GUS staining in some vascular cells located adjacent to (outside of) differentiated vessel cells, presumably including differentiating vessel cells, cambial/procambial cells, and phloem cells, in the apical part of the inflorescence stem (Figure 3.10 A, B, G, H). GUS staining was apparent in phloem cells in the apical parts of the inflorescence stem in plants harboring *VDOF2* promoter-*GUS* (Figure 3.10 G, H). In the middle part of the stem, both types of transgenic plants showed GUS staining in phloem cells and in parenchyma cells surrounding differentiated vessel cells, while only plants expressing *VDOF1* promoter-*GUS* showed GUS staining in interfascicular fiber cells, especially the outermost cells, which were likely immature/differentiating fiber cells (Figure 3.10 C, D, I, J). The GUS staining pattern in the basal part of the stem was similar to that in the middle part of the stem (Figure 3.10 E, F, K, L). These results suggest that VDOF1 and VDOF2 are involved in vascular development and/or function throughout the plant.

3.3 Effects of *VDOF1* and *VDOF2* overexpression and *vdof1 vdof2* mutations on plant growth

To observe the effects of overexpression and mutations of *VDOF1* and *VDOF2* on plant growth and vascular development, I obtained the *vdof1* and *vdof2* mutants from a publicly available collection of T-DNA insertion lines and generated the double knock-out mutant *vdof1 vdof2* by crossing the *vdof1* and *vdof2* single mutants (Figure 3.11). I generated constitutive overexpressors of *VDOF1* (*VDOF1ox*) and *VDOF2* (*VDOF2ox*) by introducing a cassette with 35S promoter-driven *VDOF1* or *VDOF2* into Arabidopsis plants (Figure 3.12).

To monitor the effects of overexpression and mutation of *VDOF1* and *VDOF2* on seedling growth, wild type, *VDOF1ox, VDOF2ox*, and *vdof1 vdof2* mutant plants were grown on MS

plates for 14 days (Figure 3.13). The growth and morphology of *vdof1 vdof2* seedlings did not differ from those of the wild type (Figure 3.13). By contrast, growth was inhibited in the *VDOF1ox* and *VDOF2ox* lines; within *VDOF1ox* line 6-6 and all of the *VDOF2ox* lines, a certain portion of the seedlings showed reduced size and yellowish leaves compared to the wild type (Figure 3.13), suggesting that overexpression of *VDOF1* and *VDOF2* affects seedling development. Interestingly, such defects in seedling growth were less prominent at later stages of development (Figure 3.14). The sizes of 40-day-old *VDOF1ox, VDOF2ox*, and *vdof1 vdof2* plants were comparable to those of the wild type (Figure 3.14). These results suggest that the growth defects caused by overexpression of *VDOF1* and *VDOF2* can be restored during subsequent development and that plants can overcome these defects in seedling growth as they mature.

3.4 Effect of *VDOF1* and *VDOF2* overexpression and *vdof1 vdof2* mutations on enzymatic saccharification efficiency in seedlings

Because VDOF1 and VDOF2 were originally isolated as enhancers of enzymatic saccharification efficiency when overexpressed (Ohtani and Ramachandran *et al*., in preparation), I performed an enzymatic saccharification analysis of *VDOF1ox, VDOF2ox*, and *vdof1 vdof2* seedlings. Ground seedlings were treated with the cellulose-degrading enzymes cellulase and cellobiase (for details, please see Materials and Methods). In accordance with the previous results, the *VDOF1ox* and *VDOF2ox* seedlings showed significantly increased glucose yields compared to the wild type (Figure 3.15). By contrast, the *vdof1 vdof2* double knock-out mutant exhibited reduced glucose yields compared to the wild type (Figure 3.15). The opposite effects of overexpression versus knock-out of the *VDOF* genes suggests that VDOF1 and VDOF2 are critical regulators of cell wall properties, which can influence the release of glucose during enzymatic saccharification.

3.5 Effects of *VDOF1* and *VDOF2* overexpression and *vdof1 vdof2* mutations on vein patterning in cotyledons

Several *Dof* genes are involved in vein formation in cotyledons and true leaves. Therefore, I examined the vein patterning in *VDOF1ox, VDOF2ox*, and *vdof1 vdof2* plants using 7- and 14-day-old cotyledons (Figure 3.16 and 3.17). In 7-day-old cotyledons of *VDOF1ox* and *VDOF2ox* plants, unconnected veins were often observed, while the secondary veins of *vdof1 vdof2* cotyledons tended to resemble closed loops (Figure 3.16 A). To quantitatively characterize vein formation in the cotyledons, I measured three descriptors from Verna *et al*. (2015) and Figure S2 to calculate the cardinality, continuity, and connectivity of vein network indexes, which reflect the number of veins in a network, the number of vein fragments (i.e., isolated veins that do not have contact with other veins) in a network, and how close a vein network is, respectively (Verna *et al*., 2015). In 7-day-old cotyledons, the cardinality and connectivity indexes of *vdof1 vdof2* tended to be higher than those of the wild type, whereas the connectivity index was significantly reduced in *VDOF1ox* and *VDOF2ox* (Figure 3.16 B). These results suggest that VDOF1 and VDOF2 have negative effects on vein development (Figure 3.16). In the cotyledons of 14-day-old plants, only the cardinality index of *vdof1 vdof2* differed significantly from that of the wild type (Figure 3.17), indicating that the reduced connectivity detected in the cotyledons of 7-day-old *VDOF1ox* and *VDOF2ox* plants was recovered in the cotyledons of 14-day-old plants, and that enhanced vein development continued to occur in *vdof1 vdof2* cotyledons. Taken together, these results suggest that VDOF1 and VDOF2 function as negative regulators of vein formation in seedlings (Figure 3.16 and 3.17).

3.6 Effects of *VDOF1* and *VDOF2* overexpression and *vdof1 vdof2* mutations on vascular cell development and secondary wall formation in inflorescence stems

Based on the expression patterns of VDOF1 and VDOF2 is vascular tissues of inflorescence

stems (Figure 3.18), I examined the structures of inflorescence stems in *VDOF1ox, VDOF2ox,* and *vdof1 vdof2* plants, paying special attention to SCW formation. I separated the inflorescence stems of 40-day-old plants into three regions (apical, middle and basal), and performed histological examination of these regions. Observations of cross-sections revealed no structural differences among *VDOF1ox, VDOF2ox*, and *vdof1 vdof2* plants in any parts of the inflorescence stem (Figure 3.18). Interestingly, phloroglucinol:HCl staining, which stains lignin red, revealed the presence of lignin deposits in the apical regions of *vdof1 vdof2* stems, while no clear deposition of lignin was found in the apical regions of wild-type stems (Figure 3.18 A and J). In the middle regions of *VDOF1ox* stems, reduced lignin signal deposition was observed in the interfascicular fibers compared to the wild type (Figure 3.18 B and E). No difference in lignin deposition was observed in the basal region of the stem for any genotype examined (Figure 3.18 C, F, I, and L).

These histological observations prompted me to quantify the lignin contents in the inflorescence stems of the transgenic plants. To determine the total lignin contents in the inflorescence stems of transgenic plants, I performed thioglycolic acid analysis of the lower halves of inflorescence stems. The extracted crude cell wall (CWR) was treated with thioglycolic acid, and the lignin content was measured with an ultraviolet spectrophotometer at 280 nm as described by Suzuki *et al*. (2009). The total lignin contents were significantly higher in *VDOF1ox* and *vdof1 vdof2* stems than in wild-type stems, whereas total lignin content tended to be reduced in *VDOF2ox* stems (Table 3.1; Figure 3.19). These results suggest that VDOF1 and VDOF2 function as negative regulators of lignin deposition and that the functioning of VDOF1 might differ depending on the stage of inflorescence stem development, with negative and positive effects on lignin biosynthesis in the middle and basal regions of the inflorescence stem, respectively.

3.7 RNA-seq analysis of inducible *VDOF1* and *VDOF2* overexpression lines to identify their target genes

To identify the downstream genes of *VDOF1* and *VDOF2*, I generated inducible *VDOF1* and *VDOF2* overexpression lines, in which the expression of *VDOF1* and *VDOF2* is induced by the application of ß-estradiol (Figure 3.20). Six-day-old seedlings of the inducible overexpression lines were treated with or without ß-estradiol for 24 h and subjected to RNA-seq analysis using a next-generation sequencer. I successfully obtained transcriptomic data for approximately 33,500 genes (Figure 3.21). When *VDOF1* expression was induced, 295 and 280 genes were significantly up- and downregulated, respectively. When *VDOF2* expression was induced, 504 and 535 genes were significantly up- and downregulated, respectively (Figure 3.21). Finally, 160 and 141 genes were commonly up- and downregulated, respectively, when either *VDOF1* or *VDOF2* was overexpressed (Table 3.2 and Table 3.3). A number of transcription factor genes are included in these lists, suggesting that the overexpression of *VDOF1* or *VDOF2* broadly affects transcriptional regulation.

I further analyzed the genes that were up-/downregulated in response to overexpression of *VDOF1* and/or *VDOF2* using the Gene Ontology (GO) term analysis software BiNGO. Interestingly, the sets of genes commonly regulated by VDOF1, VDOF2, and VDOF1/2 had similar GO term analysis results, with genes related to stress responses and to cell wall-related processes, such as lignin biosynthesis, being enriched in these gene sets (Figure 3.22–3.27). These findings support our idea that VDOF1 and VDOF2 regulate cell wall biosynthesis, especially lignin biosynthesis pathways, as hypothesized based on the inflorescence stem phenotypes of *VDOF1ox, VDOF2ox*, and *vdof1 vdof2* plants (Figure 3.18).

In addition, I looked for overlap between genes commonly regulated by VDOF1/2 and reported gene sets related to vascular development. First, I searched the literature for genes known to be involved in vascular development, which mainly included transcription factor

genes (Endo *et al*., 2015; Kondo *et al*., 2015; Yamaguchi *et al*., 2011; Ohashi-Ito *et al*., 2010; Miyashima *et al*., 2013; Furuta *et al*., 2014; Mähönen *et al*., 2006; Schlereth *et al*., 2010; Ohashi-Ito and Bergmann, 2007; Truernit and Sauer, 1995; Rybel *et al*., 2014; Table 3.4). The transcriptomic data showed that few of these genes were affected by the overexpression of *VDOF1* or *VDOF2* and that genes for key transcription factors that interact with several Dof genes, such as AtHB8 and MP/ARF5 (Guo *et al*., 2009; Gardiner *et al*., 2010; Konishi *et al*., 2015), were not influenced by *VDOF1* or *VDOF2* overexpression (Table 3.4). Moreover, no change in expression of any Dof gene (other than *VDOF1* or *VDOF2*) was detected (Table 3.5). The low impact of *VDOF1* and *VDOF2* overexpression on these gene sets suggests that the phenotypes of *VDOF1ox, VDOF2ox*, and *vdof1 vdof2* cannot be explained by disturbances to the well-known transcription factors involved in vascular development.

Next, I selected genes related to vascular cell differentiation from the transcriptomic data for the *altered phloem development (apl)* mutant and identified phloem-related genes (1,108 genes with altered expression levels with fold change >3, Furuta *et al*., 2014), as well as genes from the list of downstream targets of VND6 and/or VND7 to identify xylem vessel-related genes (561 genes, Yamaguchi *et al*., 2011; Zhong *et al*., 2010; Ohashi-Ito *et al*., 2010) and genes from the transcriptomic data for *nst1 nst3* to identify xylem fiber-related genes (1,528 genes with significantly altered expression levels at $p<0.05$ by Welch's t test, Mistsuda *et al*., 2007) (Table 3.6). One-to-one comparisons showed that approximately 20 genes overlapped among the phloem-, xylem vessel-, and xylem fiber-related gene set and genes commonly regulated by VDOF1/2 (Figure 3.28; Table 3.7 and 3.8). Notably, the number of genes that specifically overlapped between genes commonly upregulated by VDOF1/2 versus phloem- and xylem-related genes was similar, i.e., 15 and 18 genes, respectively; however, the genes commonly downregulated by VDOF1/2 appeared to preferentially overlap with xylem-related

genes (Figure 3.29). These results might be related to the observation that VDOF1 and VDOF2 influence lignin deposition in inflorescence stems (Figure 3.18 and 3.19; Table 3.1).

3.8 Changes in the expression patterns of lignin-related genes in *VDOF1ox, VDOF2ox*, and *vdof1 vdof2* plants

As mentioned above, the transcriptomic data analysis suggested that lignin-related genes are common targets of VDOF1 and VDOF2. To investigate this notion, I selected the lignin-related genes from Table 3.2 and 3.3 and investigated whether their promoter regions contained the Dof-binding core motif 5'-(A/T)AAAG-3'. As a result, I selected eight and five genes from the set of genes commonly upregulated and downregulated by VDOF1/2, respectively, to be tested by RT-PCR analysis (Figure 3.29). RT-PCR analysis of *VDOF1ox, VDOF2ox*, and *vdof1 vdof2* seedlings indicated that the expression patterns of some genes differed from the patterns detected in the transcriptomic data for the inducible overexpression lines (Figure 3.30), suggesting that the effects of transient versus constitutive overexpression of *VDOF1* and *VDOF2* might differ. However, the RT-PCR results clearly show that the overexpression and mutation of *VDOF1* and *VDOF2* influence the expression of lignin-related genes in seedlings.

Finally, I performed quantitative RT-PCR (qRT-PCR) analysis of lignin-related genes, including *CAD5* (which functions in monolignol biosynthesis) (Sibout *et al*., 2005), *MYB63* (encoding a positive transcriptional regulator of lignin biosynthesis) (Zhou *et al*., 2009), and *LAC7*, *LAC12*, *PER27,* and *PER53* (which function in lignin polymerization) (Zhao *et al*., 2015; Sibout *et al*., 2005; Østergaard *et al*., 2000) in the apical, middle, and basal portions of inflorescence stems from 40-day-old *VDOF1ox, VDOF2ox*, and *vdof1 vdof2* plants. The expression patterns of these genes were altered in *VDOF1ox, VDOF2ox*, and *vdof1 vdof2* stems compared to wild type (Figure 3.31). In accordance with the enhanced lignification phenotype of *vdof1 vdof2*, all genes examined except *PER27* were upregulated in *vdof1 vdof2*.

Interestingly, in *VDOF1ox* and *VDOF2ox*, the lignin-related genes were upregulated, although transient expression analysis suggested that VDOF1 and VDOF2 function alone have weak transcriptional repressors activity (Figure 3.4). All genes investigated possess a Dof-binding core motif in their promoters; thus, perhaps competitive occupancy by multiple Dof proteins is disturbed in *VDOF1ox* and *VDOF2ox*, as well as *vdof1 vdof2*, possibly resulting in changes in the expression patterns of these genes. Notably, *LAC7* and *PER27*, which were not expressed in wild-type stems, were expressed in *VDOF1ox*, *VDOF2ox*, and *vdof1 vdof2* (Figure 3.31). Thus, the transcriptomes of *VDOF1ox, VDOF2ox*, and *vdof1 vdof2* appear to exhibit widespread changes in inflorescence stems, likely in a developmental stage-dependent manner.

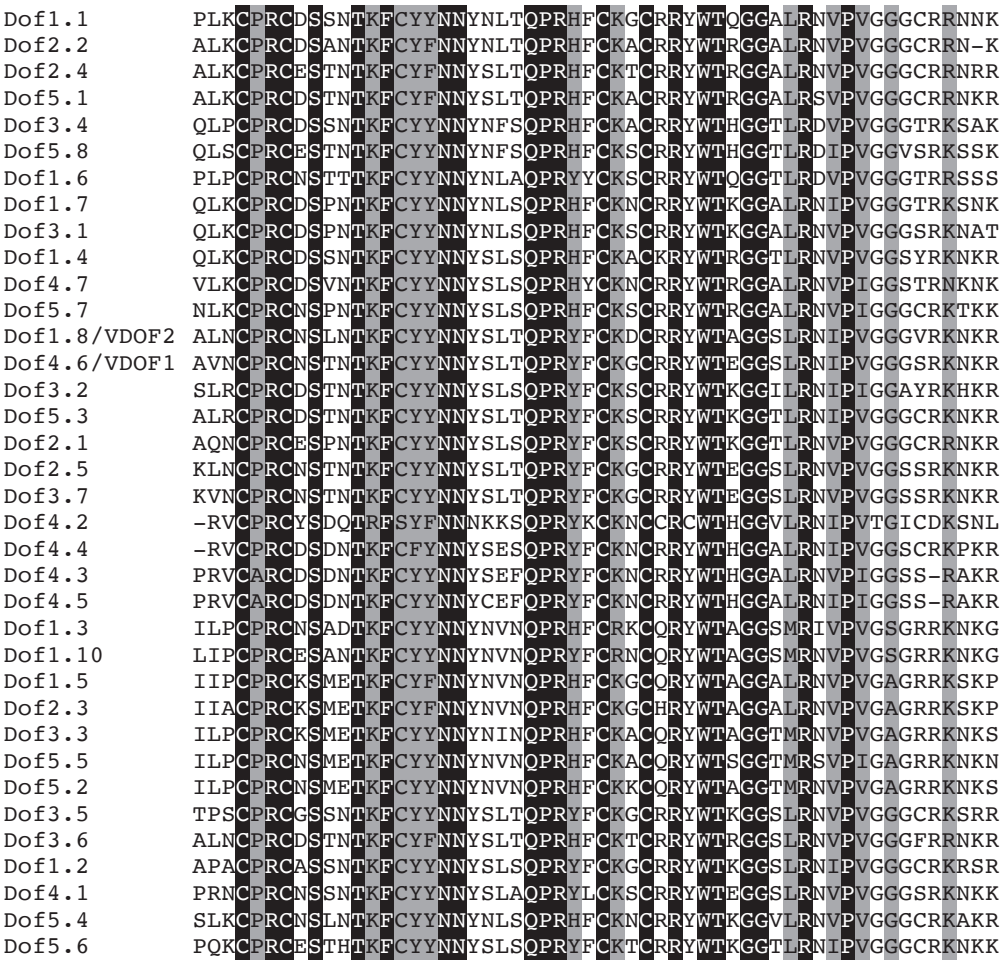

Figure 3.1 **Amino acid sequence alignment of the Dof domains in Arabidopsis Dof proteins.** The amino acid sequences of the Dof domains of Arabidopsis Dof proteins were aligned using ClustalW (http://www.genome.jp/tools-bin/clustalw). Identical and similar amino acids are highlighted in black and gray, respectively.

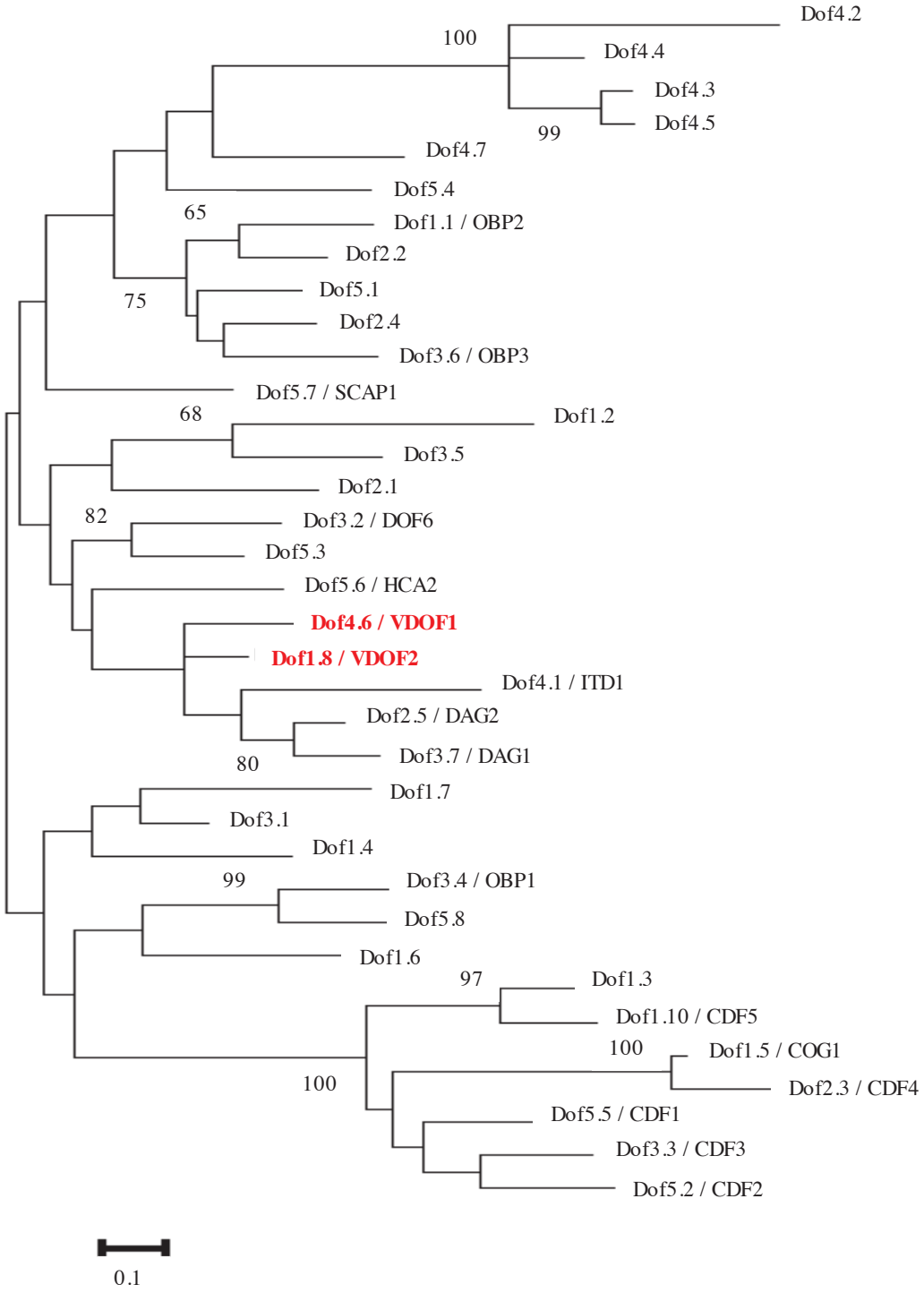

Figure 3.2 **Phylogenetic analysis of Arabidopsis Dof proteins.**
The amino acid sequences of Dof domains from 36 Arabidopsis Dof proteins were aligned using ClustalW, and a Maximum-Likelihood phylogenetic tree with 1,000 bootstraps was constructed based on the alignment. Bootstrapping values are indicated as percentages (when >60%) along the branches. The nomenclature for each gene is indicated, along with the original names used in publications. The two Dof proteins analyzed in this study are in red font. On the scale, 0.1 represents a 10% change in sequences.

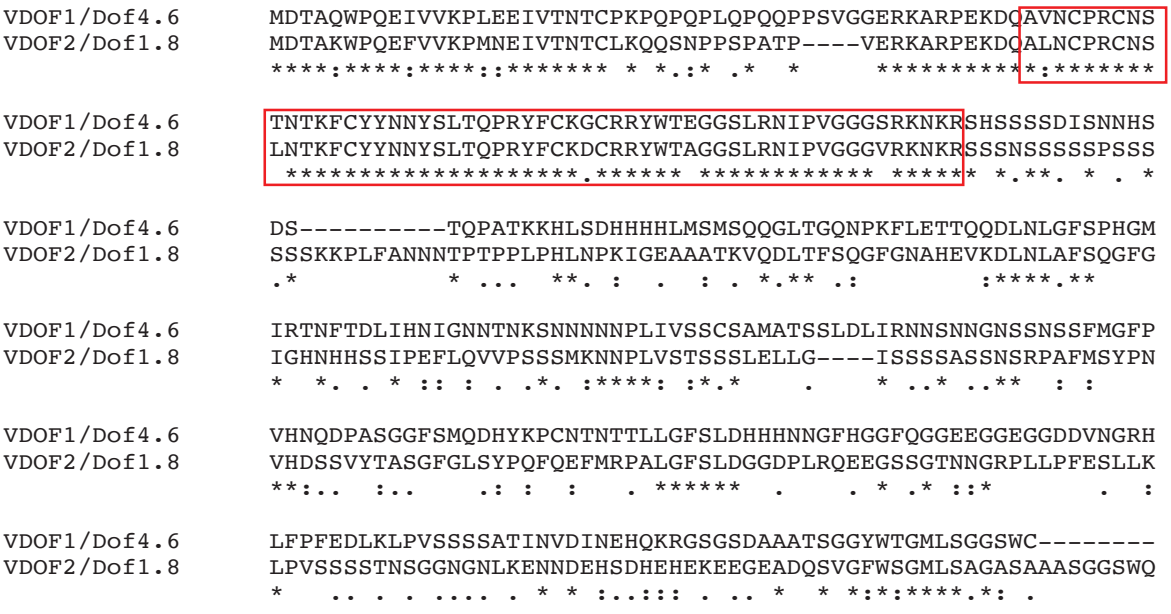

Figure 3.3 **Amino acid sequence alignment of VDOF1/Dof4.6 and VDOF2/Dof1.8.** Amino acid sequences of VDOF1/Dof4.6 and VDOF2/Dof1.8 were aligned using ClustalW (http://www.genome.jp/tools-bin/clustalw). Red boxes indicate the Dof domains. The degree of conservation is indicated by symbols below each position in the sequence alignment ('*', exact; ':', conserved substitution; and '.', semi-conserved substitution).

A)

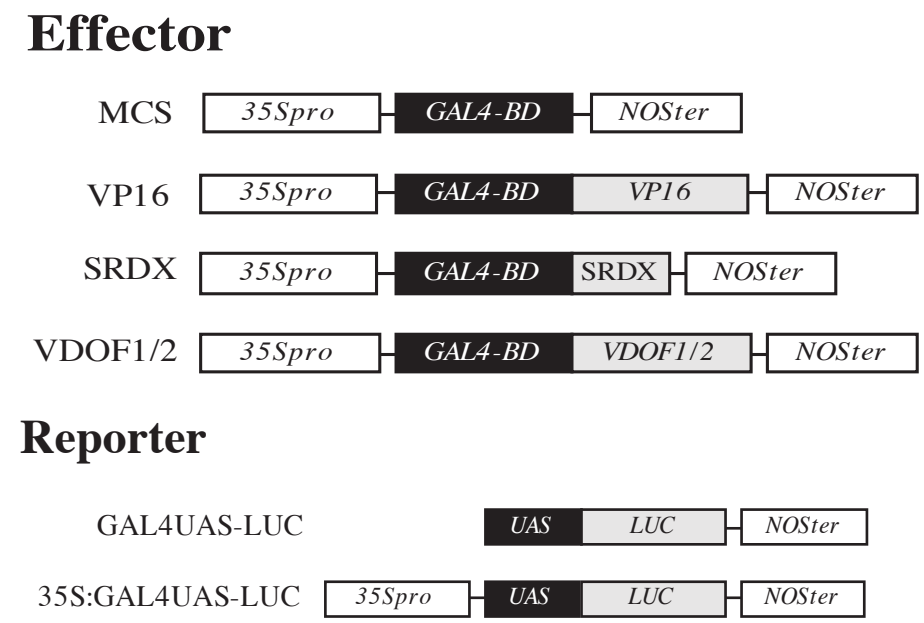

B)

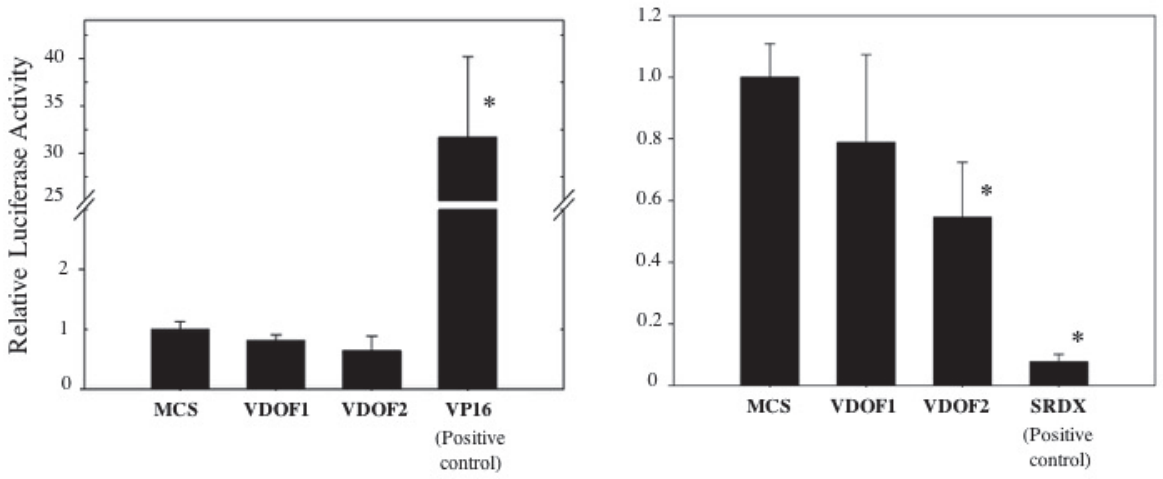

Figure 3.4 **Transcriptional activator/repressor domain activity of VDOF1 and VDOF2**.
(A) Schematic representation of the effector and reporter constructs used for the transient transcriptional activation/repression assay. GAL4-BD, GAL4 DNA-binding domain; NOSter, nopaline synthase terminator; 35Spro, CaMV 35S promoter.
(B) Transient transcriptional activator/repressor domain activity assay. The effector, reporter and reference plasmids were delivered to 14-day-old Arabidopsis leaves by particle bombardment, and luciferase activity was assayed. Data represent relative luciferase activity. Error bars, standard deviation of three biological replicates. '*', significant difference compared with the MCS control (p<0.05, Student's t-test).

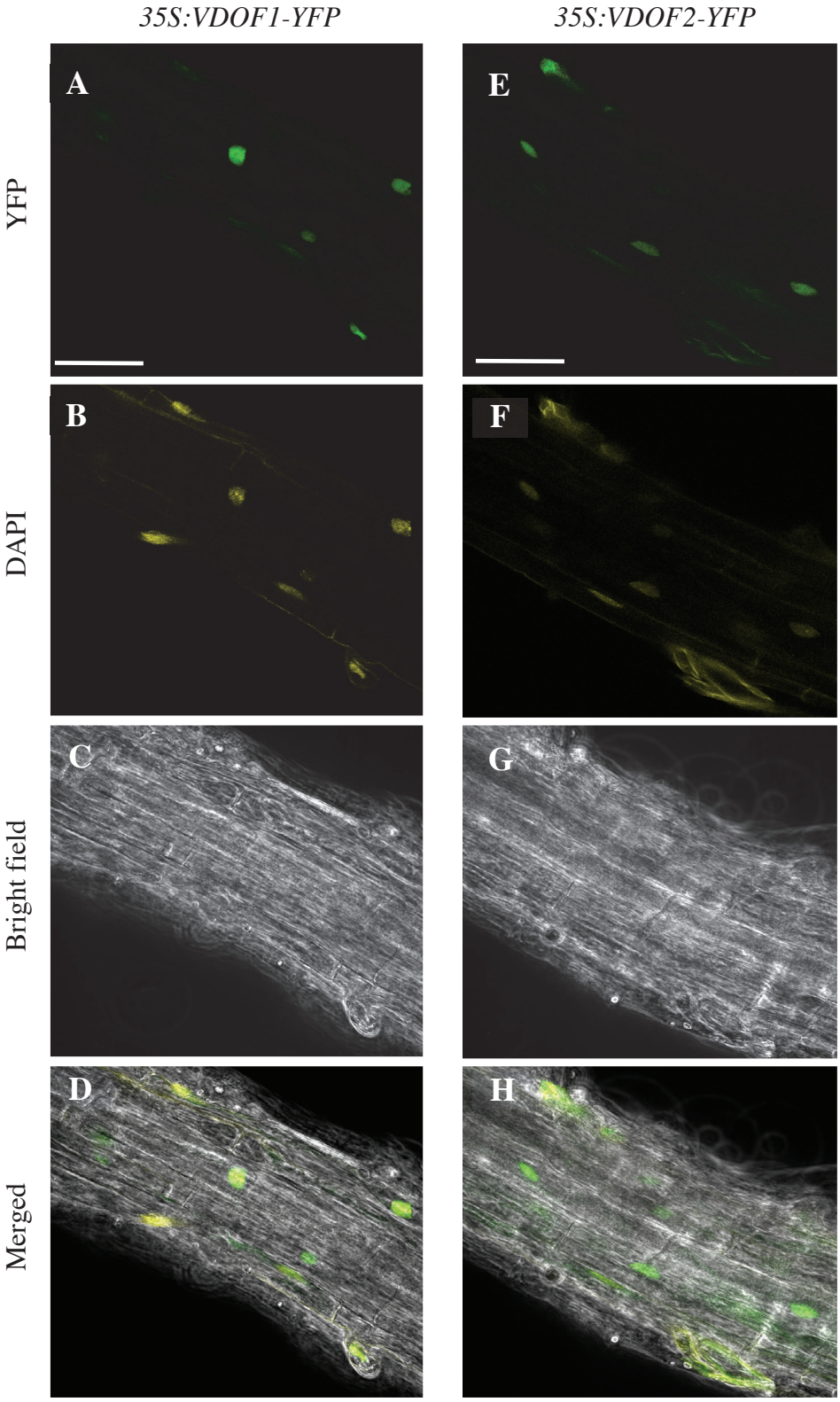

Figure 3.5 **VDOF1 and VDOF2 proteins are localized to the nucleus**.
Roots of 4-day-old transgenic Arabidopsis seedlings carrying the coding sequences of *VDOF1* (A–D) and *VDOF2* (E–H) fused with *YFP* under the control of the 35S promoter were stained with DAPI (B, F), and YFP and DAPI signals were observed. Scale bar, 50 μm.

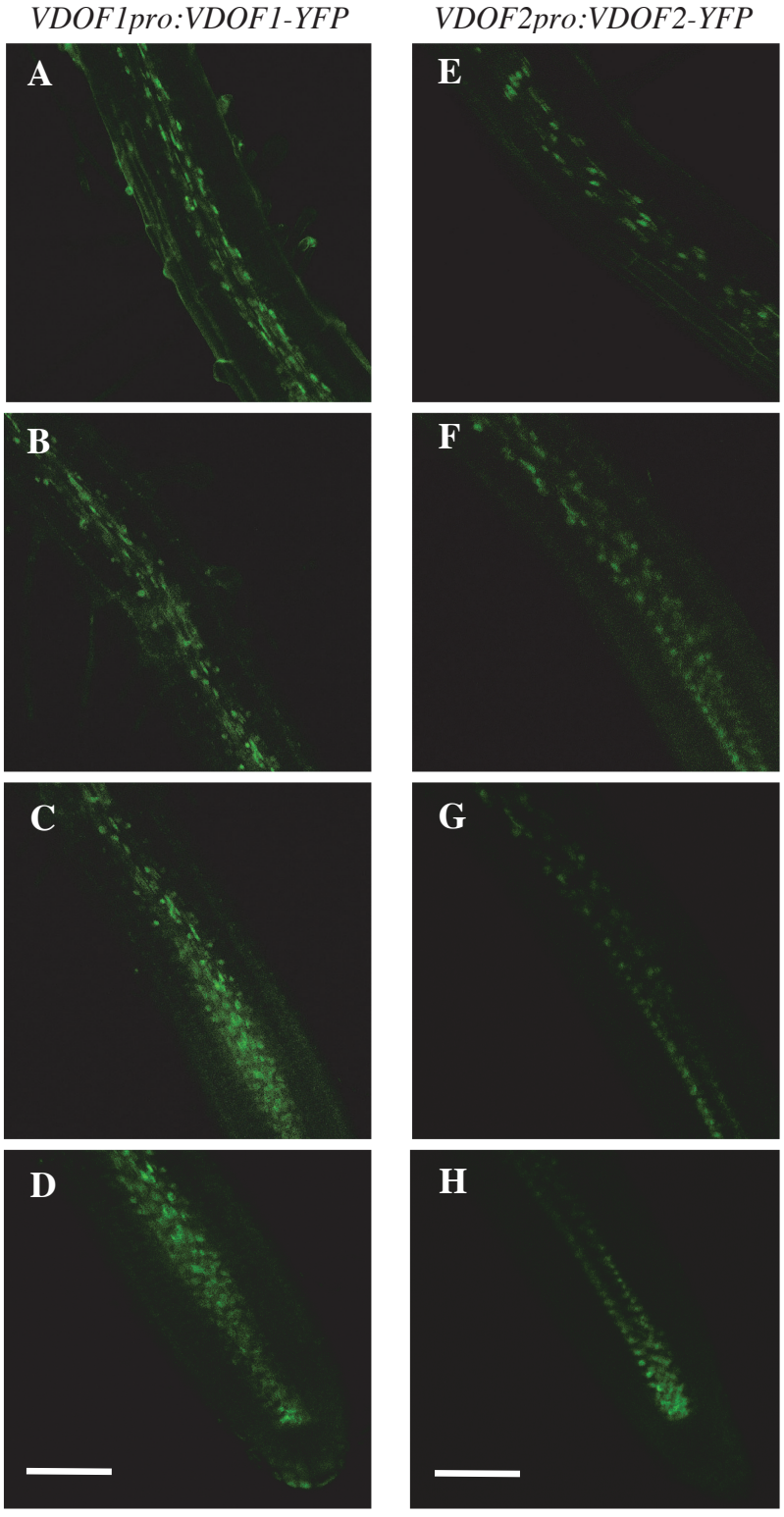

Figure 3.6 **VDOF1 and VDOF2 proteins tagged with YFP driven by their own promoters are localized to the nucleus in Arabidopsis roots.**
Subcellular localization of VDOF1 (A–D) and VDOF2 (E–H) proteins tagged with YFP driven by their own promoters in the roots of 7-day-old seedlings. Scale bars, 100 μm.

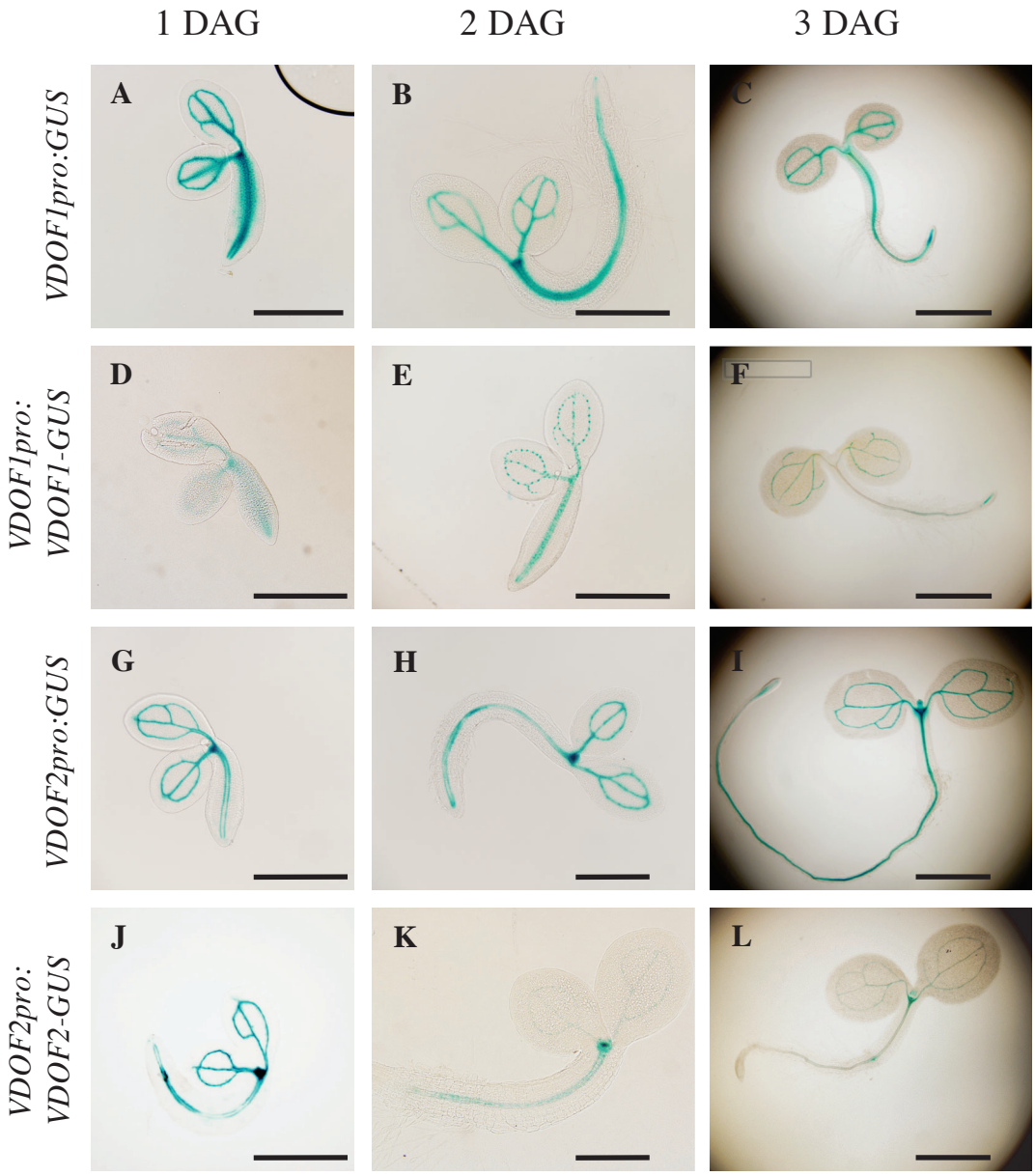

Figure 3.7 **GUS staining of transgenic Arabidopsis seedlings carrying vascular-related *VDOFpro:GUS* and *VDOFpro:VDOF CDS-GUS* gene constructs.**
GUS staining was carried out with transgenic Arabidopsis seedlings carrying *VDOF1pro:GUS* (A–C), *VDOF1pro:VDOF1 CDS-GUS* (D–F), *VDOF2pro:GUS* (G–I), and *VDOF2pro:VDOF2 CDS-GUS* (J–L) at 1 (A, D, G, J), 2 (B, E, H, K) and 3 (C, F, I, L) days after germination (DAG). Scale bars, 500 μm (A, B, D, E, G, H, J, K) or 1.0 mm (C, F, I, L).

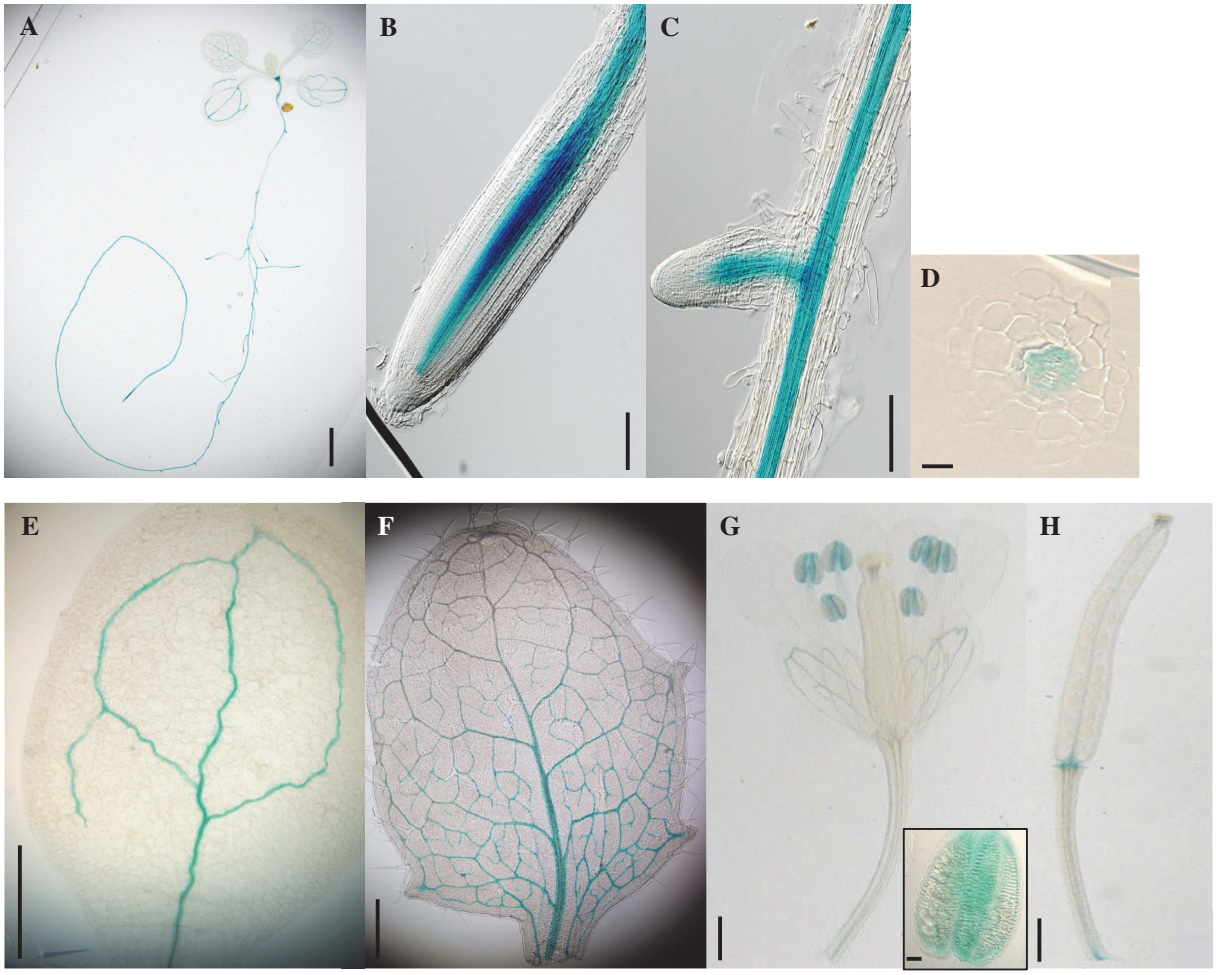

Figure 3.8 **GUS staining of transgenic Arabidopsis plants carrying vascular-related *VDOF1pro:GUS* gene constructs.**
GUS staining was carried out with 7- (A–F) and 40-day-old (G, H) transgenic Arabidopsis plants carrying *VDOF1pro:GUS*. Magnified images of a root (B, C), cotyledon (E), and leaf (F) from 7-day-old seedlings (A). A cross-section (D) was prepared from the root of a 7-day-old seedling after GUS staining. A flower and silique of a 40-day-old plant are shown in (G) and (H). Inset in G shows an anther. Scale bars: 1 mm (A, E, F, H), 500 μm (G), 200 μm (C), 100 μm (B), 50 μm (D and inset in G).

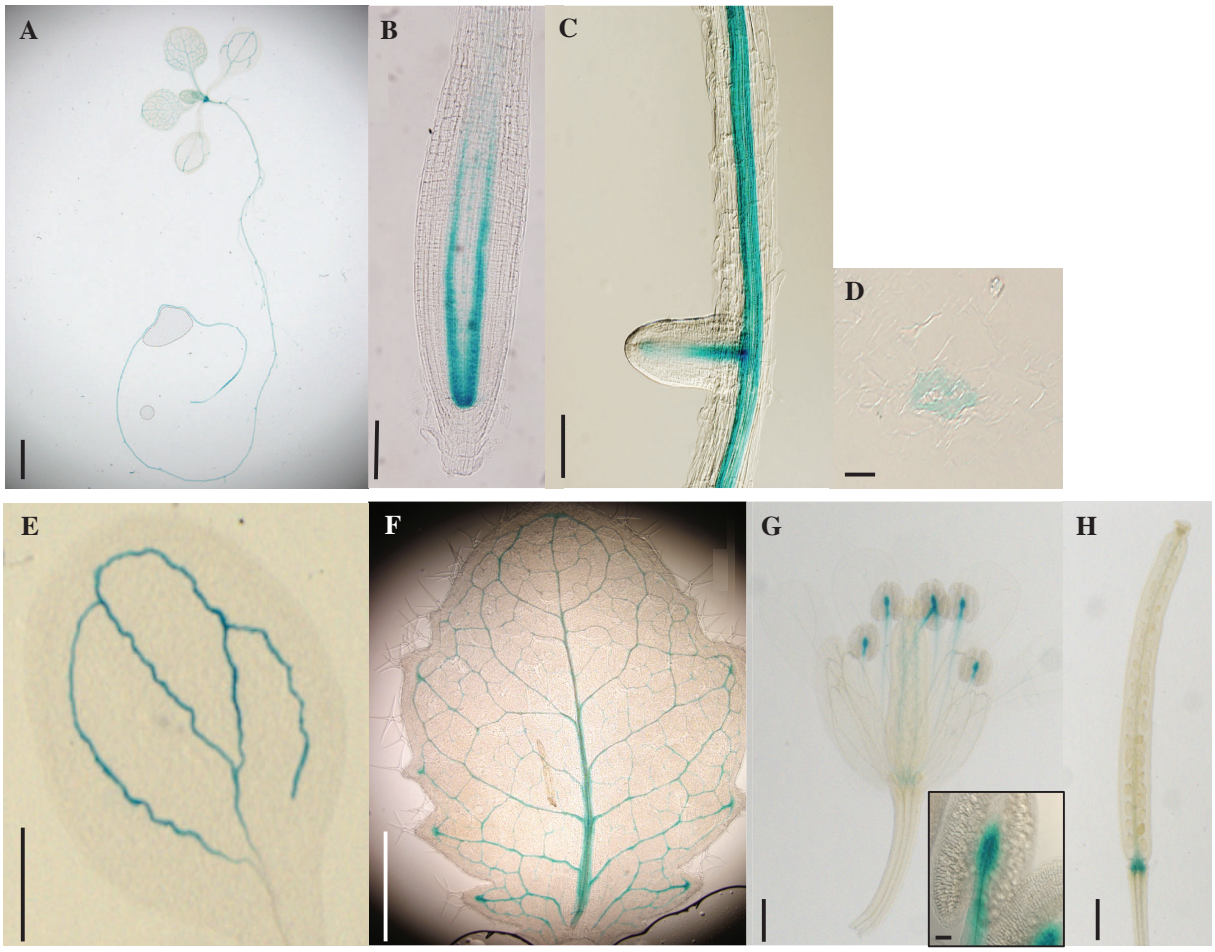

Figure 3.9 **GUS staining of transgenic Arabidopsis plants carrying vascular-related *VDOF2pro:GUS* gene constructs.**
GUS staining was carried out with 7- (A–F) and 40-day-old (G, H) transgenic Arabidopsis plants carrying *VDOF2pro:GUS*. Magnified images of a GUS-stained root (B–D), cotyledon (E) and leaf (F) from 7-day-old seedlings (A). A cross-section (D) was prepared from the root of a 7-day-old seedling after GUS staining. A flower and silique of a 40-day-old plant are shown in (G) and (H). Inset in G shows an anther. Scale bars: 1 mm (A, E, F, H), 500 μm (G), 200 μm (C), 100 μm (B), 50 μm (D and inset in G).

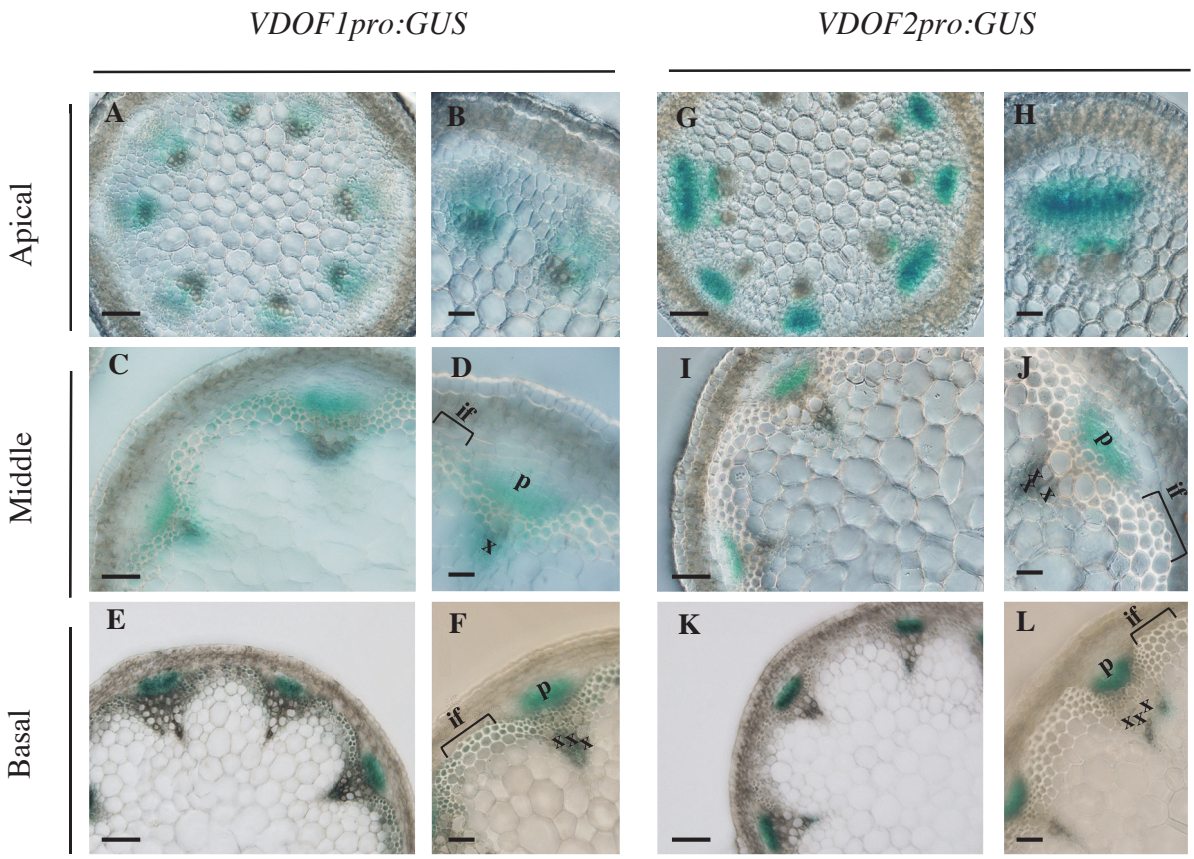

Figure 3.10 **GUS staining of inflorescence stems of transgenic Arabidopsis plants carrying vascular-related *VDOF1pro:GUS* and *VDOF2pro:GUS* gene constructs.**
Cross-sections were prepared from the apical, middle, and basal parts of inflorescence stems from 40-day-old transgenic plants carrying *VDOF1pro:GUS* (A–F) and *VDOF2pro:GUS* (G–L) after GUS staining. Scale bars, 100 μm (A, C, E, G, I, K) or 50 μm (B, D, F, H, J, L). p, phloem; x, xylem; and if, interfascicular fiber.

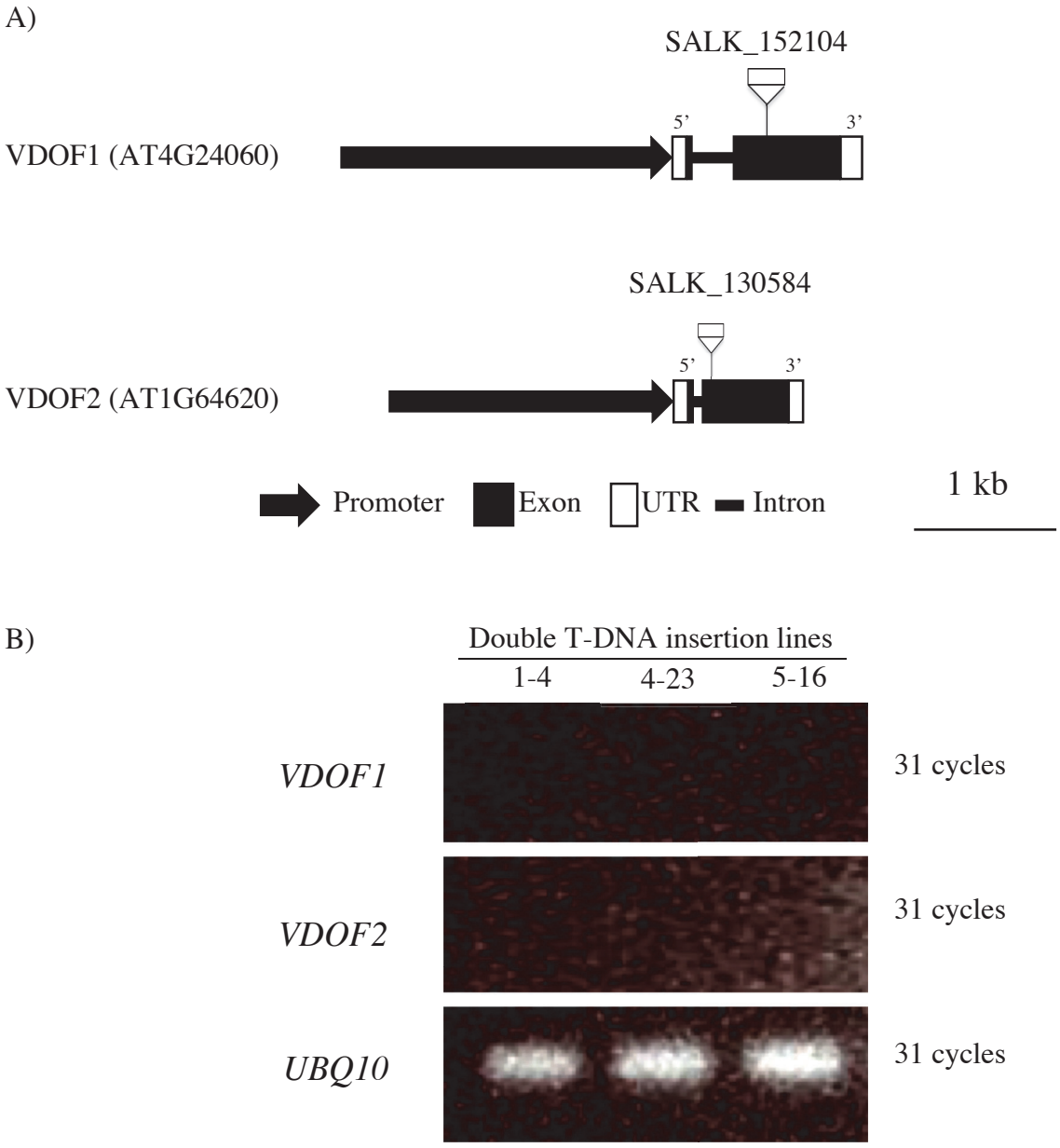

Figure 3.11 **T-DNA insertion lines of the *VDOF* genes analyzed in this study.**
(A) Schematic diagram of the structures of the *VDOF* genes and the positions of the T-DNA insertions in *vdof1* (SALK_152104) and *vdof2* (SALK_130584). Black and white boxes represent coding regions and untranslated regions, respectively. Black lines and arrows represent introns and promoter regions, respectively. Scale bar, 1 kb. (B) Semi-quantitative RT-PCR analysis of *VDOF1* and *VDOF2* expression in the double knock-out mutant homozygous lines. *UBQ10* gene was used as a loading control.

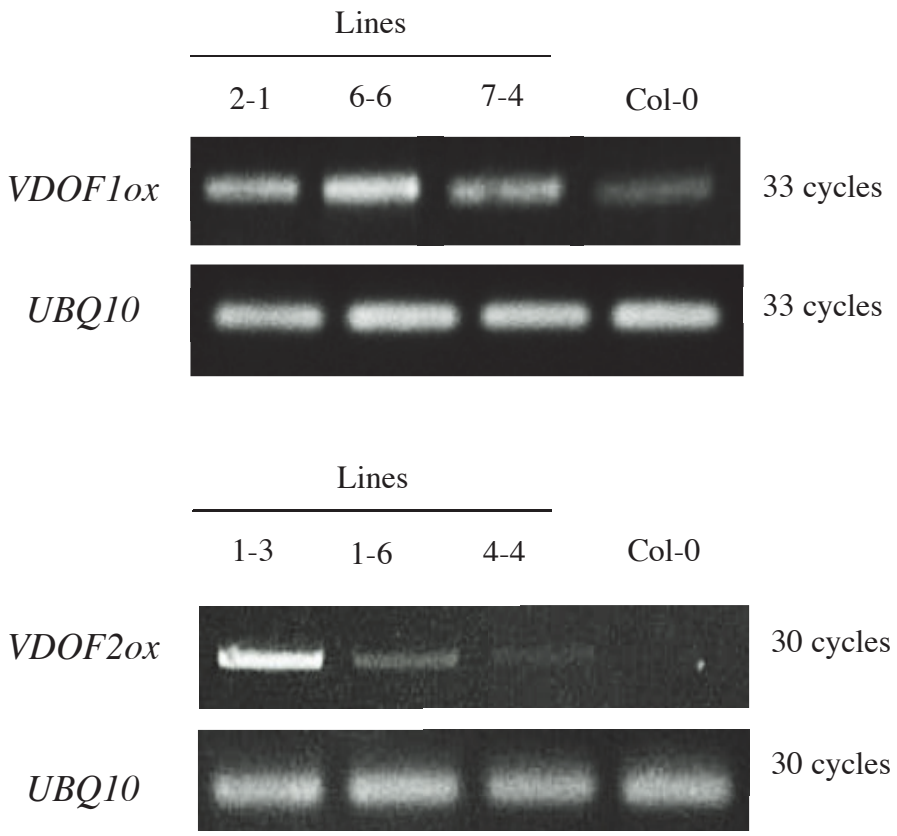

Figure 3.12 **Semi-quantitative RT-PCR analysis of the *VDOF1* and *VDOF2* overexpression lines.**
Total RNA extracted from 14-day-old seedlings of T3 homozygous lines of the *VDOF1* and *VDOF2* overexpressors (three independent lines each) was subjected to semi-quantitative RT-PCR analysis. *UBQ10* was used as a loading control.

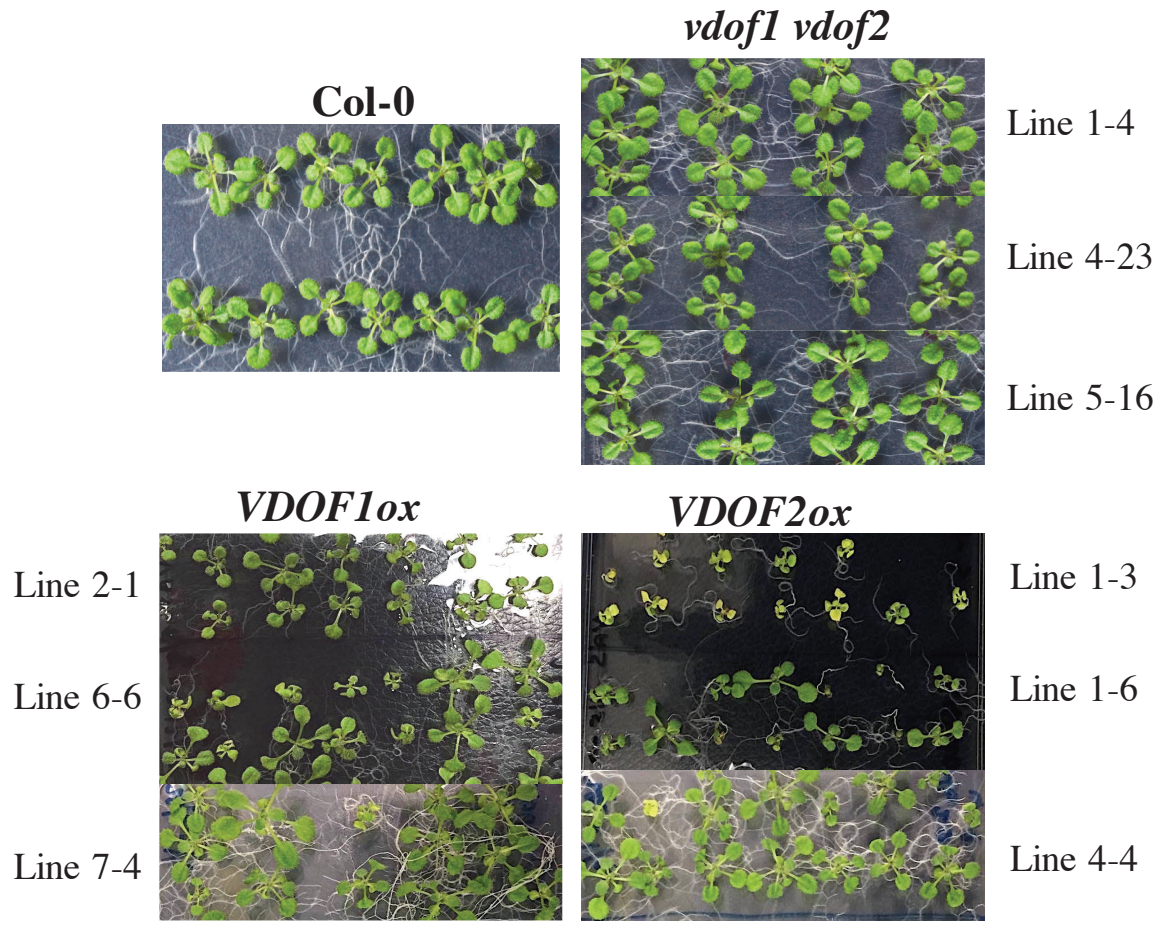

Figure 3.13 **Seedling growth in *vdof1 vdof2* double T-DNA insertion lines and the T3 generation of *VDOF1* and *VDOF2* overexpression lines.**
The double T-DNA insertion and the overexpressor lines (three lines each) were grown on agar plates for 14 days. Wild type (Col-0) was used as a control.

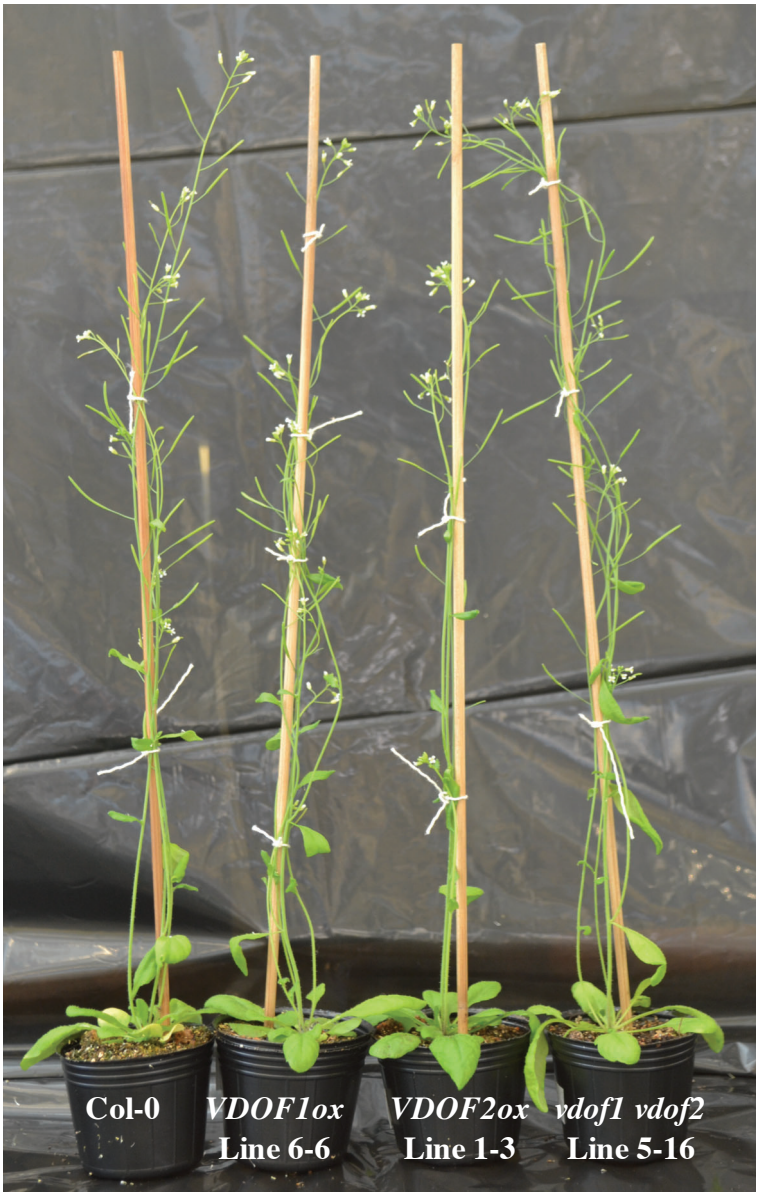

Figure 3.14 **Growth of Arabidopsis *VDOF1* and *VDOF2* overexpression lines and *vdof1 vdof2* double T-DNA insertion lines.**
The growth of 40-day-old Arabidopsis plants of the overexpressor and double T-DNA insertion lines was compared with that of the wild type (Col-0).

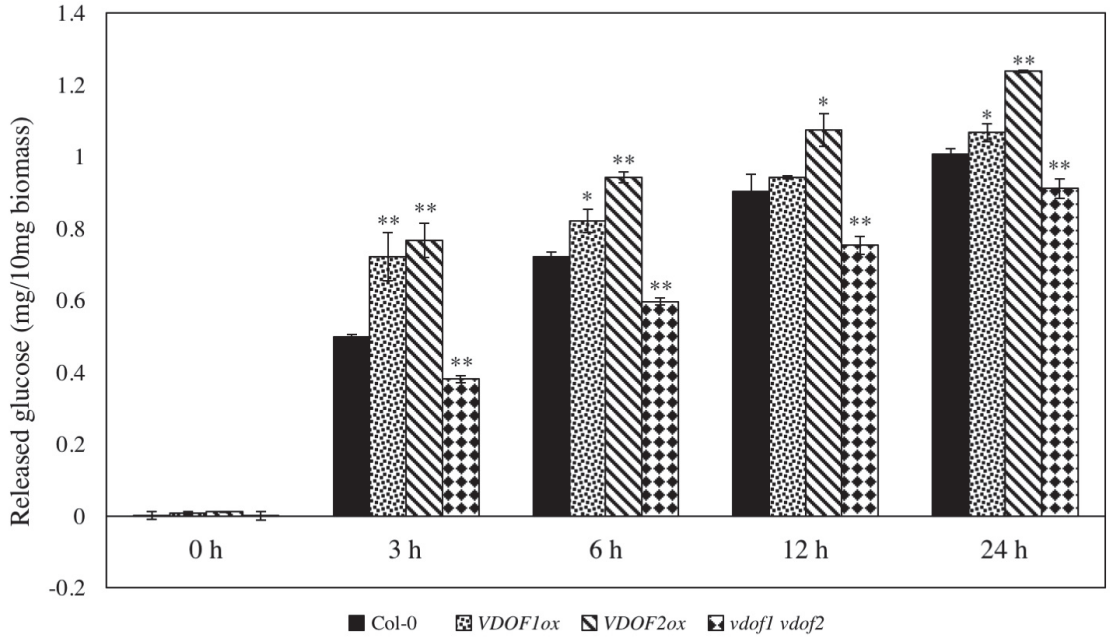

Figure 3.15 **Enzymatic saccharification efficiency of *VDOF1ox, VDOF2ox,* and *vdof1 vdof2* seedlings.**
An enzymatic saccharification assay was carried out on 14-day-old wild-type (Col-0), *VDOF1ox, VDOF2ox,* and *vdof1 vdof2* seedlings. The amounts of released glucose per 10 mg of biomass after 0, 3, 6, 12, and 24 h of enzyme treatment are shown (means ± SD, n=3). Asterisks indicate statistically significant differences compared with the wild type (*, *p*-value<0.05; **, *p*-value<0.01; Student's *t*-test).

A)

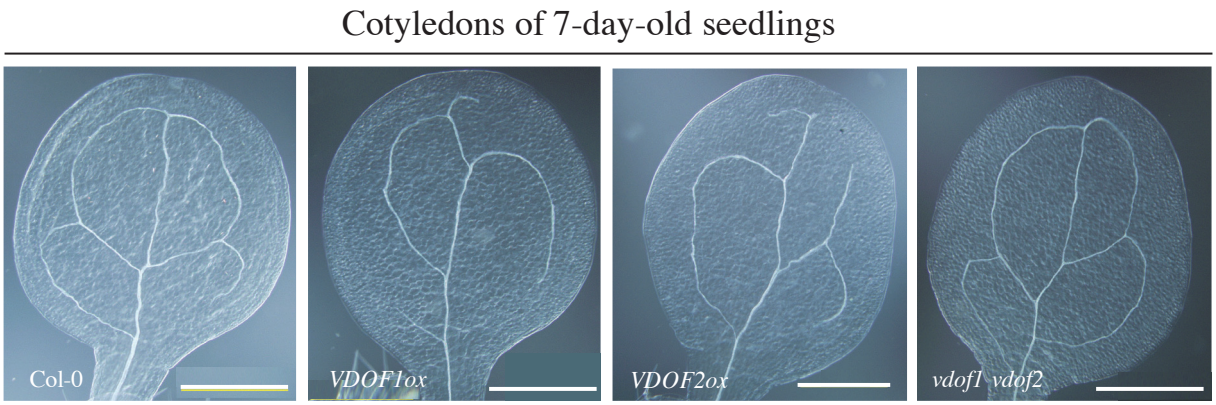

B)

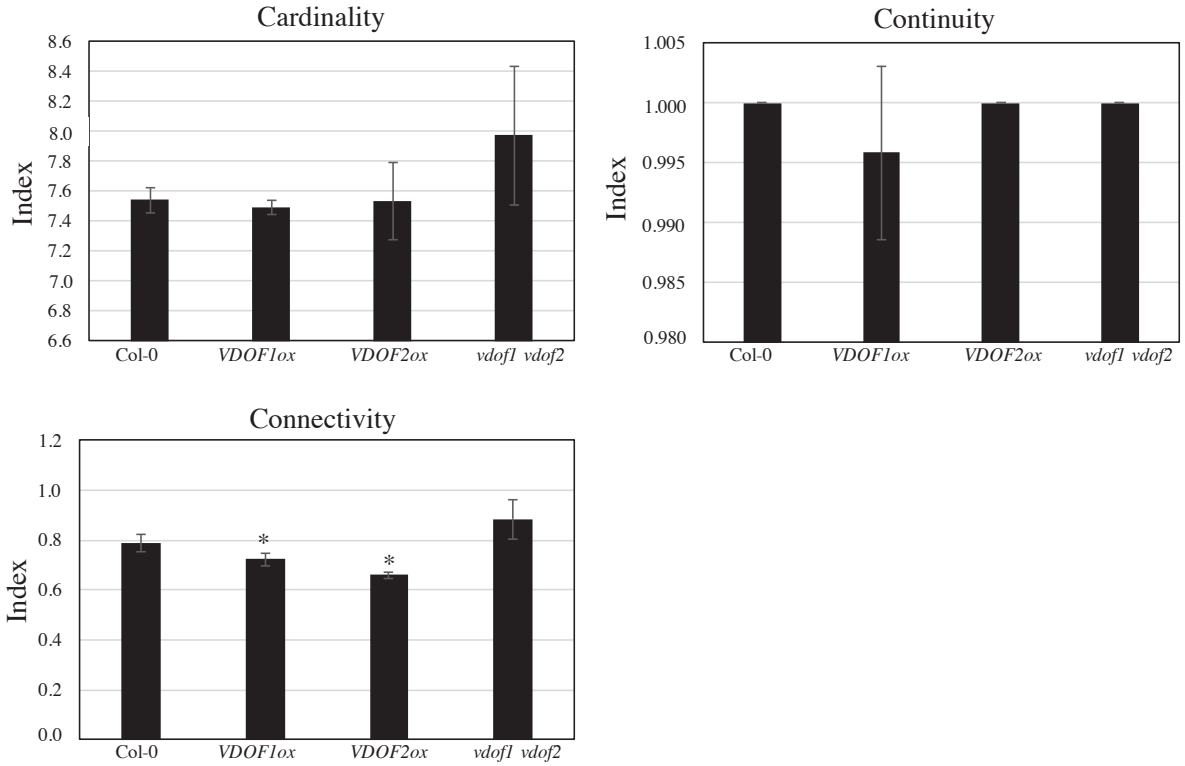

Figure 3.16 **Cotyledon vein patterns in *VDOF1* and *VDOF2* overexpressors and *vdof1 vdof2* double T-DNA insertion lines (7-day-old seedlings).**
(A) Vein patterns in cotyledons of 7-day-old seedlings from the wild type (Col-0), overexpressor lines, and *vdof1 vdof2* double T-DNA insertion lines. Scale bars, 500 μm.
(B) Cardinality, continuity, and connectivity of veins in cotyledons of *VDOF1* and *VDOF2* (T3 homozygous) overexpressors, *vdof1 vdof2* double T-DNA insertion lines, and the wild type (Col-0). Error bars, SD. For each genotype, 60 cotyledons were examined. '*', p-value<0.05 based on Student's t-test.

A)

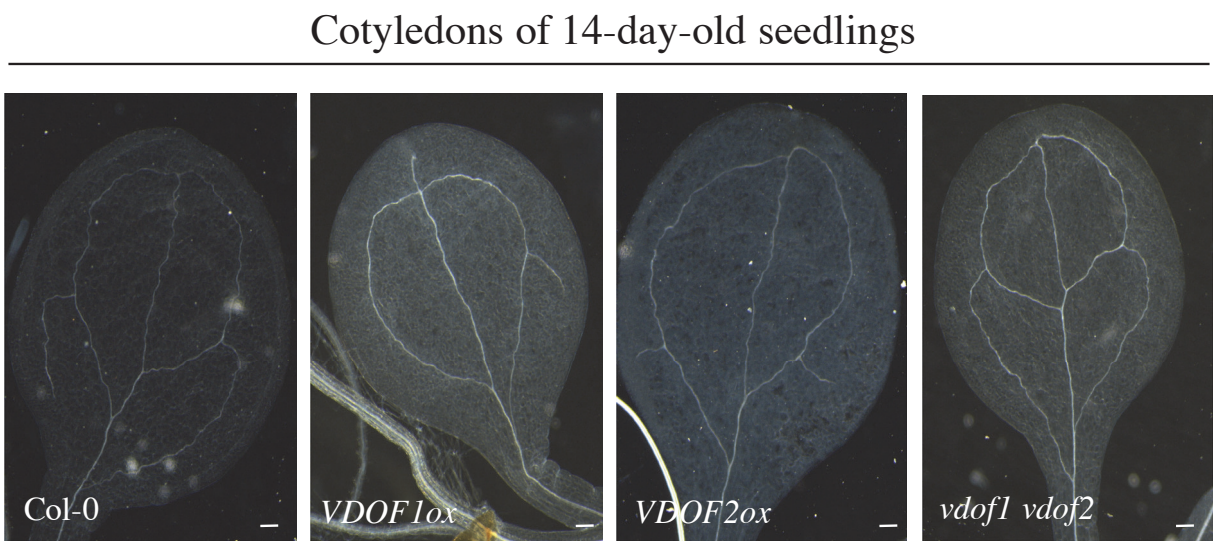

B)

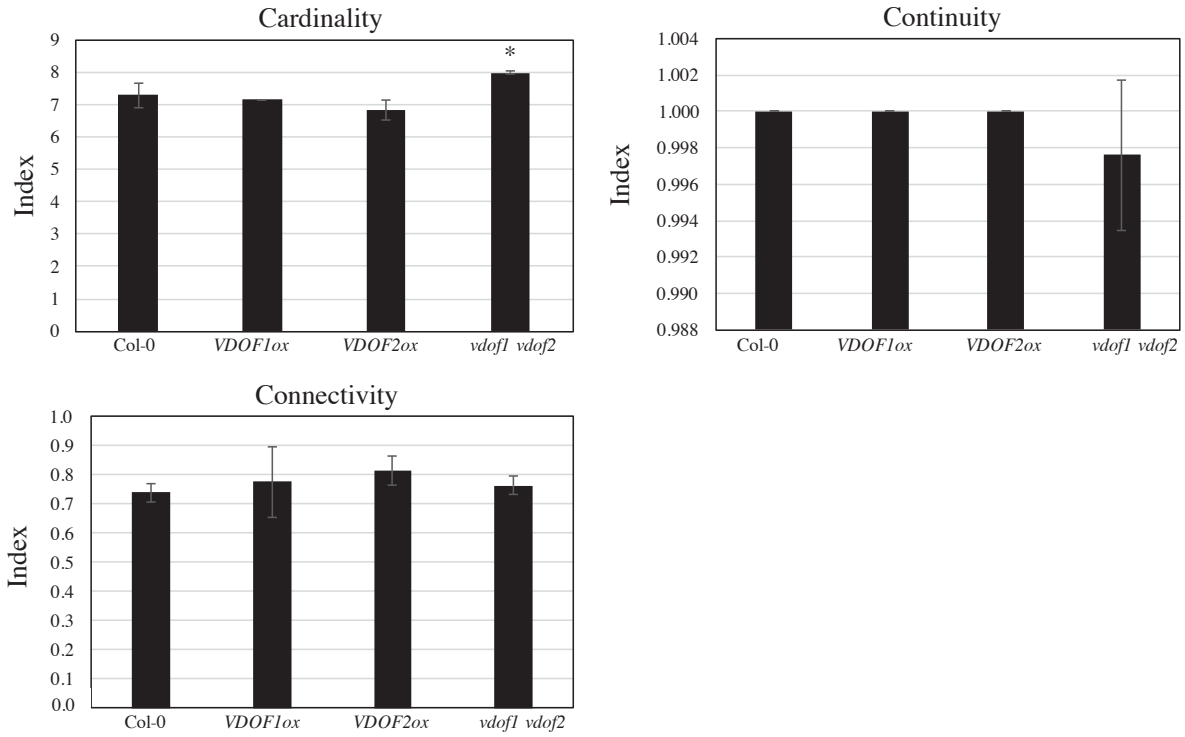

Figure 3.17 **Cotyledon vein patterns in *VDOF1* and *VDOF2* overexpressors and *vdof1 vdof2* double T-DNA insertion lines (14-day-old seedlings).**
(A) Vein patterns in cotyledons of 14-day-old seedlings of wild type (Col-0), overexpressor lines, and *vdof1 vdof2* double T-DNA insertion lines were observed. Scale bars, 200 μm.
(B) Cardinality, continuity, and connectivity of veins in cotyledons of *VDOF1* and *VDOF2* (T3 homozygous) overexpressors, *vdof1 vdof2* double T-DNA insertion lines, and the wild type (Col-0). Error bars, SD. For each genotype, 60 cotyledons were examined. '*', p-value<0.05 based on Student's t-test.

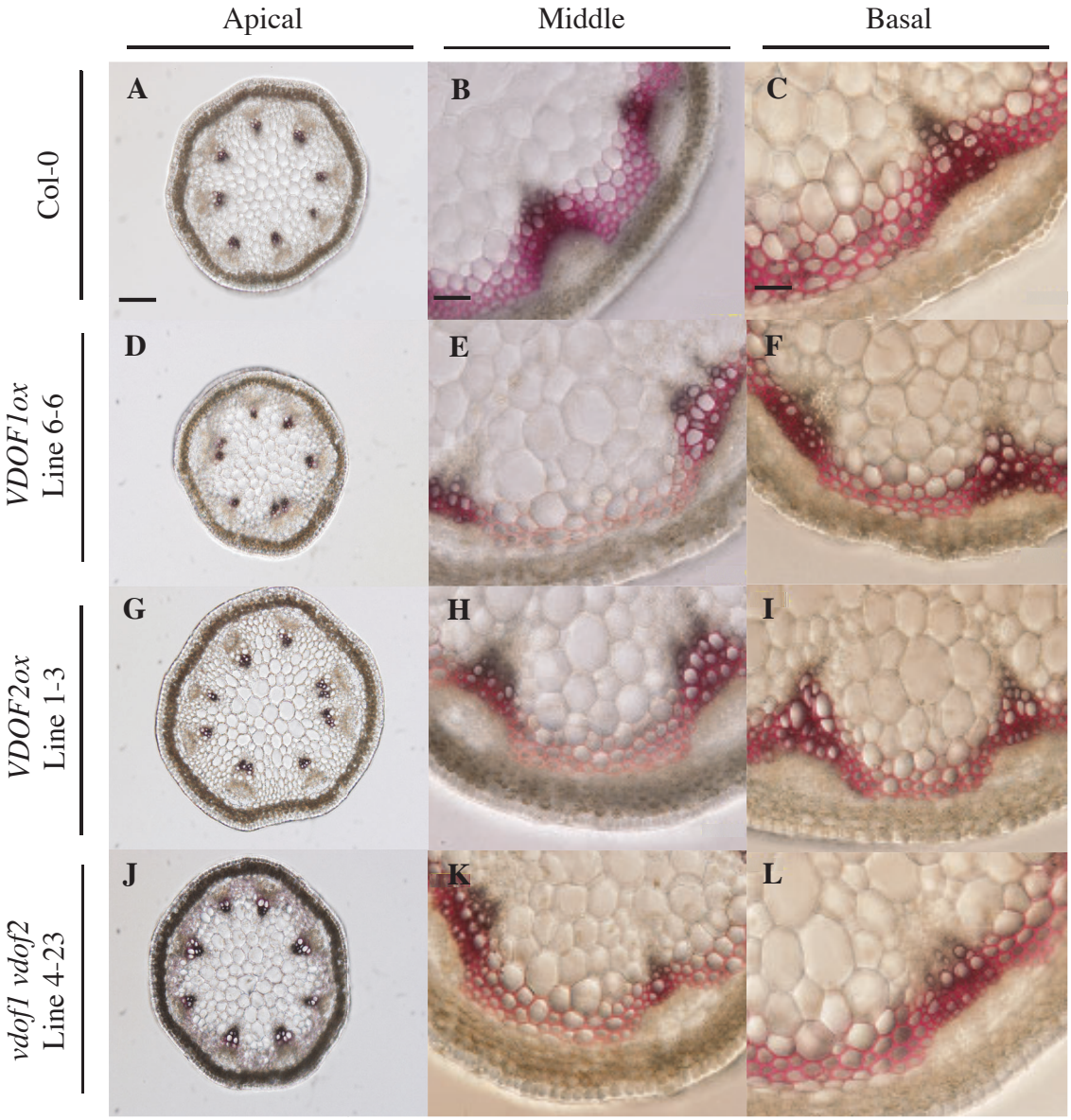

Figure 3.18 **Cross-sections of inflorescence stems stained with phloroglucinol:HCl.** Inflorescence stems of 40-day-old wild-type (Col-0, A–C), *VDOF1* (D–F) and *VDOF2* (G–I) overexpression lines, and double T-DNA insertion plants (J–L) were divided into three parts: apical (A, D, G, J), middle (B, E, H, K), and basal (C, F, I, L). Cross-sections prepared from these parts were counter-stained with phloroglucinol:HCl. Scale bar, 100 μm.

Table 3.1 **Thioglycolic acid quantification of total lignin content**

	Total lignin (%) ± SD	Mean total lignin content (%) ± SD	*p*-value
Col-0 1	17.53±0.39		
Col-0 2	16.44±0.61	16.98±0.55	
Col-0 3	16.96±0.88		
VDOF1ox Line 2-1	18.94±0.41		
VDOF1ox Line 6-6	19.01±0.46	19.21±0.41	0.0047
VDOF1ox Line 7-4	19.68±0.47		
VDOF2ox Line 1-3	15.88±0.18		
VDOF2ox Line 1-6	16.64±0.05	15.80±0.88	0.12
VDOF2ox Line 4-4	14.89±0.43		
vdof1 vdof2 Line 1-4	20.62±0.33		
vdof1 vdof2 Line 4-23	19.38±0.17	20.11±0.65	0.0031
vdof1 vdof2 Line 5-16	20.35±0.57		

SD indicates standard of three technical replicates or three biological replicates. The Student's *t*-test was performed and $p<0.01$ was considered significant.

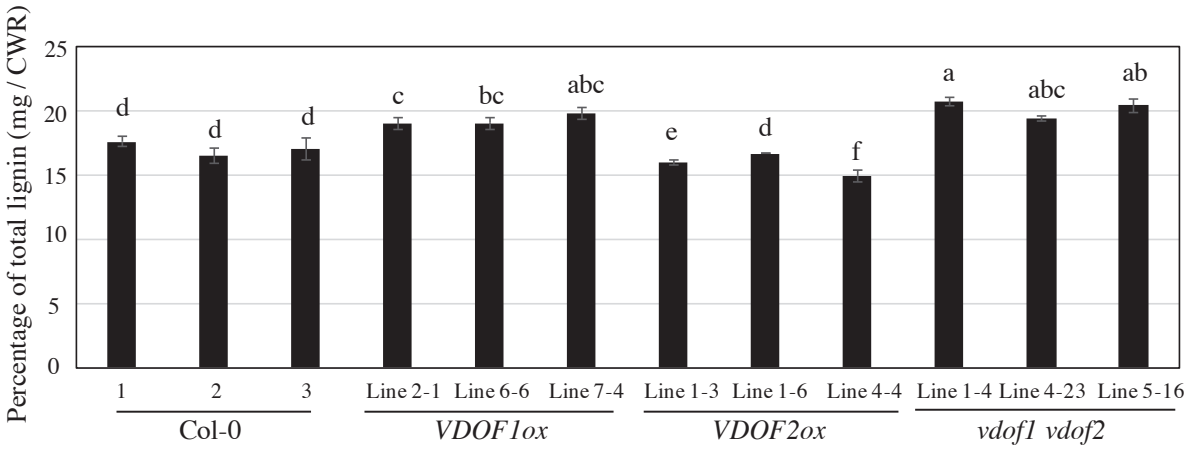

Figure 3.19 **Quantification of total lignin contents.**
Total lignin contents in cell wall residues of wild-type (Col-0), *VDOF1ox*, *VDOF2ox*, and *vdof1 vdof2* plants were determined by thioglycolic acid analysis. Means ± SD (n=3) are shown. Different letters indicate statistically significant differences (p<0.05, ANOVA followed by a post-hoc Tukey HSD test).

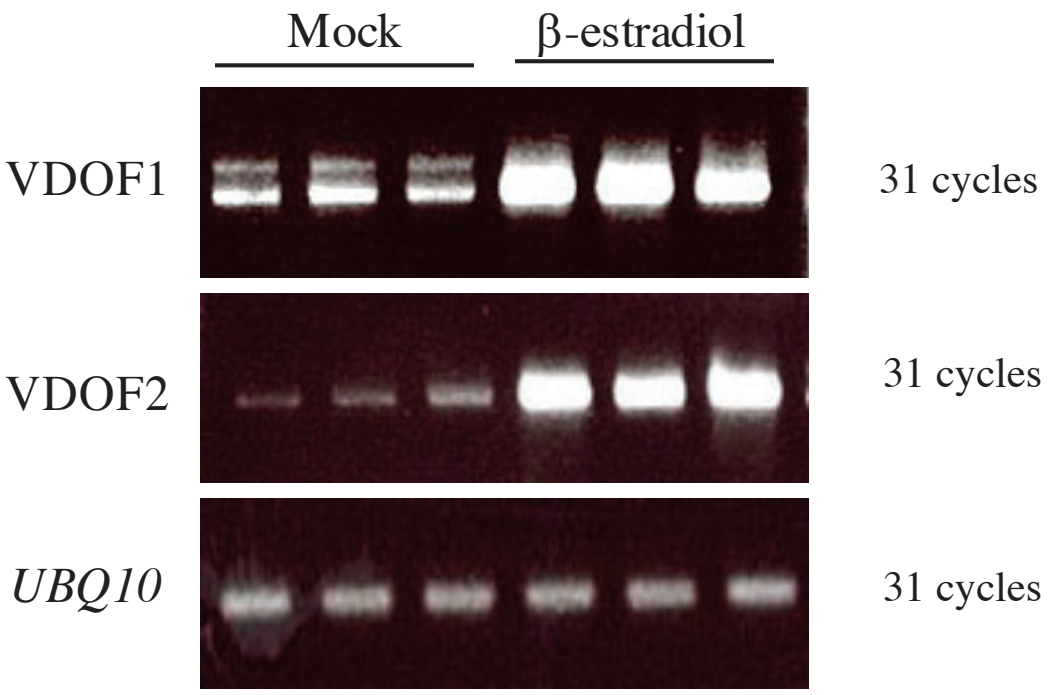

Figure 3.20 **Semi-quantitative RT-PCR analysis of inducible *VDOF1* and *VDOF2* lines.** Total RNA isolated from 7-day-old seedlings of three independent inducible *VDOF1* and *VDOF2* lines treated with DMSO (Mock) or β-estradiol for 24 hours was subjected to semi-quantitative RT-PCR analysis. *UBIQUITIN10* (*UBQ10*) was used as an internal control.

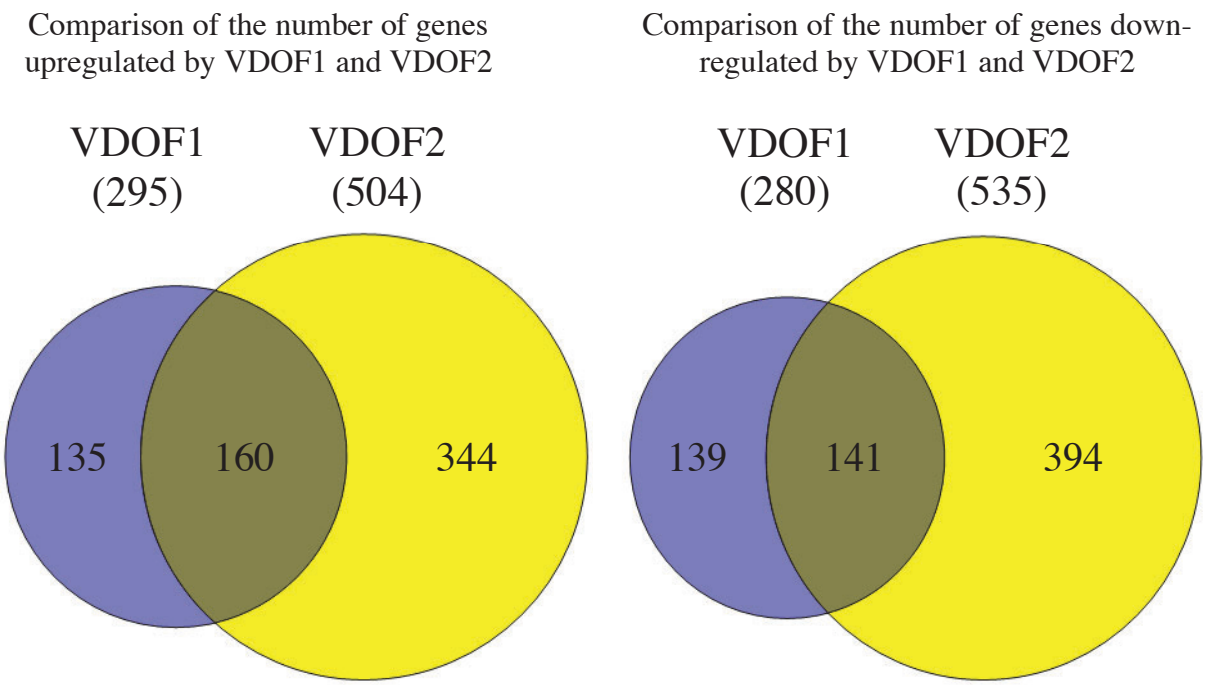

Figure 3.21 **Comparison of the number of genes significantly up- and downregulated by VDOF1 and VDOF2.**
The number of genes whose expression was significantly up- or downregulated by induced expression of *VDOF1* and *VDOF2* was compared. The number of genes in the overlapping region of each Venn diagram indicates the number of possible downstream genes of VDOF1 and VDOF2

Table 3.2 **List of genes up-regulated in both *VDOF1ox* and *VDOF2ox* plants.**

AGI Code	Description	*VDOF1ox* (Log2scale)	*VDOF2ox* (Log2scale)
AT5G24180	Lipase class 3-related protein	inf_p	inf_p
AT5G59390	XH/XS domain-containing protein	2.501	5.673
AT1G76470	NAD(P)-binding Rossmann-fold superfamily protein	4.044	5.365
AT1G03790	Zinc finger C-x8-C-x5-C-x3-H type family protein	2.828	4.465
AT5G05390	Laccase 12	2.240	4.456
AT1G64160	Disease resistance-responsive (dirigent-like protein) family protein	3.069	4.233
AT1G29860	WRKY DNA-binding protein 71	2.279	4.013
AT4G37780	Myb domain protein 87	2.925	3.783
AT5G05340	Peroxidase superfamily protein	1.869	3.762
AT1G68290	Endonuclease 2	2.583	3.387
AT2G19190	FLG22-induced receptor-like kinase 1	2.305	3.252
AT5G42830	HXXXD-type acyl-transferase family protein	1.330	3.058
AT5G58840	Subtilase family protein	2.866	3.033
AT4G36430	Peroxidase superfamily protein	1.895	2.917
AT1G20120	GDSL-like Lipase/Acylhydrolase superfamily protein	1.861	2.897
AT3G60140	Glycosyl hydrolase superfamily protein	1.715	2.562
AT1G19250	Flavin-dependent monooxygenase 1	1.874	2.417
AT1G73120	Unknown protein; FUNCTIONS IN: molecular_function unknown	1.521	2.356
AT4G28110	Myb domain protein 41	2.351	2.336
AT5G48400	Glutamate receptor family protein	1.528	2.243
AT1G50590	RmlC-like cupins superfamily protein	1.738	2.228
AT4G24040	Trehalase 1	1.012	2.165
AT5G06720	Peroxidase 2	1.248	2.151
AT3G14610	Cytochrome P450, family 72, subfamily A, polypeptide 7	1.178	2.077
AT4G18940	RNA ligase/cyclic nucleotide phosphodiesterase family protein	2.528	2.015
AT3G04960	Domain of unknown function (DUF3444)	1.576	1.984
AT1G79180	Myb domain protein 63	1.003	1.972
AT1G02470	Polyketide cyclase/dehydrase and lipid transport superfamily protein	1.276	1.971
AT2G18150	Peroxidase superfamily protein	0.973	1.876
AT2G02130	Low-molecular-weight cysteine-rich 68	1.240	1.857
AT1G06520	Glycerol-3-phosphate acyltransferase 1	1.016	1.844
AT1G14540	Peroxidase superfamily protein	1.160	1.835
AT1G02220	NAC domain containing protein 3	1.031	1.832
AT5G59845	Gibberellin-regulated family protein	1.859	1.789
AT1G10540	Nucleobase-ascorbate transporter 8	1.493	1.778
AT5G27000	Kinesin 4	0.690	1.774
AT3G23250	Myb domain protein 15	1.124	1.745
AT1G14130	2-oxoglutarate (2OG) and Fe(II)-dependent oxygenase superfamily protein	1.236	1.713
AT1G77380	Amino acid permease 3	0.891	1.701

AT3G05190	D-aminoacid aminotransferase-like PLP-dependent enzymes superfamily protein	1.239	1.695
AT2G27402	BEST Arabidopsis thaliana protein match is: plastid transcriptionally active 18 (TAIR:AT2G32180.1	0.675	1.671
AT4G15370	Baruol synthase 1	1.585	1.657
AT1G05820	SIGNAL PEPTIDE PEPTIDASE-LIKE 5	1.321	1.653
AT4G23690	Disease resistance-responsive (dirigent-like protein) family protein	0.607	1.637
AT1G80820	Cinnamoyl coa reductase	0.833	1.609
AT3G45010	Serine carboxypeptidase-like 48	0.997	1.532
AT1G50090	D-aminoacid aminotransferase-like PLP-dependent enzymes superfamily protein	1.832	1.510
AT5G40590	Cysteine/Histidine-rich C1 domain family protein	1.681	1.486
AT2G17040	NAC domain containing protein 36	1.652	1.481
AT1G08050	Zinc finger (C3HC4-type RING finger) family protein	1.118	1.452
AT1G08630	Threonine aldolase 1	0.544	1.440
AT4G39830	Cupredoxin superfamily protein	0.945	1.434
AT2G36780	UDP-Glycosyltransferase superfamily protein	1.307	1.429
AT5G61430	NAC domain containing protein 100	1.215	1.408
AT2G02820	Myb domain protein 88	0.580	1.368
AT1G69520	S-adenosyl-L-methionine-dependent methyltransferases superfamily protein	0.968	1.351
AT1G63440	Heavy metal atpase 5	0.598	1.321
AT4G12290	Copper amine oxidase family protein	0.915	1.319
AT4G34230	Cinnamyl alcohol dehydrogenase 5	0.967	1.317
AT1G17180	Glutathione S-transferase TAU 25	0.860	1.304
AT1G11730	Galactosyltransferase family protein	1.292	1.291
AT4G13660	Pinoresinol reductase 2	0.599	1.286
AT4G18170	WRKY DNA-binding protein 28	0.745	1.278
AT2G43120	RmlC-like cupins superfamily protein	1.206	1.273
AT3G17950	Unknown protein; FUNCTIONS IN: molecular_function unknown; INVOLVED IN: biological_process unknown	0.793	1.268
AT1G75750	GAST1 protein homolog 1	0.616	1.256
AT3G14990	Class I glutamine amidotransferase-like superfamily protein	0.722	1.252
AT5G11300	Mitotic-like cyclin 3B from Arabidopsis	0.724	1.213
AT1G17170	Glutathione S-transferase TAU 24	1.436	1.212
AT1G69880	Thioredoxin H-type 8	1.625	1.207
AT1G63180	UDP-D-glucose/UDP-D-galactose 4-epimerase 3	0.763	1.206
AT5G54230	Myb domain protein 49	0.998	1.175
AT1G72810	Pyridoxal-5'-phosphate-dependent enzyme family protein	0.791	1.156
AT1G49570	Peroxidase superfamily protein	1.130	1.148
AT2G28590	Protein kinase superfamily protein	0.981	1.129
AT2G18230	pyrophosphorylase 2	0.835	1.118
AT1G02360	Chitinase family protein	0.765	1.097
AT1G67080	Abscisic acid (aba)-deficient 4	0.755	1.062
AT1G78380	Glutathione S-transferase TAU 19	0.778	1.033
AT5G26340	Major facilitator superfamily protein	1.044	1.025
AT4G19700	SBP (S-ribonuclease binding protein) family protein	0.554	1.002

AT1G75040	pathogenesis-related gene 5	1.619	0.989
AT5G40780	Lysine histidine transporter 1	0.501	0.989
AT4G36988	conserved peptide upstream open reading frame 49	0.545	0.985
AT3G13650	Disease resistance-responsive (dirigent-like protein) family protein	0.852	0.981
AT1G29820	Magnesium transporter CorA-like family protein	0.611	0.972
AT4G34135	UDP-glucosyltransferase 73B2	0.837	0.957
AT1G30700	FAD-binding Berberine family protein	0.795	0.953
AT1G73680	Alpha dioxygenase	0.873	0.947
AT2G45290	Transketolase	0.513	0.939
AT3G46280	Protein kinase-related	0.694	0.937
AT4G12490	Bifunctional inhibitor/lipid-transfer protein/seed storage 2S albumin superfamily protein	1.573	0.926
AT1G55210	Disease resistance-responsive (dirigent-like protein) family protein	0.453	0.924
AT1G48600	S-adenosyl-L-methionine-dependent methyltransferases superfamily protein	0.939	0.910
AT2G23150	Natural resistance-associated macrophage protein 3	1.035	0.900
AT3G02770	Ribonuclease E inhibitor RraA/Dimethylmenaquinone methyltransferase	0.548	0.885
AT4G30860	SET domain group 4	0.541	0.883
AT1G60730	NAD(P)-linked oxidoreductase superfamily protein	1.020	0.875
AT2G44450	Beta glucosidase 15	0.535	0.872
AT5G54370	Late embryogenesis abundant (LEA) protein-related	0.646	0.869
AT3G20380	TRAF-like family protein	0.856	0.868
AT1G77330	2-oxoglutarate (2OG) and Fe(II)-dependent oxygenase superfamily protein	0.919	0.867
AT1G47395	Unknown protein; FUNCTIONS IN: molecular_function unknown; INVOLVED IN: biological_process unknown	1.147	0.862
AT5G24280	gamma-irradiation and mitomycin c induced 1	0.700	0.860
AT5G39610	NAC domain containing protein 6	0.632	0.858
AT4G30630	Unknown protein; BEST Arabidopsis thaliana protein match is: unknown protein (TAIR:AT5G57910.1	0.589	0.855
AT1G57590	Pectinacetylesterase family protein	0.965	0.847
AT5G37540	Eukaryotic aspartyl protease family protein	0.702	0.845
AT1G01010	NAC domain containing protein 1	0.702	0.831
AT4G20170	Domain of unknown function (DUF23)	0.579	0.831
AT5G48310	Unknown protein; BEST Arabidopsis thaliana protein match is: unknown protein (TAIR:AT4G24610.1)	0.436	0.827
AT5G13330	related to AP2 6l	0.641	0.809
AT5G59050	Unknown protein; BEST Arabidopsis thaliana protein match is: unknown protein (TAIR:AT3G54000.1	0.807	0.807
AT5G67160	HXXXD-type acyl-transferase family protein	0.763	0.789
AT3G56970	Basic helix-loop-helix (bHLH) DNA-binding superfamily protein	0.779	0.783
AT1G17960	Threonyl-tRNA synthetase	1.242	0.783
AT1G07750	RmlC-like cupins superfamily protein	0.636	0.776
AT1G12030	Protein of unknown function (DUF506)	0.836	0.755
AT1G30760	FAD-binding Berberine family protein	0.675	0.744
AT1G47400	unknown protein; BEST Arabidopsis thaliana protein match is: unknown protein (TAIR:AT1G47395.1	0.940	0.740
AT2G41240	basic helix-loop-helix protein 100	0.703	0.739
AT2G29420	Glutathione S-transferase tau 7	0.649	0.734

AT4G06744	Leucine-rich repeat (LRR) family protein	0.487	0.720
AT5G51550	EXORDIUM like 3	0.453	0.712
AT1G07590	Tetratricopeptide repeat (TPR)-like superfamily protein	0.533	0.699
AT5G21105	Plant L-ascorbate oxidase	0.431	0.696
AT3G11340	UDP-Glycosyltransferase superfamily protein	0.599	0.685
AT4G03400	Auxin-responsive GH3 family protein	0.651	0.663
AT1G51420	Sucrose-phosphatase 1	0.896	0.653
AT5G13790	AGAMOUS-like 15	0.855	0.648
AT1G70580	Alanine-2-oxoglutarate aminotransferase 2	0.457	0.646
AT2G41380	S-adenosyl-L-methionine-dependent methyltransferases superfamily protein	0.733	0.644
AT5G02490	Heat shock protein 70 (Hsp 70) family protein	0.623	0.641
AT5G24660	response to low sulfur 2	0.690	0.633
AT3G01970	WRKY DNA-binding protein 45	0.746	0.632
AT3G49360	6-phosphogluconolactonase 2	0.606	0.629
AT5G57887	Unknown protein; FUNCTIONS IN: molecular_function unknown; INVOLVED IN: biological_process unknown	0.532	0.624
AT3G15530	S-adenosyl-L-methionine-dependent methyltransferases superfamily protein	0.538	0.624
AT2G43290	Calcium-binding EF-hand family protein	0.481	0.622
AT3G14690	Cytochrome P450, family 72, subfamily A, polypeptide 15	0.583	0.619
AT3G27060	Ferritin/ribonucleotide reductase-like family protein	0.576	0.611
AT1G71040	Cupredoxin superfamily protein	0.586	0.610
AT2G35635	Ubiquitin 7	0.429	0.602
AT3G27870	ATPase E1-E2 type family protein / haloacid dehalogenase-like hydrolase family protein	0.649	0.592
AT3G52340	sucrose-6F-phosphate phosphohydrolase 2	0.446	0.581
AT1G17860	Kunitz family trypsin and protease inhibitor protein	0.511	0.578
AT3G11280	Duplicated homeodomain-like superfamily protein	0.502	0.569
AT1G13990	Unknown protein; FUNCTIONS IN: molecular_function unknown; INVOLVED IN: biological_process unknown	0.603	0.562
AT5G46280	Minichromosome maintenance (MCM2/3/5) family protein	0.457	0.547
AT3G04520	Threonine aldolase 2	0.532	0.540
AT4G05390	root FNR 1	0.560	0.535
AT3G55130	white-brown complex homolog 19	0.825	0.529
AT4G13180	NAD(P)-binding Rossmann-fold superfamily protein	0.643	0.528
AT1G13280	Allene oxide cyclase 4	0.498	0.514
AT3G49780	phytosulfokine 4 precursor	0.497	0.508
AT1G33560	Disease resistance protein (CC-NBS-LRR class) family	0.692	0.499
AT5G04150	Basic helix-loop-helix (bHLH) DNA-binding superfamily protein	0.825	0.492
AT2G30766	Unknown protein; FUNCTIONS IN: molecular_function unknown; INVOLVED IN: biological_process unknown	0.502	0.442
AT4G34138	UDP-glucosyl transferase 73B1	0.553	0.439
AT5G05250	Unknown protein; BEST Arabidopsis thaliana protein match is: unknown protein (TAIR:AT3G56360.1)	0.518	0.429

Table 3.3 **List of genes down-regulated in both the *VDOF1ox* and *VDOF2ox* lines.**

AGI Code	Description	*VDOF1ox* (Log_2scale)	*VDOF2ox* (Log_2scale)
AT1G01580	Ferric reduction oxidase 2	-2.292	-1.777
AT1G03850	Glutaredoxin family protein	-0.586	-0.940
AT1G03870	FASCICLIN-like arabinoogalactan 9	-0.602	-0.628
AT1G05010	ethylene-forming enzyme	-0.565	-0.665
AT1G06645	2-oxoglutarate (2OG) and Fe(II)-dependent oxygenase superfamily protein	-0.793	-0.807
AT1G07180	Alternative NAD(P)H dehydrogenase 1	-0.592	-0.788
AT1G14700	Purple acid phosphatase 3	-0.481	-0.625
AT1G14960	Polyketide cyclase/dehydrase and lipid transport superfamily protein	-1.924	-1.568
AT1G15125	S-adenosyl-L-methionine-dependent methyltransferases superfamily protein	-0.622	-1.340
AT1G15980	NDH-dependent cyclic electron flow 1	-0.525	-0.559
AT1G19050	Response regulator 7	-0.553	-0.786
AT1G19150	Photosystem I light harvesting complex gene 6	-0.445	-0.430
AT1G19900	Glyoxal oxidase-related protein	-1.048	-1.663
AT1G21910	Integrase-type DNA-binding superfamily protein	-0.743	-0.987
AT1G22430	GroES-like zinc-binding dehydrogenase family protein	-0.502	-0.520
AT1G22500	RING/U-box superfamily protein	-0.861	-1.600
AT1G26250	Proline-rich extensin-like family protein	-1.597	-2.402
AT1G32540	Lsd one like 1	-0.648	-0.778
AT1G53830	pectin methylesterase 2	-1.097	-0.854
AT1G62510	Bifunctional inhibitor/lipid-transfer protein/seed storage 2S albumin superfamily protein	-0.852	-1.168
AT1G62660	Glycosyl hydrolases family 32 protein	-0.565	-1.012
AT1G65310	Xyloglucan endotransglucosylase/hydrolase 17	-2.258	-1.883
AT1G65390	Phloem protein 2 A5	-0.600	-0.708
AT1G66100	Plant thionin	-0.539	-0.673
AT1G66800	NAD(P)-binding Rossmann-fold superfamily protein	-1.076	-1.719
AT1G72610	Germin-like protein 1	-0.781	-0.739
AT1G74670	Gibberellin-regulated family protein	-0.974	-0.634
AT1G76110	HMG (high mobility group) box protein with ARID/BRIGHT DNA-binding domain	-0.644	-0.563
AT2G01530	MLP-like protein 329	-0.893	-1.825
AT2G01880	Purple acid phosphatase 7	-0.957	-1.860
AT2G01890	Purple acid phosphatase 8	-0.704	-0.815
AT2G10940	Bifunctional inhibitor/lipid-transfer protein/seed storage 2S albumin superfamily protein	-1.005	-0.546
AT2G15080	Receptor like protein 19	-0.762	-0.981
AT2G18300	Basic helix-loop-helix (bHLH) DNA-binding superfamily protein	-0.617	-0.668
AT2G19970	CAP (Cysteine-rich secretory proteins, Antigen 5, and Pathogenesis-related 1 protein) superfamily protein	-1.327	-1.452
AT2G21210	SAUR-like auxin-responsive protein family	-0.539	-0.590
AT2G23620	Methyl esterase 1	-1.018	-1.538
AT2G25240	Serine protease inhibitor (SERPIN) family protein	-1.519	-1.615

AT2G26010	Plant defensin 1.3	-0.561	-0.863
AT2G28160	FER-like regulator of iron uptake	-0.817	-1.118
AT2G30930	Unknown protein; FUNCTIONS IN: molecular_function unknown; INVOLVED IN: biological_process unknown	-0.461	-0.902
AT2G32530	Cellulose synthase-like B3	-0.693	-1.071
AT2G36630	Sulfite exporter TauE/SafE family protein	-0.798	-0.781
AT2G38170	cation exchanger 1	-0.525	-0.599
AT2G39010	Plasma membrane intrinsic protein 2E	-0.442	-0.547
AT2G39040	Peroxidase superfamily protein	-3.772	-1.922
AT2G41560	Autoinhibited Ca(2+)-ATPase, isoform 4	-0.795	-0.873
AT2G43590	Chitinase family protein	-1.300	-1.423
AT3G01190	Peroxidase superfamily protein	-0.973	-1.145
AT3G01290	SPFH/Band 7/PHB domain-containing membrane-associated protein family	-0.562	-1.059
AT3G01420	ALPHA-DIOXYGENASE 1	-0.532	-0.845
AT3G02885	GAST1 protein homolog 5	-0.836	-1.328
AT3G06145	Unknown protein	-0.778	-0.914
AT3G09220	Laccase 7	-1.359	-2.219
AT3G09920	Phosphatidyl inositol monophosphate 5 kinase	-0.563	-0.476
AT3G16240	Delta tonoplast integral protein	-0.984	-0.730
AT3G16660	Pollen Ole e 1 allergen and extensin family protein	-0.875	-1.457
AT3G16670	Pollen Ole e 1 allergen and extensin family protein	-0.477	-0.690
AT3G17510	CBL-interacting protein kinase 1	-0.542	-0.630
AT3G18450	PLAC8 family protein	-2.023	-2.256
AT3G19850	Phototropic-responsive NPH3 family protein	-0.776	-0.768
AT3G22142	Bifunctional inhibitor/lipid-transfer protein/seed storage 2S albumin superfamily protein	-0.536	-0.904
AT3G25190	Vacuolar iron transporter (VIT) family protein	-1.661	-1.213
AT3G29250	NAD(P)-binding Rossmann-fold superfamily protein	-1.661	-1.600
AT3G45710	Major facilitator superfamily protein	-1.128	-1.456
AT3G46370	Leucine-rich repeat protein kinase family protein	-0.863	-0.932
AT3G46490	2-oxoglutarate (2OG) and Fe(II)-dependent oxygenase superfamily protein	-0.664	-0.623
AT3G46700	UDP-Glycosyltransferase superfamily protein	-0.667	-1.120
AT3G47340	Glutamine-dependent asparagine synthase 1	-0.998	-2.256
AT3G49620	2-oxoglutarate (2OG) and Fe(II)-dependent oxygenase superfamily protein	-0.624	-1.230
AT3G50740	UDP-glucosyl transferase 72E1	-0.629	-0.894
AT3G54830	Transmembrane amino acid transporter family protein	-1.031	-1.119
AT3G58810	Metal tolerance protein A2	-0.858	-1.103
AT3G61430	Plasma membrane intrinsic protein 1A	-0.453	-0.750
AT3G62680	Proline-rich protein 3	-0.728	-1.079
AT4G02380	Senescence-associated gene 21	-0.678	-0.815
AT4G04840	Methionine sulfoxide reductase B6	-0.476	-0.817
AT4G08620	sulphate transporter 1;1	-1.319	-1.334
AT4G09900	Methyl esterase 12	-0.802	-0.675
AT4G12545	Bifunctional inhibitor/lipid-transfer protein/seed storage 2S albumin	-1.826	-2.688

	superfamily protein		
AT4G12550	Auxin-Induced in Root cultures 1	-2.334	-2.279
AT4G13495	Other RNA	-0.538	-0.452
AT4G14630	Germin-like protein 9	-1.478	-2.300
AT4G15290	Cellulose synthase family protein	-1.327	-1.310
AT4G15390	HXXXD-type acyl-transferase family protein	-0.501	-1.287
AT4G15393	Cytochrome P450, family 702, subfamily A, polypeptide 5	-1.050	-1.750
AT4G17340	Tonoplast intrinsic protein 2;2	-0.548	-0.590
AT4G19030	NOD26-like major intrinsic protein 1	-0.961	-0.641
AT4G19690	Iron-regulated transporter 1	-1.346	-1.481
AT4G20450	Leucine-rich repeat protein kinase family protein	-1.282	-1.529
AT4G22666	Bifunctional inhibitor/lipid-transfer protein/seed storage 2S albumin superfamily protein	-1.588	-1.007
AT4G23290	Cysteine-rich RLK (RECEPTOR-like protein kinase) 21	-0.800	-0.797
AT4G23300	Cysteine-rich RLK (RECEPTOR-like protein kinase) 22	-0.561	-0.894
AT4G23400	Plasma membrane intrinsic protein 1;5	-0.753	-0.859
AT4G25090	Riboflavin synthase-like superfamily protein	-1.333	-1.815
AT4G25940	ENTH/ANTH/VHS superfamily protein	-0.670	-0.895
AT4G26010	Peroxidase superfamily protein	-0.558	-1.041
AT4G26530	Aldolase superfamily protein	-0.772	-0.853
AT4G28850	Xyloglucan endotransglucosylase/hydrolase 26	-1.619	-1.478
AT4G30280	Xyloglucan endotransglucosylase/hydrolase 18	-0.918	-1.233
AT4G30670	Putative membrane lipoprotein	-0.690	-0.844
AT4G31940	Cytochrome P450, family 82, subfamily C, polypeptide 4	-4.316	-1.940
AT4G33790	Jojoba acyl CoA reductase-related male sterility protein	-2.653	-2.561
AT4G36540	BR enhanced expression 2	-0.634	-0.611
AT4G36670	Major facilitator superfamily protein	-0.743	-1.077
AT4G36850	PQ-loop repeat family protein / transmembrane family protein	-0.663	-1.091
AT4G37070	Acyl transferase/acyl hydrolase/lysophospholipase superfamily protein	-1.291	-1.716
AT4G37980	Elicitor-activated gene 3-1	-0.532	-0.608
AT5G02160	Unknown protein; FUNCTIONS IN: molecular_function unknown; INVOLVED IN: biological_process unknown	-0.473	-0.460
AT5G03570	iron regulated 2	-0.916	-1.170
AT5G04960	Plant invertase/pectin methylesterase inhibitor superfamily	-0.773	-1.249
AT5G08330	TCP family transcription factor	-0.744	-0.521
AT5G11420	Protein of unknown function, DUF642	-0.672	-0.506
AT5G14120	Major facilitator superfamily protein	-0.645	-1.107
AT5G14180	Myzus persicae-induced lipase 1	-0.734	-1.463
AT5G14330	Unknown protein	-1.225	-1.285
AT5G14650	Pectin lyase-like superfamily protein	-1.637	-1.392
AT5G15780	Pollen Ole e 1 allergen and extensin family protein	-0.795	-0.470
AT5G17170	Rubredoxin family protein	-0.594	-0.691
AT5G17820	Peroxidase superfamily protein	-0.463	-0.943
AT5G20630	Germin 3	-0.617	-0.588
AT5G23980	Ferric reduction oxidase 4	-0.870	-1.083

AT5G23990	Ferric reduction oxidase 5	-0.925	-1.058
AT5G27920	F-box family protein	-0.603	-0.697
AT5G38420	Ribulose bisphosphate carboxylase (small chain) family protein	-0.541	-0.666
AT5G44420	plant defensin 1.2	-0.818	-0.677
AT5G44610	Microtubule-associated protein 18	-0.984	-1.433
AT5G44680	DNA glycosylase superfamily protein	-0.433	-0.425
AT5G45070	Phloem protein 2-A8	-1.355	-1.300
AT5G45680	FK506-binding protein 13	-0.429	-0.481
AT5G45820	CBL-interacting protein kinase 20	-0.568	-0.759
AT5G46890	Bifunctional inhibitor/lipid-transfer protein/seed storage 2S albumin superfamily protein	-2.251	-1.677
AT5G46900	Bifunctional inhibitor/lipid-transfer protein/seed storage 2S albumin superfamily protein	-2.021	-1.901
AT5G47450	Tonoplast intrinsic protein 2;3	-0.929	-0.951
AT5G47990	Cytochrome P450, family 705, subfamily A, polypeptide 5	-1.832	-1.354
AT5G48010	Thalianol synthase 1	-0.671	-1.316
AT5G53250	Arabinogalactan protein 22	-0.770	-0.983
AT5G56100	Glycine-rich protein / oleosin	-0.879	-1.278
AT5G59680	Leucine-rich repeat protein kinase family protein	-1.598	-1.760
AT5G60660	Plasma membrane intrinsic protein 2;4	-1.543	-1.371
AT5G61160	Anthocyanin 5-aromatic acyltransferase 1	-0.645	-1.902

Figure 3.22 **Enriched biological process GO term analysis for genes upregulated in Arabidopsis overexpressing *VDOF1* (295 genes).** Node size reflects the number of genes belonging to a category. Colored nodes represent GO terms that are significantly over-represented (corrected *p* value <0.05), and the color scale indicates increasing statistical significance.

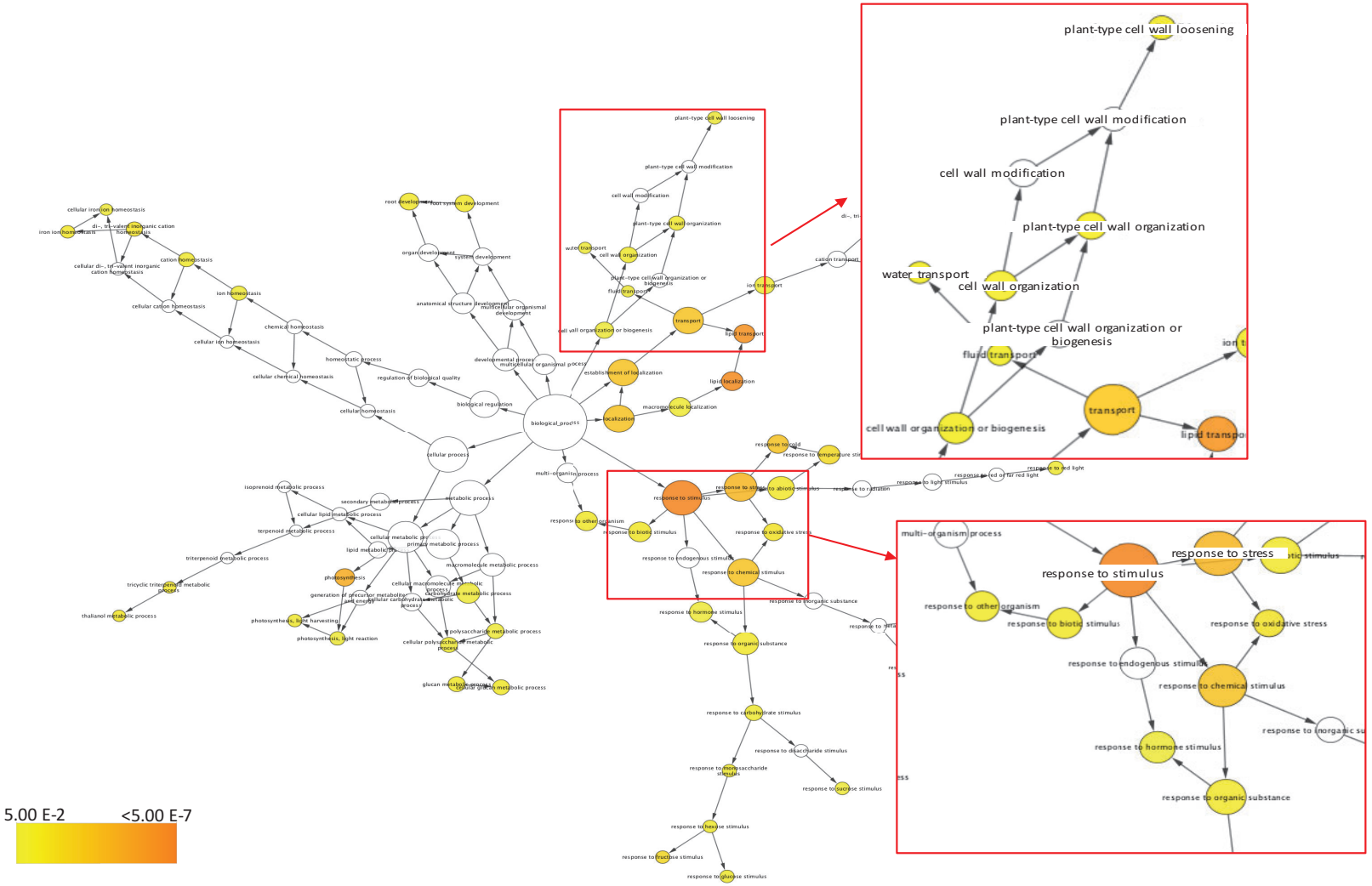

Figure 3.23 **Enriched biological process GO term analysis for genes down-regulated in Arabidopsis overexpressing *VDOF1* (280 genes).** Node size reflects the number of genes belonging to a category. Colored nodes represent GO terms that are significantly over-represented (corrected *p* value <0.05), and the color scale indicates increasing statistical significance.

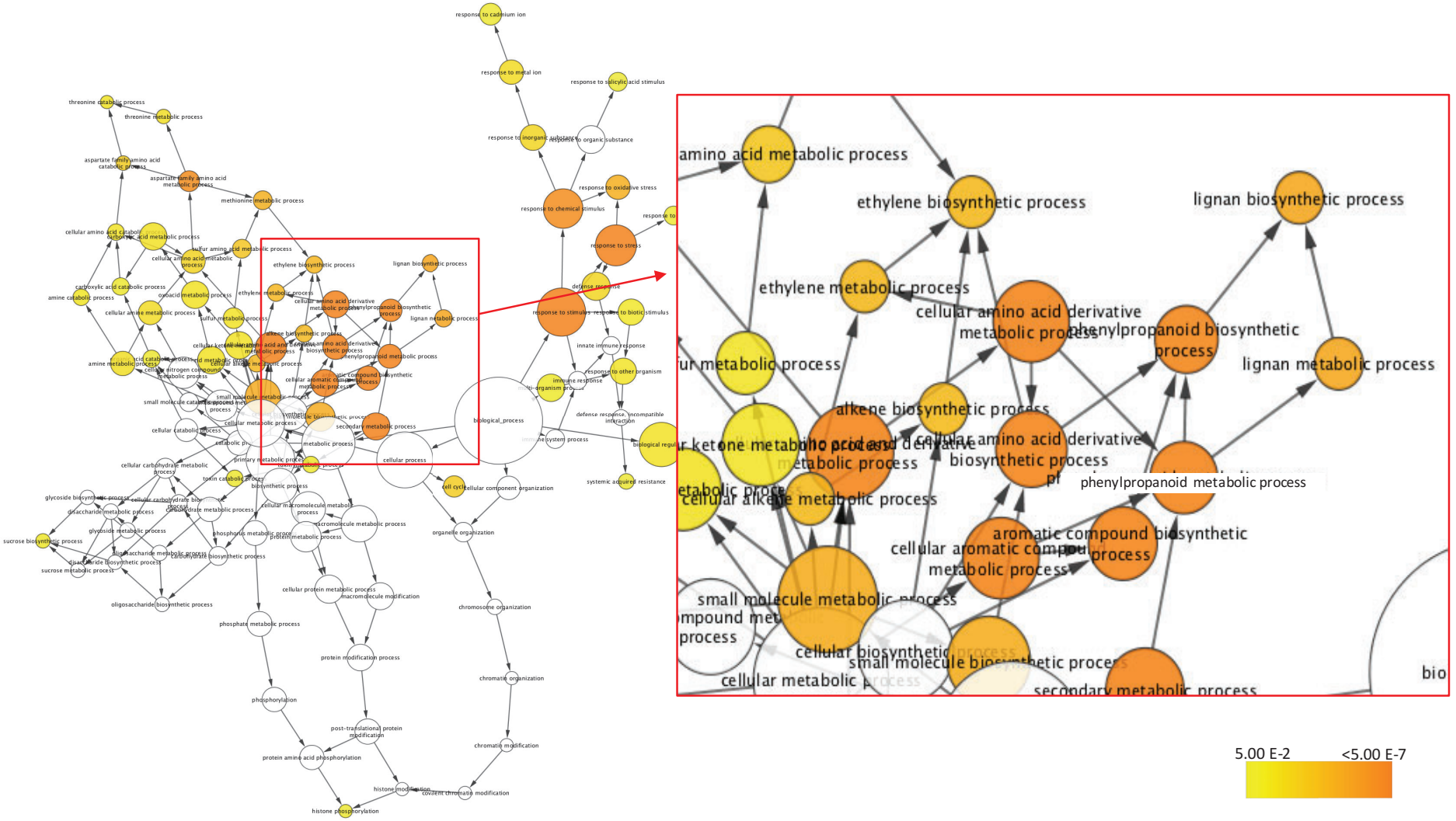

Figure 3.24 **Enriched biological process GO term analysis for genes upregulated in Arabidopsis overexpressing *VDOF2* (504 genes).** Node size reflects the number of genes belonging to a category. Colored nodes represent GO terms that are significantly over-represented (corrected *p* value <0.05), and the color scale indicates increasing statistical significance.

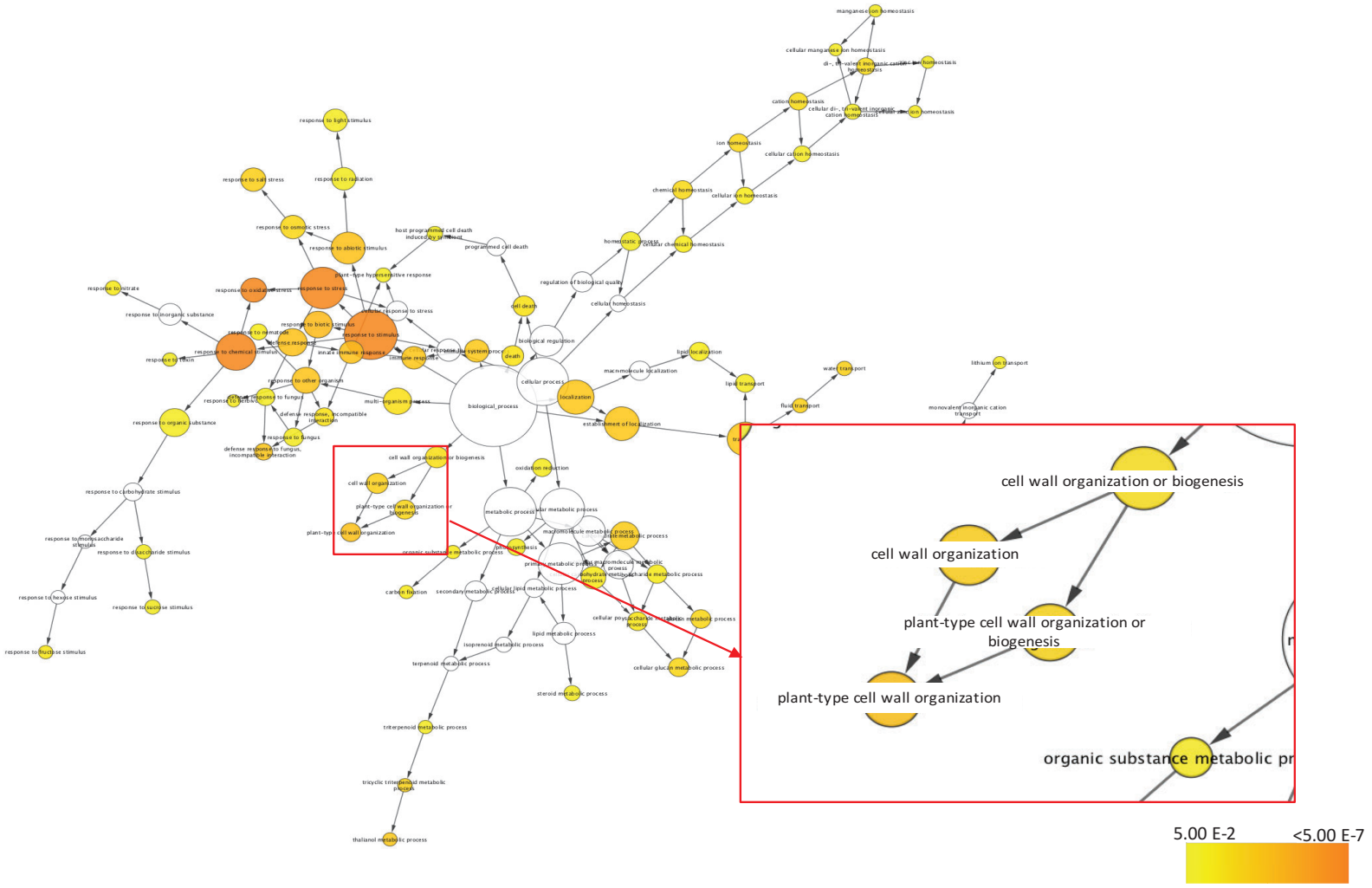

Figure 3.25 **Enriched biological process GO term analysis for genes down-regulated in Arabidopsis overexpressing *VDOF2* (535 genes).** Node size reflects the number of genes belonging to a category. Colored nodes represent GO terms that are significantly over-represented (corrected *p* value <0.05), and the color scale indicates increasing statistical significance.

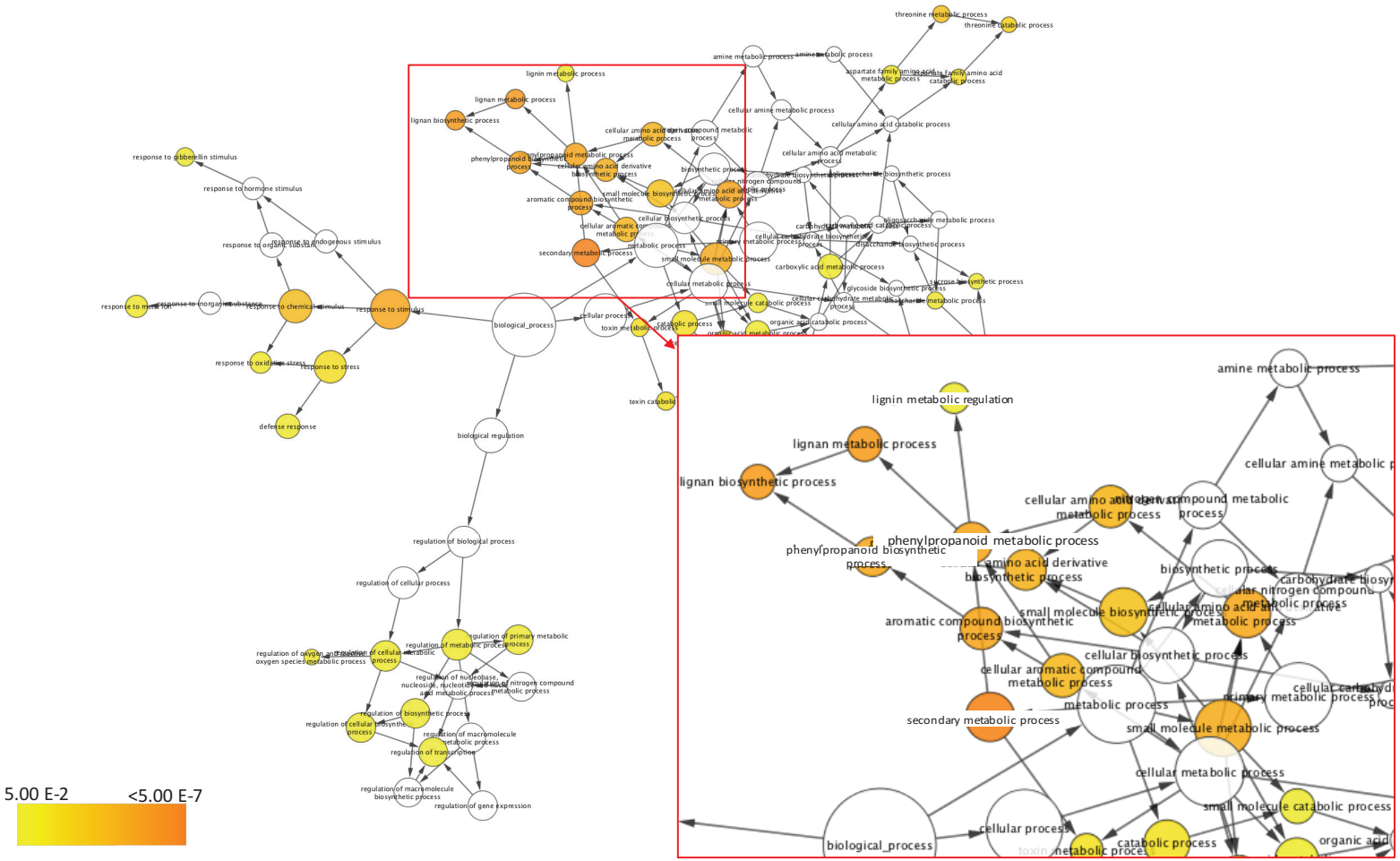

Figure 3.26 **Enriched biological process GO term analysis for genes commonly upregulated in Arabidopsis overexpressing *VDOF1* and *VDOF2* (160 genes).**
Node size reflects the number of genes belonging to a category. Colored nodes represent GO terms that are significantly over-represented (corrected *p* value <0.05), and the color scale indicates increasing statistical significance.

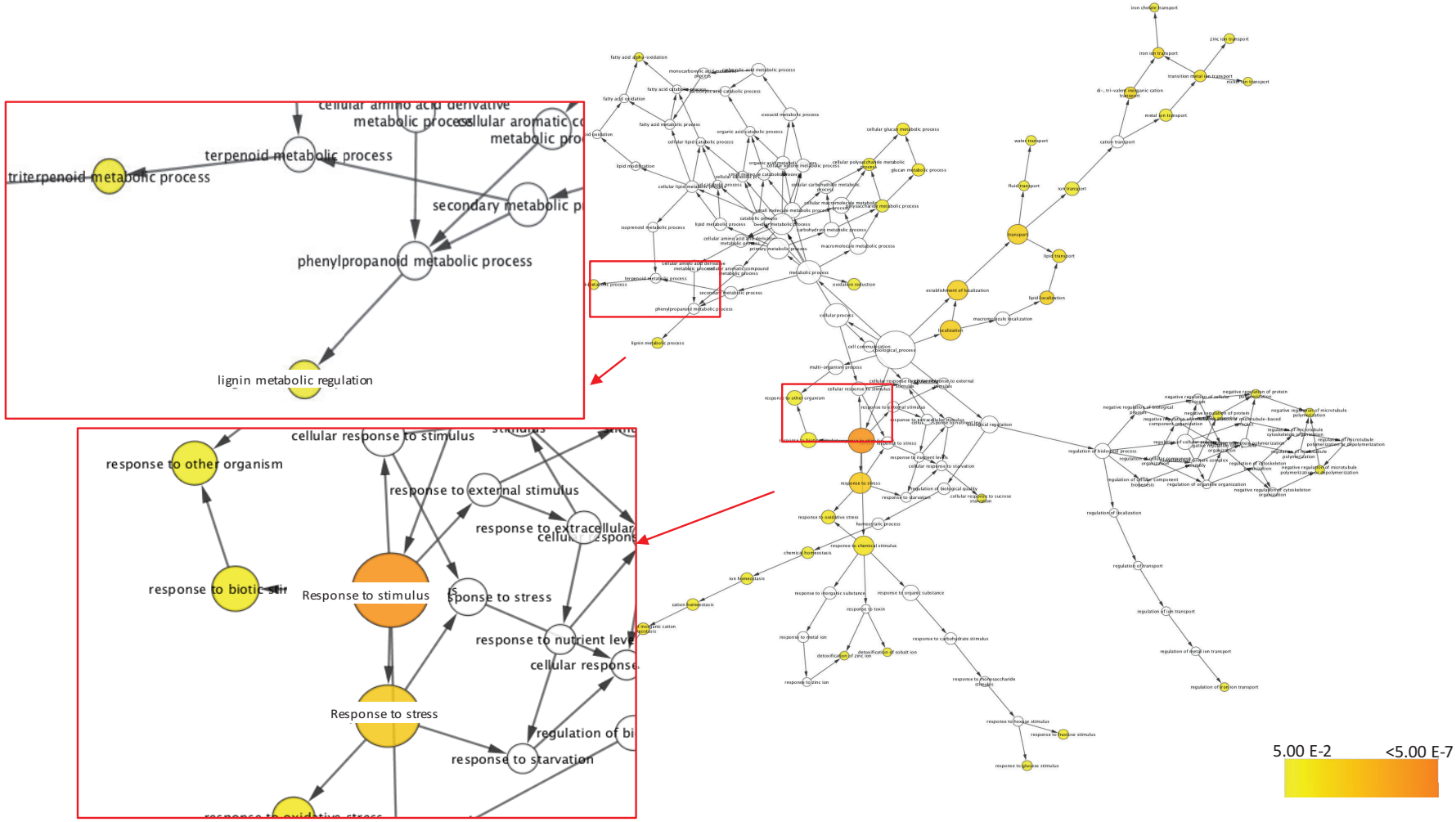

Figure 3.27 **Enriched biological process GO term analysis for genes down-regulated commonly in Arabidopsis overexpressing *VDOF1* and *VDOF2* (141 genes).**

Node size reflects the number of genes belonging to a category. Colored nodes represent GO terms that are significantly over-represented (corrected *p* value <0.05), and the color scale indicates increasingly higher statistical significance.

Table 3.4 **Expression of vascular-related genes in the *VDOF1ox* and *VDOF2ox* transcriptomic data.** Genes with significant changes in expression (q-value = 0.05) are in were bold.

AGI code	Gene name	Annotation	*VDOF1ox* (Log_2scale)	q-value	*VDOF2ox* (Log_2scale)	q-value
AT2G18060	VND1	Vascular related NAC-domain protein 1	-0.297	0.984	0.272	0.994
AT4G36160	VND2	NAC domain containing protein 76	-0.115	0.999	-0.078	0.999
AT5G66300	VND3	NAC domain containing protein 105	-0.169	0.999	-0.465	0.638
AT1G12260	VND4	NAC 007	-0.032	0.999	-0.036	0.999
AT1G62380	VND5	ACC oxidase 2	0.101	0.999	0.119	0.999
AT5G62380	VND6	NAC-domain protein 101	0.437	0.841	0.055	0.999
AT1G71930	VND7	Vascular related NAC-domain protein 7	0.313	0.999	0.152	0.999
AT1G32770	SND1/NST3	NAC domain containing protein 12	0	1	0	1
AT4G28500	SND2	NAC domain containing protein 73	-0.063	0.999	0.158	0.999
AT1G28470	SND3	NAC domain containing protein 10	0.058	0.999	-0.231	0.989
AT2G46770	NST1	NAC (No Apical Meristem) domain transcriptional regulator superfamily protein	0.53	1	INF-P	1
AT3G61910	NST2	NAC domain protein 66	0	1	0	1
AT1G19850	MONOPTEROS	Transcriptional factor B3 family protein / auxin-responsive factor AUX/IAA-related	0.15	0.896	0.036	0.999
AT4G32880	ATHB8	Homeobox gene 8	0.008	0.999	0.132	0.951
AT1G79430	APL	Homeodomain-like superfamily protein	-0.04	0.999	0.066	0.999
AT1G02730	SOS6	Cellulose synthase-like D5	0.317	0.252	**0.472**	**0.025**
AT5G03260	LAC11	Laccase 11	-0.052	0.999	0.066	0.999
AT1G20850	XCP2	Xylem cycteine peptidase 2	-0.201	0.738	-0.059	0.999
AT5G12870	MYB46	Myb domain protein 46	0.106	0.999	-0.145	0.999
AT5G13180	VNI2	NAC domain containg protein 83	-0.041	0.999	-0.066	0.999
AT5G16600	MYB43	Myb domain protein 43	0.228	0.966	0.439	0.563
AT5G60200	AtDOF5.3/TMO 6	TARGET OF MONOPTEROS6	0.093	0.999	-0.063	0.999
AT1G22640	MYB3	Myb domain protein 3	-0.129	0.999	-0.267	0.64
AT2G30590	WRKY21	WRKY DNA-binding protein 21	0.023	0.999	0.197	0.747
AT3G04670	WRKY39	WRKY DNA-binding protein 30	0.0813	0.999	0.155	0.88
AT5G64530	XND1	Xylem NAC domain 1	0.331	0.902	0.058	0.999
AT2G27250	CLV3	CLAVATA3	-0.752	0.999	-0.472	0.999
AT5G62940	AtDOF 5.6 / HCA2	Dof-typezinc finger DNA-binding family potein	-0.339	0.581	-0.13	0.999
AT1G46480	WOX4	WUSCHEL related homeobox 4	0.016	0.999	-0.215	0.974
AT1G52150	ATHB15	Homeobox-leucine zipper family protein / lipid-binding START domain-containing protein	-0.104	0.995	-0.118	0.974
AT3G09070	OCTOPUS	Protein of unknown function (DUF740)	0.087	0.999	0.167	0.892
AT5G16560	KAN1	Homeodomain-like superfamily protein	-0.008	0.999	-0.003	0.999

AT4G08150	KNAT1	KNOTTED-like from Arabidopsis thaliana	0.009	0.999	-0.077	0.999
AT1G22710	SUC2	Sucrose-proton symporter 2	0.081	0.999	0.051	0.999
AT2G37210	LOG3	Lysine decarboxylase family protein	0.057	0.999	-0.302	0.885
AT3G53450	LOG4	Putative lysine decarboxylase family protein	0.168	0.999	-0.039	0.999
AT3G25710	TMO5	Basic helix-loop-helix 32	-0.037	0.999	0.040	0.999
AT2G27230	LHW	Transcription factor-related	-0.035	0.999	0.137	0.999
AT3G10740	ATASD1	Alpha-L-arabinofuranosidase 1	-0.105	0.995	-0.202	0.691
AT1G20930	CDKB2;2	Cyclin-dependent kinase B2;2	0.282	0.503	0.528	0.019
AT1G34460	CYCB1;5	CYCLIN B1;5	0.522	0.856	-0.882	0.601
AT2G27970	CKS2	CDK-subunit 2	0.391	0.205	0.873	0.003
AT3G01330	E2L2	DP-E2F-like protein 3	0.429	0.274	0.577	0.063
AT3G06030	NP3	NPK1-related protein kinase 3	0.099	0.999	0.243	0.626
AT3G16920	CTL2	chitinase-like protein 2	-0.089	0.999	-0.138	0.999
AT3G17360	POK1	Phragmoplast orienting kinesin 1	0.086	0.999	0.135	0.950
AT3G23890	TOPII	Topoisomerase II	0.221	0.634	0.221	0.627
AT3G25980	MAD2	DNA-binding HORMA family protein	0.282	0.779	0.515	0.502
AT3G43210	TES	ATP binding microtubule motor family protein	0.170	0.896	0.345	0.324
AT3G45610	AtDOF 3.2 / DOF6	Dof-typezinc finger DNA-binding family potein	-0.094	0.999	-0.216	0.971
AT3G45970	EXPL1	Expansin-like A1	-0.148	0.999	-0.412	0.943
AT3G60840	MAP65-4	Microtubule-associated protein 65-4	0.402	0.209	**0.706**	**0.003**
AT5G15630	IRX6	COBRA-like extracellular glycosyl-phosphatidyl inositol-anchored protein family	0.072	0.999	0.157	0.999
AT5G54690	LGT6	Galacturonosyltransferase 12	0.226	0.999	0.042	0.999
AT5G56580	MKK6	MAP kinase kinase 6	0.257	0.690	0.301	0.53
AT1G01620	TMP-B	Plasma membrane intrinsic protein 1C	-0.303	0.372	-0.188	0.788
AT1G32100	PRR1	Pinoresinol reductase 1	0.072	0.999	0.707	0.003
AT4G00950	MEE47	Protein of unknown function (DUF688)	-0.418	0.187	-0.229	0.759
AT5G17420	MUR10	Cellulose synthase family protein	-0.058	0.999	-0.066	0.999
AT1G10540	NAT8	nucleobase-ascorbate transporter 8	**1.493**	**0.009**	**1.778**	**0.003**
AT5G47500	PME5	Pectin lyase-like superfamily protein	-0.144	0.904	0.121	0.96
AT5G39610	ORE1	NAC domain containing protein 6	**0.632**	**0.003**	**0.858**	**0.003**
AT2G40470	LBD15	LOB domain-containing protein 15	-0.383	0.858	-0.24	0.999
AT2G45420	LBD18	LOB domain-containing protein 18	-0.351	0.999	-0.413	0.981
AT4G37650	SHR	GRAS family transcription factor	0.009	0.999	-0.159	0.924
AT5G60690	REV	Homeobox-leucine zipper family protein / lipid-binding START domain-containing protein	0.081	0.999	-0.008	0.999
AT5G66320	GATA5	GATA transcription factor 5	0.051	0.999	0.123	0.985
AT5G15830	bZIP3	Basic leucine-zipper 3	0.258	0.766	0.611	0.057
AT5G41410	BEL1	POX (plant homeobox) family protein	0.065	0.999	0.22	0.769
AT1G63650	EGL3	Basic helix-loop-helix (bHLH) DNA-binding superfamily protein	0.226	0.867	0.178	0.958

AT4G36540	BEE2	BR enhanced expression 2	**-0.634**	**0.003**	**-0.611**	**0.003**
AT1G30490	PHV	Homeobox-leucine zipper family protein / lipid-binding START domain-containing protein	0.041	0.999	0.099	0.999
AT1G31320	LBD4	LOB domain-containing protein 4	0.257	0.896	-0.147	0.999
AT3G04420	NAC048	NAC domain containing protein 48	0.565	0.499	1.607	0.003
AT4G29230	NAC075	NAC domain containing protein 75	0.188	0.999	0.122	0.999
AT2G31070	TCP10	TCP domain protein 10	-0.255	0.561	-0.213	0.713
AT5G05410	DREB2A	DRE-binding protein 2A	0.135	0.999	0.236	0.917
AT1G63910	MYB103	Myb domain protein 103	-0.399	0.991	0.052	0.999
AT3G52820	PAP22	Purple acid phosphatase 22	-0.228	0.999	0.056	0.999
AT4G12910	scpl20	Serine carboxypeptidase-like 20	-0.279	0.645	-0.246	0.735
AT5G15490	UGD3	UDP-glucose 6-dehydrogenase family protein	0.019	0.999	-0.009	0.999
AT2G38080	LMCO4	Laccase/Diphenol oxidase family protein	-0.072	0.999	0.111	0.999
AT4G18780	LEW2	Cellulose synthase family protein	0.021	0.999	0.06	0.999
AT5G03170	FLA11	FASCICLIN-like arabinogalactan-protein 11	0.094	0.999	0.106	0.999
AT5G44030	NWS2	Cellulose synthase A4	-0.105	0.999	0.101	0.999
AT1G27920	MAP65-8	Microtubule-associated protein 65-8	-0.084	0.999	0.125	0.999
AT5G01930	MAN6	Glycosyl hydrolase superfamily protein	-0.196	0.999	-0.109	0.999
AT5G56540	ATAGP14	Arabinogalactan protein 14	-0.331	0.671	-0.332	0.654
AT4G00230	XSP1	Xylem serine peptidase 1	-0.072	0.999	-0.107	0.999
AT1G73590	PIN1	Auxin efflux carrier family protein	0.163	0.882	0.078	0.999
AT3G16857	ARR1	Response regulator 1	-0.06	0.999	-0.052	0.999
AT1G19850	MP	Transcriptional factor B3 family protein / auxin-responsive factor AUX/IAA-related	0.150	0.896	0.036	0.999
AT3G23630	IPT7	Isopentenyltransferase 7	0.186	0.999	0.400	0.887
AT3G02130	TOAD2	Receptor-like protein kinase 2	0.062	0.999	0.103	0.999
AT5G17260	NAC086	NAC domain containing protein 86	0.057	0.999	-0.236	0.999
AT3G03200	NAC045	NAC domain containing protein 45	-0.141	0.999	-0.419	0.777
AT1G80100	AHP6	Histidine phosphotransfer protein 6	0.393	0.913	0.158	0.999
AT1G68460	IPT1	Isopentenyltransferase 1	-0.66	0.808	0.611	0.809
AT5G13300	VAN3/SFC	ARF GTPase-activating protein	0.047	0.999	0.088	0.999
AT1G66140	ZFP4	Zinc finger protein 4	-0.041	0.999	-0.072	0.999

Table 3.5: **Expression of Dof transcription factors differentially expressed in *VDOFox* and *VDOF2ox*.** Dof genes that significantly differ in expression (q-value = 0.05) are in bold.

Gene Name	AGI code	Log_2FC VDOF1	q-value	Log_2FC VDOF2	q-value
AtDOF1.1 / OPB2	AT1G07640	0.020	0.999	-0.150	0.931
AtDOF1.2	AT1G21340	-0.216	0.999	0.493	0.953
AtDOF1.4	AT1G28310	-0.246	0.762	-0.229	0.799
AtDOF1.5 / COG1	AT1G29160	0.130	0.999	-0.231	0.958
AtDOF1.6	AT1G47655	-0.371	0.760	-0.134	0.999
AtDOF1.8 / VDOF2	AT1G64620	-0.191	0.920	**6.726**	**0.003**
AtDOF1.10 / CDF5	AT1G69570	-0.060	0.999	0.633	0.589
AtDOF2.1	AT2G28510	-0.111	0.999	-0.122	0.998
AtDOF2.2	AT2G28810	-0.359	0.356	-0.404	0.245
AtDOF2.3 / CDF4	AT2G34140	-0.086	0.999	-0.089	0.999
AtDOF3.1 / ADOF2	AT3G21270	-0.343	0.452	-0.303	0.564
AtDOF3.2 / DOF6	AT3G45610	-0.216	0.971	-0.094	0.999
AtDOF3.5	AT3G52440	-1.144	0.999	-1.185	0.877
AtDOF3.7 / DAG1	AT3G61850	-0.151	0.968	-0.192	0.885
AtDOF4.1 / ITD1	AT4G00940	-0.718	0.256	-0.686	0.294
AtDOF4.5	AT4G21080	INF_M	0.690	INF_P	1
AtDOF4.6 / VDOF1	AT4G24060	**5.196**	**0.003**	-0.295	0.433
AtDOF5.2 / CDF2	AT5G39660	0.413	0.127	0.178	0.855
AtDOF5.5 / CDF1	AT5G62430	-0.523	0.178	-0.193	0.901
AtDOF5.6 / HCA2	AT5G62940	-0.130	0.999	-0.339	0.581
AtDOF5.8	AT5G66940	-0.057	0.999	0.180	0.999

Table 3.6 **List of selected genes related to phloem and xylem cell differentiation.**

Transcriptomic data	Description	References	Selected genes
apl Vs WT	Altered Phloem Development (APL) gene required for phloem development	Furuta *et al*., 2014	1,108
VND6/7ox Vs WT	VND6 and VND7 genes are key regulators of xylem vessels differentiation	Yamaguchi *et al*., 2011; Zhong *et al*., 2010; Ohashi-Ito *et al*., 2010	561
nst1 nst3 Vs WT	NST1 and NST3 regulate secondary cell wall thickening in fibers	Mistsuda *et al*., 2007	1,528

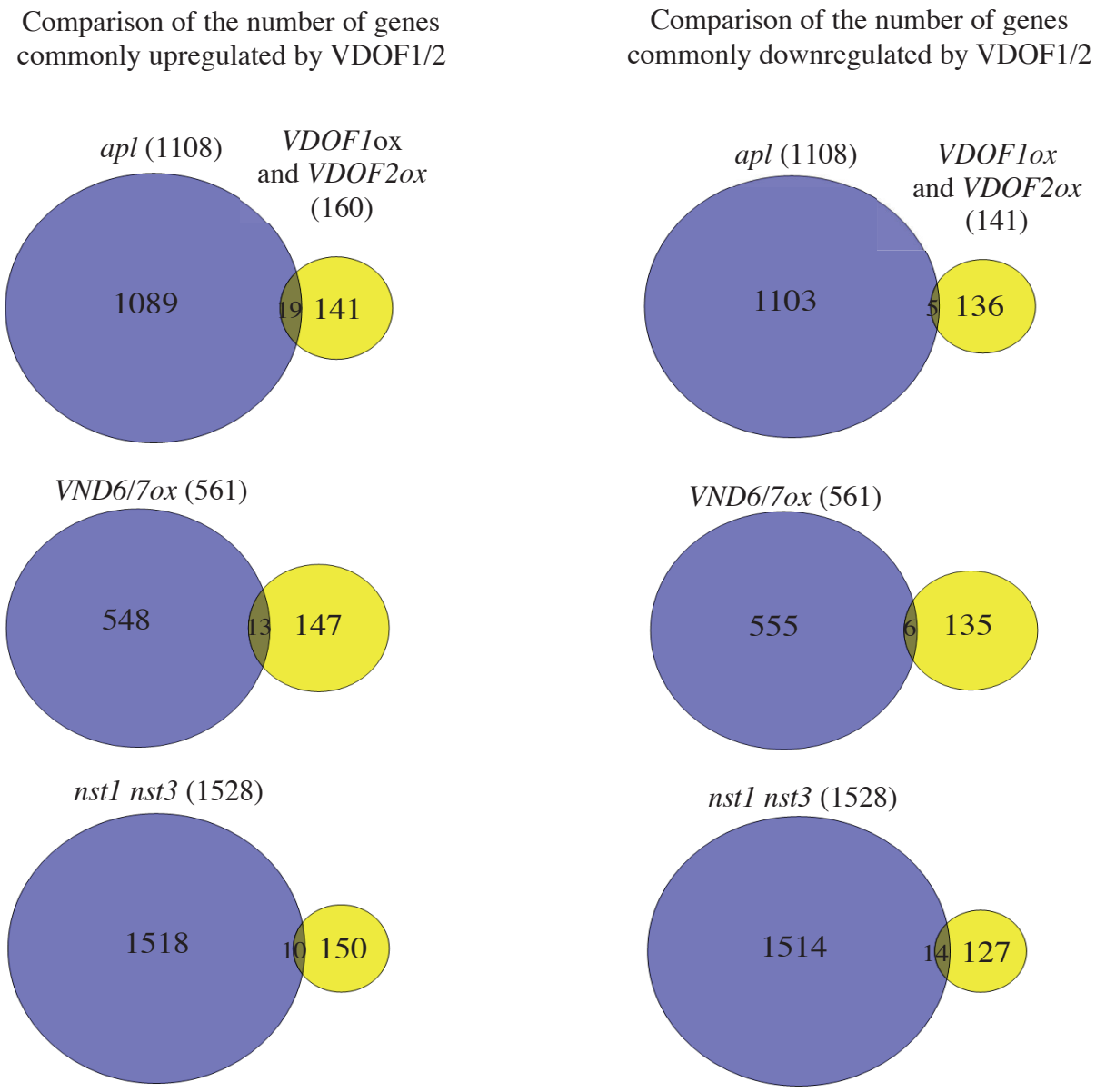

Figure 3.28 **Comparison of selected genes possibly related to phloem and xylem cell differentiation that might be common targets of VDOF1 and VDOF2.**
Genes differentially expressed in the *apl* mutant, *VDN6* or *VND7* overexpressors, and the *nst1 nst3* double knock-out mutant were selected from published transcriptomic data and compared with genes commonly up- or downregulated in *VDOF1* and *VDOF2* overexpression lines.

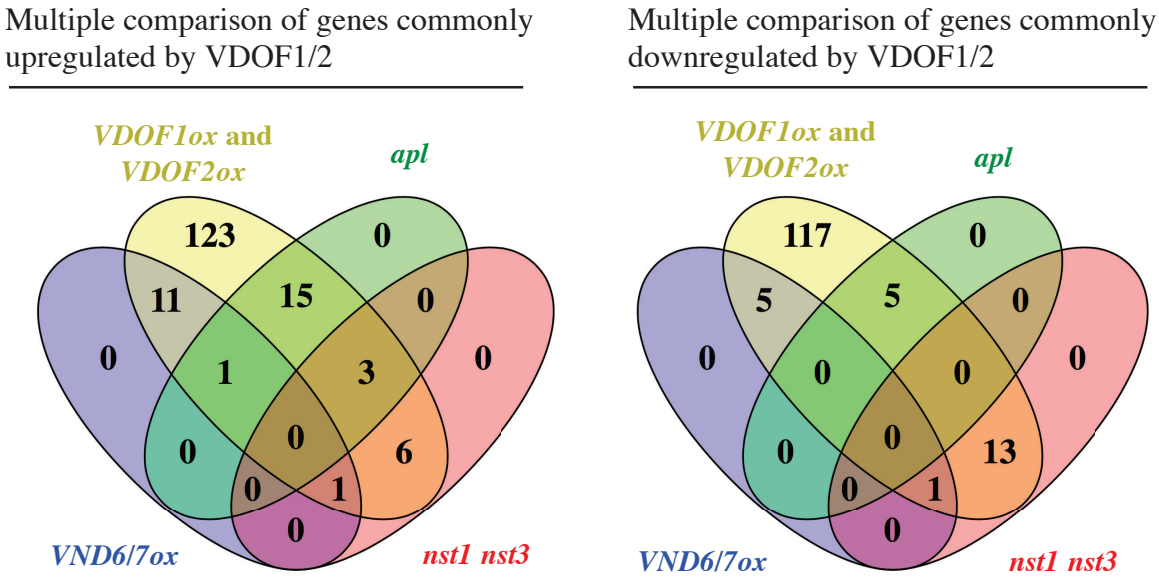

Figure 3.29 **Multiple comparison of selected genes possibly related to phloem and xylem cell differentiation that might be common targets of VDOF1 and VDOF2.**
Genes differentially expressed in the *apl* mutant, VDN6 or VND7 overexpressors, and the *nst1 nst3* double knock-out mutant were selected from published transcriptomic data and compared with genes commonly up- or downregulated in *VDOF1* and *VDOF2* overexpression lines.

Table 3.7 **List of genes that overlap with genes up-regulated in *VDOF1ox* and *VDOF2ox* compared with *VND6/7ox*, *apl,* and *nst1 nst3***

AGI code	Description	*VDOF1ox* (Log_2scale)	*VDOF2ox* (Log_2scale)	*VND6/7 ox*	*apl*	*nst1 nst3*
AT4G36430	Peroxidase superfamily protein	1.895	2.917	Yes	-	-
AT5G59845	Gibberellin-regulated family protein	1.859	1.789	Yes	-	-
AT5G05390	laccase 12	2.240	4.456	Yes	-	-
AT3G60140	Glycosyl hydrolase superfamily protein	1.715	2.562	Yes	-	-
AT3G45010	serine carboxypeptidase-like 48	0.997	1.532	Yes	-	-
AT4G23690	Disease resistance-responsive (dirigent-like protein) family protein	0.607	1.637	Yes	-	-
AT3G23250	myb domain protein 15	1.124	1.745	Yes	-	-
AT1G73120	unknown protein; FUNCTIONS IN: molecular_function unknown	1.521	2.356	Yes	-	-
AT1G17180	glutathione S-transferase TAU 25	0.860	1.304	Yes	-	-
AT2G18150	Peroxidase superfamily protein	0.973	1.876	Yes	-	-
AT1G77330	2-oxoglutarate (2OG) and Fe(II)-dependent oxygenase superfamily protein	0.919	0.867	Yes	-	-
AT1G47400	Unknown protein; FUNCTIONS IN: molecular_function unknown	0.940	0.740	Yes	Yes	-
AT1G64160	Disease resistance-responsive (dirigent-like protein) family protein	3.069	4.233	-	Yes	-
AT5G06720	Peroxidase 2	1.248	2.151	-	Yes	-
AT5G27000	Kinesin 4	0.690	1.774	-	Yes	-
AT1G08050	Zinc finger (C3HC4-type RING finger) family protein	1.118	1.452	-	Yes	-
AT3G17950	Unknown protein; FUNCTIONS IN: molecular_function unknown; INVOLVED IN: biological_process unknown	0.793	1.268	-	Yes	-
AT1G72810	Pyridoxal-5'-phosphate-dependent enzyme family protein	0.791	1.156	-	Yes	-
AT2G28590	Protein kinase superfamily protein	0.981	1.129	-	Yes	-
AT2G45290	Transketolase	0.513	0.939	-	Yes	-
AT1G55210	Disease resistance-responsive (dirigent-like protein) family protein	0.453	0.924	-	Yes	-
AT3G02770	Ribonuclease E inhibitor RraA/Dimethylmenaquinone methyltransferase	0.548	0.885	-	Yes	-
AT5G37540	Eukaryotic aspartyl protease family protein	0.702	0.845	-	Yes	-
AT1G01010	NAC domain containing protein 1	0.702	0.831	-	Yes	-
AT5G67160	HXXXD-type acyl-transferase family protein	0.763	0.789	-	Yes	-
AT3G27060	Ferritin/ribonucleotide reductase-like family protein	0.576	0.611	-	Yes	-
AT5G04150	Basic helix-loop-helix (bHLH) DNA-binding superfamily protein	0.825	0.492	-	Yes	-
AT2G02130	Low-molecular-weight cysteine-rich 68	1.240	1.857	-	Yes	Yes
AT2G23150	Natural resistance-associated macrophage protein 3	1.035	0.900	-	Yes	Yes
AT1G71040	Cupredoxin superfamily protein	0.586	0.610	-	Yes	Yes
AT1G79180	Myb domain protein 63	1.003	1.972	-	-	Yes
AT1G08630	Threonine aldolase 1	0.544	1.440	-	-	Yes
AT5G61430	NAC domain containing protein 100	1.215	1.408	-	-	Yes

AT4G34230	Cinnamyl alcohol dehydrogenase 5	0.967	1.317	-	-	Yes
AT1G67080	Abscisic acid (aba)-deficient 4	0.755	1.062	-	-	Yes
AT3G49780	Phytosulfokine 4 precursor	0.497	0.508	-	-	Yes
AT1G17960	Threonyl-tRNA synthetase	1.242	0.783	Yes	-	Yes

Table 3.8 **List of genes that overlap with genes down-regulated in *VDOF1ox* and *VDOF2ox* compared to *VND6/7ox*, *apl,* and *nst1 nst3***

AGI code	Description	*VDOF1ox* (Log_2FC)	*VDOF2ox* (Log_2FC)	*VND6/7 ox*	*apl*	*nst1 nst3*
AT4G31940	Cytochrome P450, family 82, subfamily C, polypeptide 4	-4.316	-1.940	Yes	-	-
AT4G19690	Iron-regulated transporter 1	-1.481	-1.346	Yes	-	-
AT3G02885	GAST1 protein homolog 5	-0.836	-1.328	Yes	-	-
AT1G21910	Integrase-type DNA-binding superfamily protein	-0.743	-0.987	Yes	-	-
AT5G60660	Plasma membrane intrinsic protein 2;4	-1.543	-1.371	Yes	-	-
AT3G49620	2-oxoglutarate (2OG) and Fe(II)-dependent oxygenase superfamily protein	-0.624	-1.230	-	Yes	-
AT5G14180	Myzus persicae-induced lipase 1	-0.734	-1.463	-	Yes	-
AT5G44680	DNA glycosylase superfamily protein	-0.433	-0.425	-	Yes	-
AT5G47990	Cytochrome P450, family 705, subfamily A, polypeptide 5	-1.832	-1.354	-	Yes	-
AT5G48010	Thalianol synthase 1	-0.671	-1.316	-	Yes	-
AT4G36540	BR enhanced expression 2	-0.634	-0.611	Yes	-	Yes
AT1G19050	Response regulator 7	-0.553	-0.786	-	-	Yes
AT1G19150	Photosystem I light harvesting complex gene 6	-0.445	-0.430	-	-	Yes
AT1G22430	GroES-like zinc-binding dehydrogenase family protein	-0.502	-0.520	-	-	Yes
AT1G65390	Phloem protein 2 A5	-0.600	-0.708	-	-	Yes
AT1G72610	Germin-like protein 1	-0.781	-0.739	-	-	Yes
AT2G18300	Basic helix-loop-helix (bHLH) DNA-binding superfamily protein	-0.617	-0.668	-	-	Yes
AT3G09920	Phosphatidyl inositol monophosphate 5 kinase	-0.563	-0.476	-	-	Yes
AT4G09900	Methyl esterase 12	-0.802	-0.675	-	-	Yes
AT4G15290	Cellulose synthase family protein	-1.327	-1.310	-	-	Yes
AT4G26530	Aldolase superfamily protein	-0.772	-0.853	-	-	Yes
AT5G15780	Pollen Ole e 1 allergen and extensin family protein	-0.795	-0.470	-	-	Yes
AT5G38420	Ribulose bisphosphate carboxylase (small chain) family protein	-0.541	-0.666	-	-	Yes
AT5G45680	FK506-binding protein 13	-0.429	-0.481	-	-	Yes

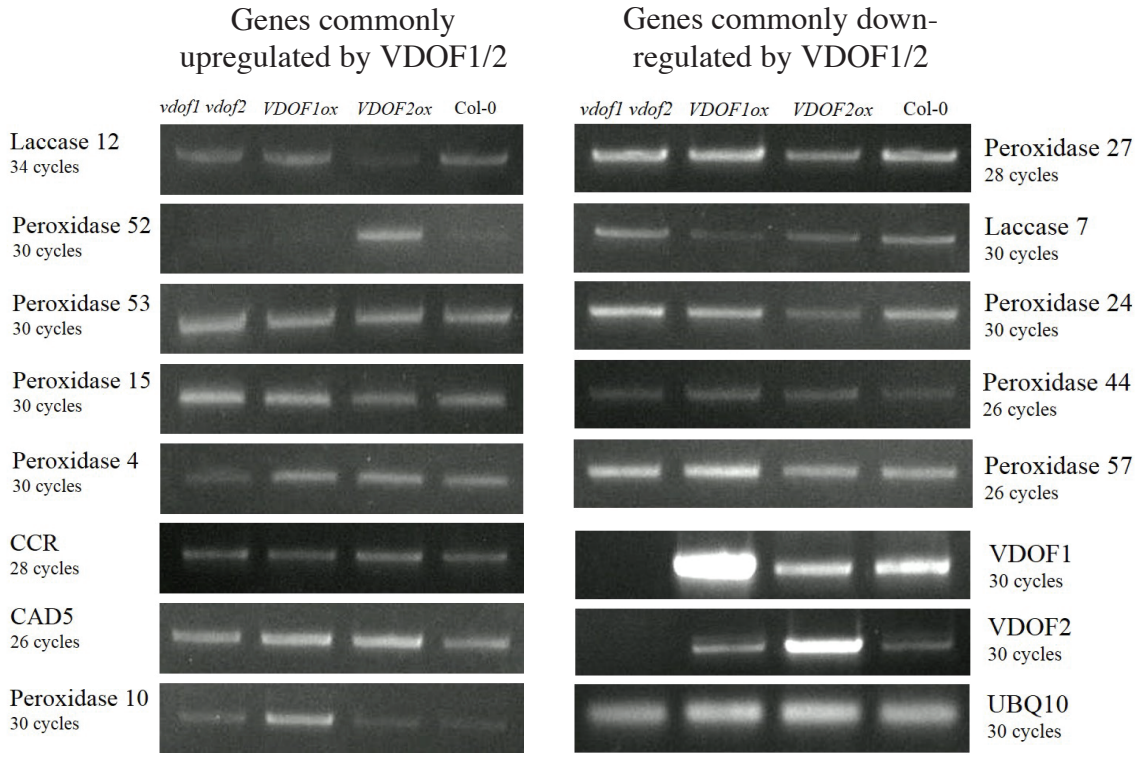

Figure 3.30 **Expression analysis of selected genes commonly up- or downregulated by VDOF1 and VDOF2.**
Semi-quantitative RT-PCR analysis of several genes commonly up- or down-regulated by VDOF1 and VDOF2 was carried out with 8-day-old seedlings of a *vdof1 vdof2* double T-DNA insertion line (Line 5-16), constitutive overexpressors of *VDOF1* and *VDOF2* (Line 6-6 and Line 1-3, respectively), and wild-type (Col-0). *UBQ10* was used as a loading control. CCR, cinnamoyl-CoA reductase; CAD5, cinnamyl alcohol dehydrogenase 5.

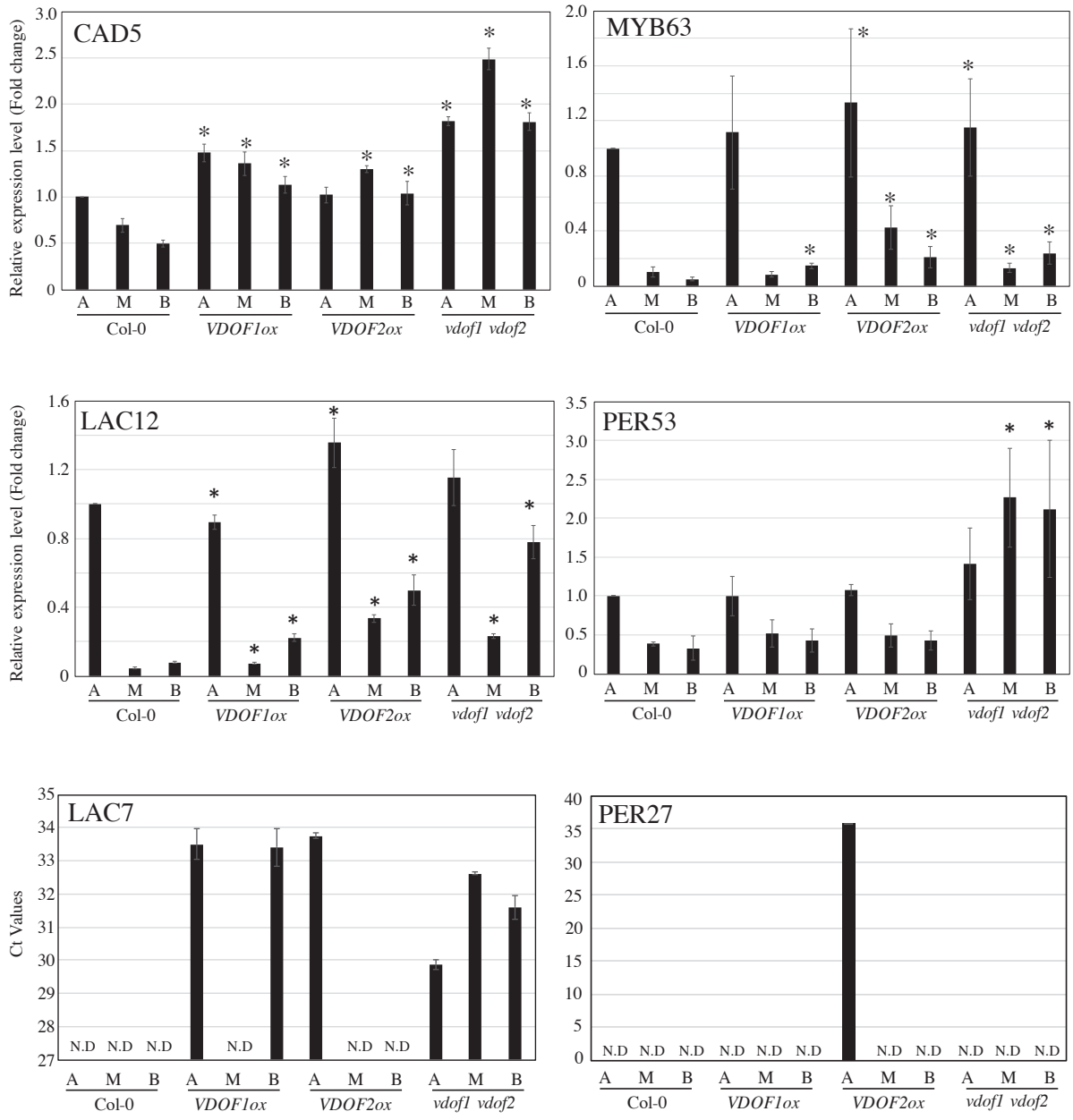

Figure 3.31 **Quantitative expression analysis of lignin-related genes in inflorescence stems.** Quantitative RT-PCR (qRT-PCR) analysis was carried out for lignin-related genes in inflorescence stems of 40-day-old plants. Inflorescence stems of 40-day-old plants including wild type (Col-0), *VDOF1* and *VDOF2* overexpression lines (*VDOF1ox* and *VDOF2ox*, respectively), and the double T-DNA insertion line (*vdof1 vdof2*) were divided into three parts: apical (A), middle (M), and basal (B). Total RNA was extracted from each of these parts and subjected to qRT-PCR analysis. The value for the apical part of wild-type inflorescence stems (Col-0, T) was set to 1. *UBQ10* was used as an internal control. Results were shown as mean ±SD (n=3). '*', significant difference compared with the wild type, $p<0.05$ by Student's *t*-test. CAD5, cinnamyl alcohol dehydrogenase 5; LAC, laccase; PER, peroxidase; N.D., not detected.

CHAPTER 4

DISCUSSION

4.1 VDOF1 and VDOF2 act as transcription factors

Dof transcription factors are unique to plant species, and more than half of the members of the Dof family are expressed in vascular tissues (Hir and Bellini, 2013). It has been proposed that all Arabidopsis *Dof* genes could be involved in vascular development, although many *Dof* genes have not been characterized. This work aimed to elucidate the molecular functions of VDOF1/Dof4.6 and VDOF2/Dof1.8. The VDOF proteins were localized to the nucleus, consistent with a role as Dof transcription factors (Figure 3.5). Transient expression assays indicated that VDOF2 could be a transcription factor with weak repressor domain, whereas VDOF1 did not display activator or repressor domain activity (Figure 3.4).

The modes of Dof activity in transcriptional regulation are likely complex. Several studies showed that Dof proteins can act as transcriptional activators or transcriptional repressors depending on the target gene. OBP3/Dof3.6 acts as a positive regulator of *PhyB* expression and a negative regulator of *Cry1* expression (Ward *et al*., 2005). Dof5.8 contains transcriptional activation domains, but they can strongly repress MP/ARF5-activated Dof5.8 upregulation (Konishi and Yanagisawa, 2015). Dof5.8 acts as a negative regulator to repress the expression of the auxin-related genes *DORNRÖSCHEN* and *SHI-RELATED SEQUENCE 5* (Konishi and Yanagisawa, 2015). Thus, it is possible that VDOF1 and VDOF2 activities depend on the target genes. The qRT-PCR analyses of inflorescence stems showed that both overexpression and knockout of *VDOF* genes upregulated the expression levels of *CAD5* and *LAC12* (Figure 3.31). *CAD5* and *LAC12* promoters contain Dof-binding motifs, suggesting that VDOF proteins may interact with these promoters and activate their expression either directly or indirectly by interacting with other transcription factors, including other Dof proteins. Further detailed

molecular analyses of VDOF proteins, especially of their DNA–protein and protein–protein interaction activities, will provide further insight into the underlying mechanisms.

4.2 Roles for VDOF1 and VDOF2 in vascular development

In Arabidopsis, vascular cell formation is initiated at the early globular stage of embryogenesis. The identity of xylem cells is established at this stage, whereas the identity of phloem cells is established later, near the end of embryogenesis (Rybel *et al*., 2016). Vascular tissue patterning is established during embryogenesis, but vascular cell differentiation arrests at the procambial stage and resumes after seed germination during post-embryonic development (Turner and Sieburth, 2003). My data show that *VDOF* genes are expressed in vascular regions throughout the plant's life cycle, from the early post-embryonic developmental stages, suggesting that VDOF proteins are always involved in vascular development (Figure 3.6–3.10). Different *VDOF1* and *VDOF2* expression patterns in root tips and inflorescence stems could reflect their different roles in vascular development (Figure 3.10).

Overexpression and knockout mutations of *VDOF1* and *VDOF2* affected cotyledon vein formation (Figure 3.16 and 3.17). *VDOF1* and *VDOF2* overexpression reduced vein connectivity, whereas vein connectivity was enhanced in the *vdof1 vdof2* double mutant (Figure 3.16 and 3.17). Therefore, *VDOF* genes could negatively regulate cotyledon vein formation (Figure 3.16 and 3.17). In the current model of vein formation, auxin is a first cue of provascular cell differentiation from undifferentiated leaf meristem cells (Rybel *et al*., 2016). Auxin signals are mediated by the transcription factor MP/ARF5 (Mattsson *et al*., 2003), leading to the expression of AtHB8, the key regulator of (pro)cambial cell establishment, in provascular cells. Previous studies suggest that several Dof proteins, including VDOF1/Dof4.6, may function after MP/ARF5-mediated auxin signaling but before AtHB8 activity (i.e., during vascular cell development) (Gardiner *et al*., 2010; Konishi and Yanagisawa, 2015). One of these Dof proteins

is Dof5.8, which is a direct target of MP/ARF5 (Konishi *et al*., 2015). Dof5.8 does not alter the expression of genes that are preferentially expressed in provascular cells, such *AtHB8*; instead, Dof5.8 influences the expression of auxin-associated transcription factor genes (Konishi and Yanagisawa, 2015). Thus, Dof5.8 is presumed to be a modulator of the auxin response for vein formation (Konishi and Yanagisawa, 2015). Similarly, my observations indicate that *AtHB8* expression was not changed by overexpression of *VDOF1* and *VDOF2* (Table 3.4), suggesting that VDOF1 and VDOF2 are not directly involved in the MP/ARF5-AtHB8 pathway. Transcriptomic analysis of inducible overexpression of *VDOF1* and *VDOF2* indicates that *VDOF* can downregulate brassinosteroid (BR) signaling genes such as *BR ENHANCED EXPRESSION 2* (*BEE2*) and *HOMOLOG OF BEE2 INTERACTING WITH IBH1* (*HBI1*) (Bai *et al*., 2012, Fan *et al*., 2014) (Table 3.4).

BR is a crucial phytohormone regulating vascular cell differentiation. Previous studies of *in vitro* xylem induction (Yamamoto *et al*., 1997) and BR-related mutants (Clay and Nelson, 2002; Caño-Delgado *et al*., 2004) indicate that BR is involved in xylem development. The leucine-rich repeat receptor-like kinase BRASSINOSTEROID INSENSITIVE1 (BRI1) and its homologs BRL1 and BRL3 mediate BR signaling; this pathway is thought to regulate the relative production ratios of differentiated xylem to phloem, probably by positively regulating xylem cell proliferation (Caño-Delgado *et al*., 2004). Xylem cell differentiation is also regulated by another pathway that depends on the leucine-rich repeat receptor-like kinase PHLOEM INTERCALLATED WITH XYLEM (PXY)/TDIF RECEPTOR (TDR) (Nieminen *et al*., 2015). Glycogen synthase kinase 3 proteins (GSK3s), especially BRASSINOSTEROID-INSENSITIVE 2 (BIN2), are key components of BR signaling pathways, and can interact with PXY/TDR to increase BIN2 kinase activity and inactivate the transcription factor BRI1-EMS SUPPRESSOR 1 (BES1), a positive regulator of xylem differentiation (Kondo *et al*., 2014). My results show that VDOF1 and VDOF2 can downregulate the expression of *BEE2* and *HBI1*,

positive regulators of BR signaling (Table 3.3). Public gene expression data show that *VDOF1* and *VDOF2* can be upregulated by BR (Arabidopsis eFP browser, Winter *et al*., 2007). Therefore, VDOF1 and VDOF2 could function as modulators of the BR response during vascular development. Further analysis of BR-related events during vascular development in *VDOF1ox, VDOF2ox,* and *vdof1 vdof2* is expected to strengthen this hypothesis.

In addition to the effects of *VDOF1ox* and *VDOF2ox* on vein formation, I also observed growth inhibition in these seedlings (Figure 3.13). However, this defect was restored during vegetative stages, and no differences between wild-type and *VDOF* overexpressors were observed at the reproductive stages (Figure 3.14). The *vdof1 vdof2* double mutant did not display any growth defects (Figure 3.13), implying that the growth inhibition in *VDOF1ox* and *VDOF2ox* were not due to enhancement of native VDOF1 and VDOF2 functions, but to ectopic activation and/or repression of molecular events by VDOF1 and VDOF2 overexpression. Transcriptomic analysis using inducible overexpression constructs showed that VDOF1 and VDOF2 upregulate many transcription factors (Table 3.2), including several stress-related transcription factors such as bHLH38, bHLH100, and bHLH101 involved in iron homeostasis (Sivitz *et al*., 2012), WRKY45 in phosphate starvation (Wang *et al*., 2014), WRKY28 and MYB15 in abiotic stress responses and plant immunity (Ding *et al*., 2009; Chen *et al*., 2013; Chezem *et al*., 2017), and ANAC036 putatively involved in stress responses (Kato *et al*., 2010). These combined results suggest that *VDOF* genes function in plant stress responses. In some cases, overexpression of stress-related transcription factors can induce dwarfism due to inhibition of cell elongation (Kato *et al*., 2010). Thus, it is possible that growth inhibition in *VDOF1ox* and *VDOF2ox* plants can be attributed to upregulation of stress-related transcription factors. A recent study proposed the existence of a BR-based growth-immunity trade-off system mediated by BRASSINAZOLE-RESISTANT 1 (BZR1) and HBI1 (Lozano-Duran and Zipfel,

2015). The VDOF-mediated upregulation of stress-related factors might be interpreted within the context of VDOF function in the BR signaling pathway.

4.3 Roles for VDOF1 and VDOF2 in lignin biosynthesis

The reporter GUS assays of *VDOF* expression during the reproductive stages demonstrated that *VDOF* genes are expressed in vascular tissues and in the anther endothecium (non-vascular tissue) (Figure 3.8). The anther endothecium includes cells accumulated in the SCW, which generate enough tensile force to rupture the stomium and release pollen grains (Yang *et al*., 2007). This observation suggests that VDOF1 and VDOF2 have distinct roles in SCW formation during vascular development.

No changes were detected in the structures of vascular tissues in the inflorescence stem under normal growth condition; however, a reduction in lignin was detected in the middle region of the *VDOF1ox* stem (Figure 3.18). Conversely, enhanced lignin deposition was observed in the *vdof1 vdof2* double mutant inflorescence stems (Figure 3.18 and 3.19), suggesting that VDOF1 and VDOF2 could work cooperatively as negative regulators of lignin deposition. Transcriptomic data of inducible overexpressors of *VDOF1* and *VDOF2* identified many lignin-related factors as possible target genes of VDOF1 and VDOF2 (Figure 3.22-3.27; Table 3.2). I examined whether the expression levels of these lignin-related genes were affected by overexpression and mutation of *VDOF1* and *VDOF2* (Figure 3.30 and 3.31); genes encoding CAD5, a specialized enzyme involved in the last step of monolignol biosynthesis (Sibout *et al*., 2005); MYB63, a positive transcriptional regulator of lignin biosynthesis (Zhou *et al*., 2009); and the oxidative lignin polymerization enzymes LAC7, LAC12, and PER53 (Sibout *et al*., 2005; Østergaard *et al*., 2000; Zhao *et al*., 2015) were all upregulated in the inflorescence stems of *VDOF1ox, VDOF2ox*, and *vdof1 vdof2* plants. These results indicate that VDOF1 and VDOF2 might regulate the expression of lignin biosynthetic genes. However, the lignin content

was not increased in *VDOF2ox*, and lignin deposition was reduced in the middle region of the *VDOF1ox* stem (Figure 3.18 and 3.19). This discrepancy between increased expression levels of lignin biosynthesis genes and the final lignin levels might suggest that additional layers regulate lignin deposition mediated by VDOF proteins and/or their interactors after transcriptional regulation of lignin-related genes. Although this work focused on commonly regulated genes, the transcriptomic data also identified a set of VDOF1- and VDOF2-specific target genes (Figure 3.21). The different effects of *VDOF1* and *VDOF2* overexpression may result from VDOF1- and VDOF2-specific downstream molecular processes.

Originally, VDOF1 and VDOF2 were identified as positive factors for the enzymatic saccharification efficiency in seedlings (Ohtani and Ramachandran *et al*., in preparation; Figure 3.15). I found that *vdof1 vdof2* seedlings displayed reduced glucose release from powdered biomass samples (Figure 3.15). As seedlings lack fibers, all lignin in seedlings is basically derived from xylem vessels. Lignin is a strong negative factor for saccharification of lignocellulosic biomass; therefore, the reduced saccharification efficiency in *vdof1 vdof2*, in which lignin deposition should be increased (Figure 3.19), and the increased saccharification efficiency in *VDOF1ox* and *VDOF2ox*, which have fewer veins (Figure 3.16 and 3.17) and therefore less lignin, would be reasonable. Increased biomass availability is currently a central issue for industrial applications (Henry, 2010). Knowledge of the functions of VDOF1 and VDOF2 could be harnessed to increase saccharification efficiency.

4.4 Conclusions

The data presented in this thesis indicate that VDOF1 and VDOF2 are transcription factors that regulate vascular cell differentiation in Arabidopsis. VDOF1 and VDOF2 negatively regulate vein formation in cotyledons and lignin deposition in inflorescence stems. The results of transcriptome analysis of *VDOF* overexpressors suggest that VDOF1 and VDOF2 function as

modulators of BR signaling during vascular cell differentiation. VDOF1 and VDOF2 also regulate lignin deposition, at least in part, through transcriptional alteration of lignin-related genes. The manipulation of *VDOF* expression is suggested as a new biotechnology strategy to design desirable SCW properties through lignin modification.

CHAPTER 5

FUTURE PERSPECTIVES

Based on this study, I concluded that VDOF1 and VDOF2 are novel regulators of vascular cell differentiation through the course of a lifetime, possibly with shifting their transcriptional target genes. The transcriptomic analysis of inducible overexpression of *VDOF1* and *VDOF2* indicates that *VDOF* can downregulate brassinosteroid (BR) signaling genes such as *BEE2* and *HBI1*, suggesting VDOF1 and VDOF2 could function as modulators of the BR response during vascular development. Further analysis of the expression of BR-related genes and BR responses in the *VDOF1ox*, *VDOF2ox*, and *vdof1 vdof2* will prove this hypothesis and provide new insights into phytohormonal regulation of vascular development.

My expression and phenotype analyses suggested that VDOF1 and VDOF2 have distinct roles in SCW formation during vascular development, especially through the transcriptional regulation of lignin-related genes. Interestingly, *VDOF1ox* and *VDOF2ox* showed opposite phenotypes of lignin accumulation in mature inflorescence stems. Additionally, the transcriptomic analysis of inducible overexpressors indicated the VDOF1- and VDOF2-specific downstream molecular processes. Therefore, it is possible that VDOF1 and VDOF2 could have different molecular activities for the transcriptional regulation of their target genes. Detailed molecular functional analysis using *vdof* single mutants would be critical to elucidate VDOF1 and VDOF2-specific aspects of the transcriptional regulation of vascular development. More than half of Dof transcription factors are expressed in vascular tissues in Arabidopsis plants. Future molecular functional analysis of VDOF1 and VDOF2 would shed light on the complicated functional redundancy of Dof transcription factors.

Finally, through this study, VDOF1 and VDOF2 are identified as positive factors for the enzymatic saccharification efficiency in seedlings, and negative regulators in lignin deposition

in inflorescence stems. Further analysis on this aspect could provide new biotechnological strategy to design desirable secondary cell wall properties, e.g. lignin contents, for industrial applications.

SUPPLEMENTARY MATERIALS

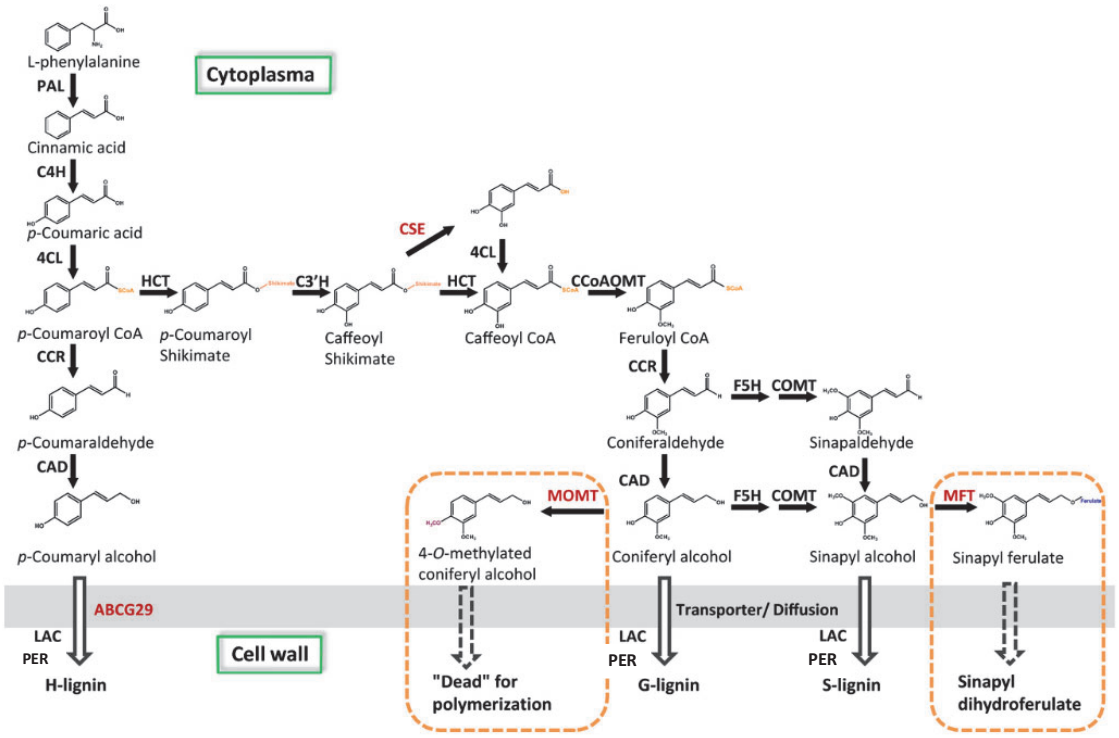

Figure S1 **The phenylpropanoid-lignin biosynthesis pathway.**
PAL, phenylalanine ammonia lyase; C4H, cinnamic acid 4-hydroxylase; 4CL, 4-hydroxycinnamoyl-CoA ligase; HCT, hydroxycinnamoyl-CoA: shikimate/quinate hydroxycinnamoyltransferase; C3'H, p-coumaroyl shikimate 3'-hydroxylase; CSE, caffeoyl shikimate esterase; CCoAOMT, caffeoyl-CoA O-methyltransferase; CCR, cinnamoyl-CoA reductase; F5H, coniferaldehyde/ ferulate 5-hydroxylase; COMT, caffeic acid/5-hydroxyferulic acid O-methyltransferase; CAD, (hydroxy)cinnamyl alcohol dehydrogenase; LAC, laccase; PER, peroxidase. The boxes with dashed line indicate the engineered steps; MOMT, monolignol 4-O-methyltransferase; MFT, monolignol ferulate transferase. (Edited from Liu *et al*., 2014).

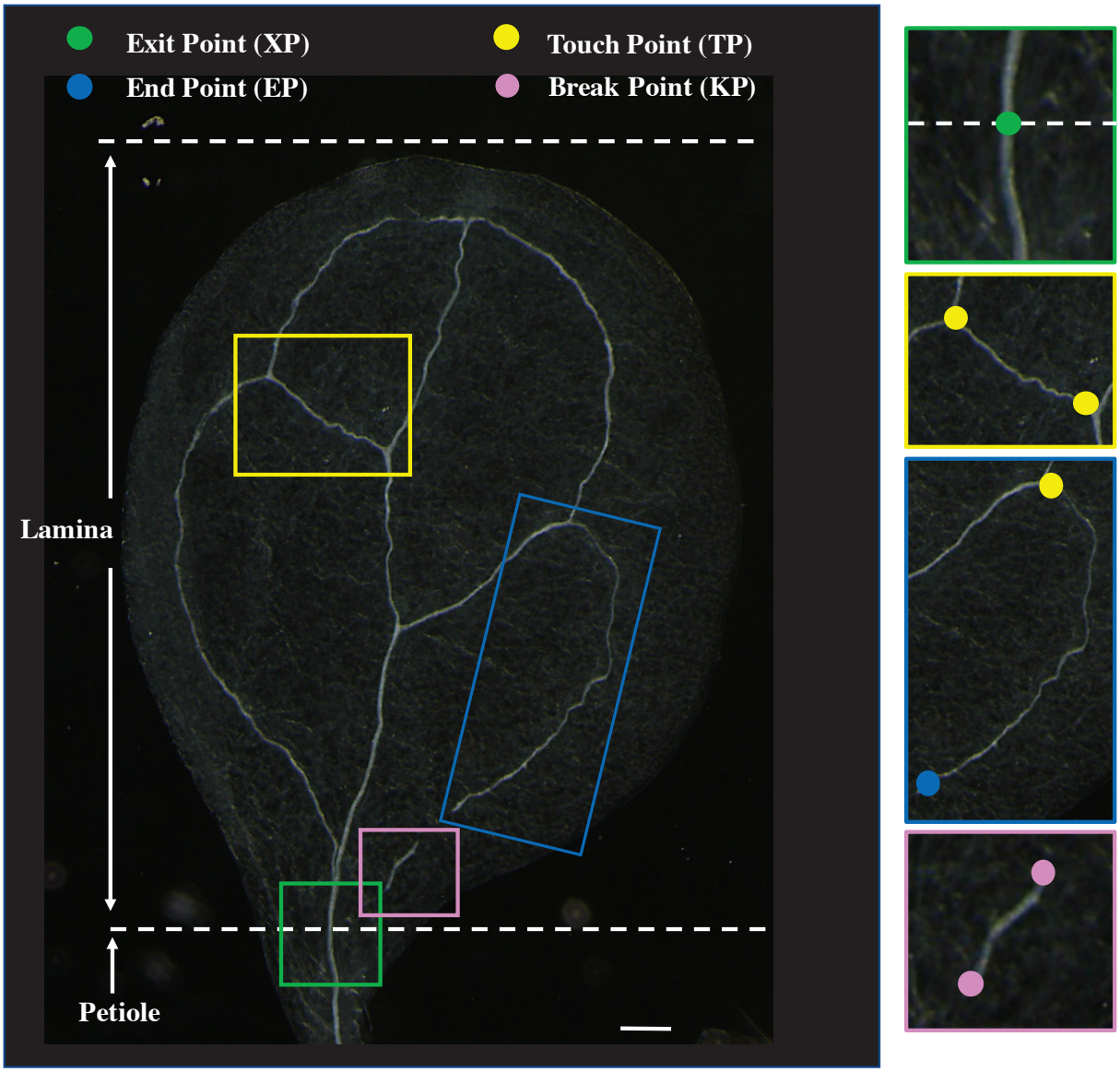

Figure S2 **Analysis of vein network topology of cotyledon**
A "vein fragment" (magenta box) is incident to two "break points" (KPs; magenta dots), the points where a vein fragment terminates free of contact with veins or other vein fragments. An "open vein" (blue box) is incident to a "touch point" (TP; yellow dot), a point of contact between a vein and vein fragments or other veins and an "end point" (EP; blue dot), the point where an open vein terminates free of contact with another vein or a vein fragment. A "closed vein" (yellow box) is incident to two TPs. A vein or a vein fragment exits the leaf lamina and enters the leaf petiole (green box) by an "exit point" (XP; green dot). Cardinality index represents the number veins which can be calculated as: (TP + XP – EP)/2] + EP, or: (TP + XP + EP)/2. Continuity index represents quantification of how close a vein network is to a network with the same number of veins but in which at least one end of each vein fragment contacts a vein: [(TP + XP + EP)/2]/[(TP + XP + EP + KP)/2], or: (TP + XP + EP)/(TP + XP + EP + KP). Connectivity index quantifies how close a vein network is to a network with the same number of veins but in which both ends of each vein or vein fragment contact other veins [(TP + XP – EP)/2]/[(TP + XP + EP + KP)/2], or: (TP + XP – EP)/(TP + XP + EP + KP). (Edited from Verna *et al*., 2015).

ACKNOWLEDGEMENTS

I would like to express my sincere appreciation to my supervisor, Professor Dr Taku Demura for his constant guidance, encouragement and moral support, without which this work would not have been possible. I truly grateful to the committee members of my dissertation, Professor Dr Masaaki Umeda and Professor Dr Toshiro Ito for their time and constructive comments.

My special thanks go to Assistant Professor Dr Misato Ohtani for her unconditional support, advice and insightful discussion; "You are truly my role model". My gratitude also dedicated to Associate Professor Dr Minoru Kubo, Associate Professor Dr Ko Kato, Assistance Professor Dr Arata Yoneda for technical advice and assistance, Dr Ryosuke Sano for assistance on bioinformatics, Dr Hitoshi Endo for his help and guidance especially during my early years in the laboratory. I also would like to thank Professor Toshiaki Umezawa, Associate Professor Dr. Yuki Tobimatsu and Assistant Professor Dr Masaomi Yamamura (Kyoto University) for allowing me to use their resources and help for this project.

Many thanks to my laboratory mates and friends for their kindness, friendship and generous assistance throughout my studies here. I also appreciate the scholarship awarded by Ministry of Education, Culture, Sports, Science, and Technology (MEXT).

Last not the least, my family and my husband, Segar for their sacrifice, love and continuous encouragement to be where am I now. This dissertation is dedicated to you.

REFERENCES

Bai, M-Y., Fan, M., Oh, E., and Wang, Zhi-Yong. (2012). A triple Helix-Loop-Helix/Basic Helix-Loop-Helix cascade controls cell elongation downstream of multiple hormonal and environmental signaling pathways in Arabidopsis. Plant Cell 24:12, 4917-4929.

Baima, S. Possenti, M. Matteucci, A., Wisman, E., Altamura, M. M. Ruberti, I., and Morelli, G. (2001). The arabidopsis ATHB-8 HD-Zip protein acts as a differentiation-promoting transcription factor of the vascular meristems. Plant Physiology 126, 643-655.

Baima, S., Forte, V., Possenti, M., Peñalosa, A., Leoni, G., Salvi, S., Felici, B., Ruberti, I., and Morelli, G. (2014). Negative feedback regulation of auxin signaling by ATHB8/ACL5-BUD2 transcription module. Molecular Plant 7, 1006–1025.

Barrière, Y., Ralph, J., Méchin, V., Guillaumie, S., Grabber, J. H., Argillier, O., Chabbert, B., and Lapierre, C. (2004). Genetic and molecular basis of grass cell wall biosynthesis and degradability. II. Lessons from brown-midrib mutants. Plant Biology and Pathology 327, 847-860.

Boccaccini, A., Santopolo, S., Capauto, D., Lorrai, R., Minutello, E., Belcram, K., Palauqui, J-C., Costantino, P., and Vittorioso, P. (2014). Independent and interactive effects of DOF affecting germination 1 (DAG1) and the Della proteins GA insensitive (GAI) and repressor of *ga1-3* (RGA) in embryo development and seed germination. BMC Plant Biology 14, 1-11.

Boerjan, W., Ralph, J., and Baucher, M. (2003). Lignin Biosynthesis. Annu. Rev. Plant Biol. 54, 519-546.

Bonawitz, N.D., Kim, J. I., Tobimatsu, Y., Ciesielski, P. N., Anderson, N. A., Ximenes, E., Maeda, J., Ralph, J., Donohoe, B. S., Ladisch, M., and Chapple, C. (2014). Disruption of Mediator rescues the stunted growth of a lignin-deficient Arabidopsis mutant. Nature 509, 376-380.

Bonke, M., Thitamadee, S., Mähönen, A. P., Hauser, M-T., and Helariutta, Y. (2003). APL regulates vascular tissue identity in *Arabidopsis*. Nature 426, 181-185.

Caffall, K. H., and Mohnen, D. (2009). The structure, function, and biosynthesis of plant cell wall pectic polysaccharides. Carbohydrates Research 344, 1879-1900.

Caño-Delgado, A., Yin, Y., Yu, C., Vafeados, D., Mora-García, S., Cheng, J.C., Nam, K.H., Li, J., and Chory, J. (2004). BRL1 and BRL3 are novel brassinosteroid receptors that function in vascular differentiation in Arabidopsis. Development 131:21, 5341-5351.

Chen, F., and Dixon, R. (2007). Lignin modification improves fermentable sugar yields for biofuel production. Nature Biotechnology 25, 759-761.

Chen, X., Liu, J., Lin, G., Wang, A., Wang, Z., and Lu, G. (2013). Overexpression of AtWRKY28 and AtWRKY75 in Arabidopsis enhances resistance to oxalic acid and *Sclerotinia sclerotiorum*. Plant Cell Reports 32:10, 1589-1599.

Chezem, W. R., Memon, A., Li, F-S., Weng, J-K., and Clay, N. K. (2017). SG2-type R2R3-MYB transcription factor MYB15 controls defense-induced lignification and basal immunity in Arabidopsis. The Plant Cell 29:6.

Clay, N. K., and Nelson, T. (2002). VH1, a provascular cell-specific receptor kinase that influences leaf cell patterns in Arabidopsis. Plant Cell 14:1, 2707-2722.

Cosgrove, D. J. (2005). Growth of the plant cell wall. Nature 6, 850-861.

Cosgrove, D. J., and Jarvis, M. C. (2012). Comparative structure and biomechanics of plant primary and secondary cell walls. Fro. Plant Sci. 3, 1-6.

Demura, T., and Ye, Z-H. (2010). Regulation of plant biomass production. Curr. Opin. Plant Biol. 13, 299-304.

Diaz, I., Vicente-Carbajose, J., Abraham, Z., Martinez, M., Isabel-La Moneda, I., and Carbonera, P. (2002). Te GAMYB protein from barley interacts with the DOF transcription factor BPBF and activates endosperm-specific genes during seed development. Plant Journal 29, 453-464.

Ding, Z., Li, S., An, X., Liu, X., Qin, H., and Wang D. (2009). Transgenic expression of MYB15 confers enhanced sensitivity to abscisic acid and improved drought tolerance in *Arabidopsis thaliana*. J. Genet. Genomics 36:1, 17-29.

Donner, T. J., Sherr, I., and Scarpella, E. (2009). Regulation of preprocambial cell state acquisition by auxin signaling in Arabidopsis leaves. Development 136, 3235-3246.

Endo, S., Pesquet, E., Yamaguchi, M., Tashiro, G., Sato, M., Toyooka, K., Nishikubo, N., Udagawa-Motose, M., Kubo, M., Fukuda, H., and Demura, T. (2009). Identifying new components participating in the secondary cell wall formation of vessel elements in Zinnia and Arabidopsis. The Plant Cell 21, 11555-1165.

Etchells, J. P., and Turner, S. R. (2010). The PXY-CLE41 receptor ligand pair defines a multifunctional pathway that controls the rate and orientation of vascular cell division. Development 137, 767-774.

Etchells, J. P., Provost, C. M., Mishra, L., and Turner, S. R. (2013). *WOX4* and *WOX14* act downstream of the PXY receptor kinase to regulate plant vascular proliferation independently of any role in vascular organisation. Development 140, 2224-2234.

Fan, M., Bai, M-Y., Kim, J-G., Wang, T., Oh, E., Chen, L., Park, C. H., Son, S-H., Kim, S-K., Mudgett, M. B., and Wang, Z-Y. (2014). The bHLH transcription factor HBI1 mediates the trade-off between growth and pathogen-associated molecular pattern–triggered immunity in Arabidopsis. Plant Cell 26:2, 828-841.

Fisher, K., and Turner, S. (2007). PXY, a Receptor-like kinase essential for maintaining polarity during plant vascular-tissue development. Current Biology 17:12, 1061-1066.

Festucci-Buselli, R. A., Otoni, W. C., and Joshi, C. P. (2007). Structure, organization, and functions of cellulose synthase complexes in higher plants. Braz. J. Plant Physiol. 19, 1-13.

Furuta, K. M., Hellmann, E., and Helariutta, Y. (2014). Molecular control of cell specification and cell differentiation during procambial development. Ann. Rev. Plant Biology 65, 607-638.

Franceschi, V.R., Krokene, P., Christiansen, E., and Krekling, T. (2005). Anatomical and chemical defenses of conifer bark against bark beetles and other pests. New Phytologist 167: 353-376.

Gardiner, J., Sherr, I., and Scarpella, E. (2010). Expression of DOF genes identifies early stages of vascular development in *Arabidopsis* leaves. Int. J. Dev. Biol. 54, 1389-1396.

Gaur, V. S., Singh, U., and Kumar, A. (2011). Transcriptional profiling and in silico analysis of Dof transcription factor gene family for understanding their regulation during seed development of rice Oryza sativa L.Mol. Biol. Rep. 38, 2827-2848.

Gorshkova, T., Brutch, N., Chabbert, B., Deyholos, M., hayashi, T., Lev-yadun, S., Mellerowicz, E.J., Morvan, C., Neutelings, G., and Pilate, G. (2012). Plant fiber formation: State of the art, recent and expected progress, and open questions. Cri. Rev. Plant Sci. 31, 201-228.

Gualberti, G., Papi, M., Bellucci, L., Ricci, I., Bouchez, D., Camilleri, C., Costantino, P., and Vittorioso. (2002) Mutations in the Dof zinc finger genes DAG2 and DAG1 influence with opposite effects the germination of *Arabidopsis* seeds. Plant Cell 14, 1253-1263.

Guo, Y., Qin, G., Gu, H., and Qu, L-J. (2009). *Dof5.6/HCA2*, a Dof Transcription Factor Gene, Regulates Interfascicular Cambium Formation and Vascular Tissue Development in *Arabidopsis*. Plant Cell 21:11, 3518–3534.

Haigler, C. H., Ivanova-Datcheva, M., Hogan, P. S., Salnikov, V. V., Hwang, S., Martin, K., and Delmer, D. P. (2001). Carbon partitioning to cellulose synthesis. Plant Mol. Biol. 47, 29–51.

Hardtke, C. S., and Berleth, T. (1998). The Arabidopsis gene MONOPTEROS encodes a transcription factor mediating embryo axis formation and vascular development. The EMBO 17, 1405-1411.

Henry, R. J. (2010). Evaluation of plant biomass resources available for replacement of fossil oil. Plant Biotechnology 8:3, 288-293.

Herr, J. M. Jr. (1992). New uses for calcium chloride solution as a mounting medium. Biotech & Histochem 67:9-13.

Heo, J-O., Roszak, P., Furuta, K. M., and Helariutta, Y. (2014). Phloem development: Current knowledge and future perspectives. American J. Bot. 101:9, 1393-1402.

Hir, R. L., and Bellini, C. (2013). The plant-specific Dof transcription factors family: new players involved in vascular system development and functioning in *Arabidopsis*. Fro. Plant Sci. 4:164, 1-10.

Hirakawa, Y., Shinohara, H., Kondo, Y., Inoue, A., Nakanomyo, I., Ogawa, M., Sawa, S., Ohashi-Ito, K., Matsubayashi, Y., and Fukuda, H. (2008). Non-cell-autonomous control of vascular stem cell fate by a CLE peptide/receptor system. PNAS 105:39, 15208-15213.

Hoffmann, L., Besseau, S., Geoffroy, P., Ritzenthaler, C., Meyer, D., Lapierre, C., Pollet, B., and Legrand, M. (2004). Silencing of hydroxycinnamoyl-Coenzyme A shikimate/quinate hydroxycinnamoyltransferase affects phenylpropanoid biosynthesis. The Plant Cell 16, 1446-1465.

Huang, J., Gu, M., Lai, Z., Fan, B., Zhou, Y-H., Yu, J-Q., and Chen, Z. (2010). Functional analysis of the arabidopsis *PAL* gene family in plant growth, development, and response to environmental stress. Plant Physiology 153, 1526-1538.

Kato, H., Motomura, T., Komeda, Y., Saito, T., and Kato, A. (2010). Overexpression of the NAC transcription factor family gene ANAC036 results in a dwarf phenotype in A*rabidopsis thaliana*. Plant Physiology 167:7, 571-577.

Keegstra, K. (2010). Plant Cell Wall. Fut. Per. Plant Bio. 154, 483-486.

Kim, H. S., Kim, S. J., Abbasi, N., Bressan, R. A., Yun, G. J., Yoo, S. D., Kwon, S. Y., and Choi, S. B. (2010). The DOF transcription factor Dof5.1 influences leaf axial patterning by promoting Revoluta transcription in *Arabidopsis*. The Plant Journal 64, 524-535.

Kondo, Y., Ito, T., Nakagami, H., Hirakawa, Y., Saito, M., Tamaki, T., Shirasu, K., and Fukuda, H. (2014). Plant GSK3 proteins regulate xylem cell differentiation downstream of TDIF-TDR signalling. Nature communications 5, 3504.

Konishi, M., Donner, T. J., Scarpella, E., and Yanagisawa, S. (2015). MONOPTEROS directly actvates the auxin-inducible promoter of the Dof5.8 transcription factor gene in Arabidopsis thaliana leaf provascular cells. Journal of Exp. Bot. 66:1, 283-291.

Konishi, M., and Yanagisawa, S. (2007). Sequential activation of two Dof transcription factor gene promoters during vascular development in *Arabidopsis thaliana*. Plant Physiology and Biochemistry 45, 623-629.

Konishi, M., and Yanagisawa, S. (2015). Transcriptional repression caused by Dof5.8 is involved in proper vein network formation in Arabidopsis thaliana leaves. J. Plant Research 128:4, 643-652.

Kubo, M., Udagawa, M., Nishikubo, N., Horiguchi, G., Yamaguchi, M., Ito, J., Mimura, T., Fukuda, H., and Demura, T. (2005). Transcription switches for protoxylem and metaxylem vessel formation. Genes and Development 19:16, 1855-1860.

Krebs, J., Mueller-Roeber, B., and Ruzicic, S. (2010). A novel bipartite nuclear localization signal with an atypically long linker in DOF transcription factors. J. of Plant Physiology 167:7, 583-586.

Li, J., Ou-Lee, T-M., Raba, R., Amundson, R. G., and Last, R. L. (1993). Arabidopsis flavonoid mutants are hypersensitive to UV-6 irradiation. The Plant Cell 5, 171-179.

Li, X., Yang, Y., Yao, J., Chen, G., Li, X., Zhang, Q., and Wu, C. (2009). *FLEXIBLE CULM 1* encoding a cinnamyl-alcohol dehydrogenase controls culm mechanical strength in rice. Plant Molecular Biology 69:6, 685-697.

Liebminger, E., Grass, J., Altmann, F., Mach, L., and Strasser, R. (2013). Characterizing the link between glycosylation state and enzymatic activity of the endo-ß1,4-glucanase KORRIGAN1 from *Arabidopsis thaliana*. J. Biol. Chem. 288, 22270-22280.

Lijavetzky, D., Carbonero, P., and Vicente-Carbajosa, J. (2013). Genome-wide comparative phylogenetic analysis of the rice and Arabidopsis Dof gene families. BMC Evolutionary Biology 3:17, 1-11.

Liu, C-J., Cai, Y., Zhang, X., Gou, M., and Yang, H. (2014). Tailoring lignin biosynthesis for efficient and sustainable biofuel production. Plant Biotechnology 1-9.

Lozano-Durán, R., and Zipfel, C. (2015). Trade-off between growth and immunity: role of brassinosteroids. Trends Plant Sci. 20:1, 12-19.

Lucas, W.J., Groover, A., Lichtenberger, R., Furuta, K., Yadav, S-R., Helariutta, Y., He, X-Q., Fukuda, H., Kang, J., Brady, S.M., Patrick, J.W., Sperry, J., Yoshida, A., López-Millán, A-F., Grusak, M.A., and Kachroo, P. (2013). J. Int. Plant Biol. 55:4, 294-388.

Mattson, J., Ckurshumova, W., and Berleth, T. (2003). Auxin signaling in Arabidopsis leaf vascular development. Plant Physiology 131(3): 1327-1339.

Mendu, V., Stork, J., Harris, D., and DeBolt, S. (2011). Cellulose synthesis in two secondary cell wall processes in a single cell type. Plant sig. and Beh. 6:11, 1638-1643.

Milhinhos, A., Prestele, J., Bollhoner, B., Matos, A., Vera-Sirera, F., Rambla, J. L., Ljung, K., Carbonell, J., Blázquez, M. A., Tuominen, H., and Miguel, C. M. (2013). Thermospermine levels are controlled by an auxin-dependent feedback loop mechanism in Populus xylem. The Plant Journal 75, 685–698.

Mitsuda, N., Iwase, A., Yamamoto, H., Yoshida, M., Seki, M., Shinozaki, K., and Ohme-Takagi, M. (2007). NAC transcription factors, NST1 and NST3, are key regulators of the formation of secondary walls in woody tissues of Arabidopsis. The Plant Cell 19, 270-280.

Mitsuda, N., Seki, M., Shinozaki, K., and Ohme-Takagi, M. (2005). The NAC transcription factors NST1 and NST2 of *Arabidopsis* regulate secondary wall thickening and are required for anther dehiscence. American Soc.Plant Bio. 17, 2993-3006.

Miyashima, S., Sebastian, J., Lee, J-Y., and Helariutta, Y. (2013). Stem cell function during plant vascular development. The EMBO Journal 32, 178-193.

Moreno-Risueno, M. Á., Martínez, M., Vicente-Carbajosa, J., and Carbonero, P. (2006). The family of DOF transcription factors: from green unicellular algae to vascular plants. Mol. Genet. Genomics 277, 379-390.

Myburg, A., Lev-Yadun, S., and Sederoff, R. R. (2001). Xylem structure and function. eLS.

Nakano, Y.,Yamaguchi, M., Endo, H., Rejab, N. A., and Ohtani, M. (2015). NAC-MYB-based transcriptional regulation of secondary cell wall biosynthesis in land plants. Front. Plant Sci. 6, 288.

Nieminen, K., Blomster, T., Helariutta, Y., and Mähönen, A.P. (2015). Vascular cambium development. The Arabidopsis Book.

Ohashi-Ito, K., and Bergmann, D. C. (2007). Regulation of the Arabidopsis root vascular initial population by *LONESOME HIGHWAY*. Development 134, 2959-2968.

Ohtani, M., Nishikubo, N., Xu, B., Yamaguchi, M., Mitsuda, N., Goue, N., Shi, F., ohme-Takagi, M., and Demura, T. (2011). A NAC domain protein family contributing to the regulation of wood formation in poplar. The Plant Journal 67, 499-512.

Ohtani, M., Akiyoshi, N., Takenaka, Y., Sano, R., and Demura, T. (2017). Evolution of plant conducting cells: perspectives from key regulators of vascular cell differentiation. Journal of Exp. Bot. 68:1, 17-26.

Østergaard, L., Teilum, K., Mirza, O., Mattsson, O., Petersen, M., Welinder, K.G., Mundy, J., Gajhede, M., and Henriksen, A. (2000). Arabidopsis ATP A2 peroxidase. Expression and high-resolution structure of a plant peroxidase with implications for lignification. Plant Mol. Biol. 44:2, 231-243.

Pauly, M., and Keegstra, K. (2010). Curr. Opin. Plant Biol. 13, 305-312.

Pinçon, G., Maury, S., Hoffmann, L., Geoffroy, P., Lapierre, C., Pollet, B., and Legrand, M. (2001). Repression of O-methyltransferase genes in transgenic tobacco affects lignin synthesis and plant growth. Phytochemistry 57:7, 1167-1176.

Read, S. M., and Bacic, T. (2002). Prime time for cellulose. Science 295, 59-60.

Reiter, W-D. (2002). Biosynthesis and properties of the plant cell wall. Curr. Opi. Plant Bio. 5, 536-542.

Rejab, N. A., Nakano, Y., Yoneda, A., Ohtani, M., and Demura, T. (2015). Possible contribution of TED6 and TED7, secondary cell wall-related membrane proteins, to evolution of tracheary element in angiosperm lineage. Plant Biotechnology 32, 343-347.

Rogers, L. A., and Campbell, M. M. (2004). The genetic control of lignin deposition during plant growth and development. New Phytologist 164, 17-30.

Rogers, L. A., Dubos, C., Surman, C., Willment, J., Cullis, I. F., Mansfield, S. D., and Campbell, M. M. (2005). Comparison of lignin deposition in three ectopic lignification mutants. New Phytologist 168, 123-140.

Ruiz-Medrano, R., Xoconostle-Cázares, B., Ham, B.K., Li, G., and Lucas, W.J. (2011). Vascular expression in Arabidopsis is predicted by the frequency of CT/GA-rich repeats in gene promoters. The Plant Journal 67:1, 130-144.

Rueda-Romero, P., Barrero-Sicilia, C., Gómez-Cadenas, A., Carbonero, P., and Oñate-Sánchez, L. (2012). *Arabidopsis thaliana* DOF6 negatively affects germination in non-after-ripened seeds and interacts with TCP14. J. Exp. Bot. 63, 1937-1949.

Rybel, B. D., Möller, B., Yoshida, S., Grabowicz, I., Reuille, P. B. D., Boeren, S., Smith, R. S., Borst, J. W., and Weijers, D. (2013). A bHLH complex controls embryonic vascular tissue establishment and indeterminate growth in Arabidopsis. Developmental Cell 24:4, 426-437.

Rybel, B. D., Mähönen, A. P., Helariutta, Y., and Weijers, D. (2016). Plant vascular development: from early specification to differentiation. Nature 17, 30-40.

Sakamoto, S., and Mitsuda, N. (2015). Reconstitution of a secondary cell wall in a secondary cell wall-deficient Arabidopsis mutant. 56:2, 299-310.

Schuetz, M., Smith, R., and Ellis, B. (2013). Xylem tissue specification, patterning, and differentiation mechanisms. J. Exp. Bot. 64:1, 11-31.

Sibout, R., Eudes, A., Mouille, G., Pollet, B., Lapierre, C., Jouanin, L., and Séguina, A. (2005). *CINNAMYL ALCOHOL DEHYDROGENASE-C* and *-D* are the primary genes involved in lignin biosynthesis in the floral stem of Arabidopsis. Plant Cell 17:7, 2059-2076.

Simmons, B. A., Loque, D., and Ralph, J. (2010). Advances in modifying lignin for enhanced biofuel production. Curr. Opin. Plant Biol. 13, 313-320.

Sivitz, A. B., Hermand, V., Curie, C., and Vert, G. (2012). Arabidopsis bHLH100 and bHLH101 control iron homeostasis via a FIT-Independent pathway. PLoS ONE 7:9, e44843.

Somerville, C. (2006). Cellulose synthesis in higher plants. Annu. Rev. Cell Dev. Biol. 22, 53-78.

Skirycz, A., Jozefczuk, S., Stobiecki, M., Muth, D., Zanor, M. I., Witt, I., and Mueller-Roeber, B. (2007). Transcription factor AtDOF4;2 affcets phenylpropanoid metabolism in *Arabidopsis thaliana*. New Phytologist 175, 425-438.

Skirycz, A., Radziejwoski, A., Busch, W., Hannah, M. A., Czeszejko, J., Kwaśniewski, M., Zanor, M-I., Lohmann, J. U., Veylder, L. D., Witt, I., and Mueller-Roeber, B (2008). The DOF transcription factor OBP1 is involved in cell cycle regulation in *Arabidopsis thaliana*. The Plant Journal 56, 779-792.

Skirycz, A., Reichelt, M., Burow, M., Birkemeyer, C., Rolcik, J., Kopka, J., Zanor, M. I., Gershenzon, J., Strnad, M., Szopa, J., Mueller-Roeber, B., and Witt, I. (2006). DOF transcription factor AtDof1.1 (OBP2) is part of a regulatory network controlling glucosinate biosynthesis in Arabidopsis. The Plant Journal 47, 10-24.

Stewart, J. J., Akiyama, T., Chapple, C., Ralph, J., and Mansfield, S. D. (2009). Plant Physiology 150, 621-635.

Taylor, N. G., Scheible, W-R., Cutler, S., Somerville, C.R., and Turner, S.R. (1999). The *irregular xylem3* locus of Arabidopsis encodes a cellulose synthase required for secondary cell wall synthesis. The Plant Cell 11, 769-779.

Taylor, N.G., Laurine, S., and Turner, S.R. (2000). Multiple cellulose synthase catalytic subunits are required for cellulose synthesis in Arabidopsis. The Plant Cell 12, 2529-2539.

Taylor, N. G., Howells, R. M., Huttly, A.K., Vickers, K., and Turner, S.R. (2003). Interactions among three distinct CesA proteins essential for cellulose synthesis. PNAS 100:3, 1450-1455.

Taylor, N. G. (2008). Cellulose biosynthesis and deposition in higher plants. New Phytologist 178, 239-252.

Turner, S., and Sieburth, L. E. (2003). Vascular patterning. Arabidopsis Book 1-23.

Van Acker, V., Vanholme, R., Storme, V., Mortimer, J. C., Dupree, P., and Boerjan, W. (2013). Lignin biosynthesis perturbations affect secondary cell wall composition and saccharification yield in *Arabidopsis thaliana*. Biotechnology for Biofuels 6:46, 1-17.

Vanholme, R., Demedts, B., Morreel, K., Ralph, J., and Boerjan, W. (2010). Lignin biosynthesis and structure. Plant Physiology 153, 895-905.

Wang, H-W., Zhang, B., Hao, Y-J., Huang, J., Tian, A-G., Liao, Y., Zhang, J-S., and Chen, S-Y. (2007). The soybean Dof-type transcription factor genes, *GmDof4* and *GmDof11*, enhance lipid content in the seeds of transgenic Arabidopsis plants. The Plant Journal 52, 716-729.

Wang, H., Xu, Q., Kong, Y-H., Chen, Y., Duan, J-Y., Wu, W-H., and Chen, Y-F. (2014). Arabidopsis WRKY45 transcription factor activates PHOSPHATE TRANSPORTER1;1 expression in response to phosphate starvation. Plant Physiology 164:3, 2020-2029.

Ward, J. M., Cufr, C. A., Denzel, M. A., and Neff, M. M. (2005). The Dof transcription factor OBP3 modulates phytochrome and crytochrome signalling in *Arabidopsis*. Plant Cell 17, 475-485.

Welker, C. M., Balasubramanian, V. K., Petti, C., Rai, K. M., Debolt, S., and Mendu, V. (2015). Engineering plant biomass lignin content and composition for biofuels and bioproducts. Energies 8, 7654-7676.

Weng, J-K., and Chapple, C. (2010). The origin and evolution of lignin biosynthesis. New Phytologist 187, 273-285.

Wightman, R., and Turner, S. (2010). Trafficking of the plant cellulose synthase complex. Plant Physiology 153, 427-432.

Winter, D., Vinegar, B., Nahal, H., Ammar, R., Wilson, G.V., and Provart, N. J. (2007). An "Electronic Fluorescent Pictograph" Browser for Exploring and Analyzing Large-Scale Biological Data Sets. PLoS ONE 2:8, e718.

Xu, P., Chen, H., Ying, L., and Cai, W. (2016). AtDOF5.4/OBP4, a DOF transcription factor gene that negatively regulates cell cycle progression and cell expansion in *Arabidopsis thaliana*. Science Reports 6:27705, 1-13.

Yamaguchi, M., Kubo, M., Fukuda, H., and Demura, T. (2008). VASCULAR-RELATED NAC_DOMAIN7 is involved in the differentiation of all types of xylem vessels in Arabidopsis roots and shoots. The Plant Journal 55, 652-664.

Yamaguchi, M., Ohtani, M., Mitsuda, N., Kubo, M., Ohme-Takagi, M., Fukuda, H., and Demura, T. (2010). VND-INTERACTING2, a NAC domain transcription factor, negatively regulates xylem vessel formation in Arabidopsis. The Plant Cell 22, 1249-1263.

Yamamoto, R., Demura, T., and Fukuda, H. (1997). Brassinosteroids induce entry into the final stage of tracheary element differentiation in cultured Zinnia cells. Plant Cell physiol. 38:8, 980-983.

Yanagisawa, S. (1995). A novel DNA-binding domain that may form a single zinc finger motif. Nucleic Acid Res. 23:17, 3403-3410.

Yanagisawa, S. (2015). Chapter 12 : Structure, function, and evolution of the Dof transcription factor family (Plant transcription Factors; edited by Gonzalez, D. H.). 183-197.

Yanagisawa, S., and Schmidt, R. J. (1999). Diversity and similarity among recognition sequences of Dof transcription factors. The Plant Journal 17:2, 209-214.

Yang, C., Xu, Z., Song, J., Conner, K., Vizcay, B. G., and Wilson, Z. A. (2007). Arabidopsis MYB26/MALE STERILE35 regulates secondary thickening in the endothecium and is essential for anther dehiscence. Plant Cell 19:2, 534-548.

Ye, Z-H. (2002). Vascular tissue differentiation and pattern formation in plants. Annu. Rev. plant Bio. 53, 183-202.

Yoshida, K., Sakamoto, S., Kawai, T., Kobayashi, Y., Sato, K., Ichinose, Y., Yaoi, K., Akiyoshi-Endo, M., Sato, H., Takamizo, T., Ohme-Takagi, M., and Mitsuda, N. (2013). Engineering the *Oryza sativa* cell wall with rice NAC transcription factors regulating secondary wall formation. Fro. Plant. Sci. 4, 383.

Zhao, Y., Lin, S., Qiu, Z., Cao, D., Wen, J., Deng, X., Wang, X., Lin, J., and Li, X. (2015). MicroRNA857 is involved in the regulation of secondary growth of vascular tissues in Arabidopsis. Plant Physiology 169:4, 2539-2552.

Zhong, R., Demura, T., and Ye, Z-H. (2006). SND1, a NAC domain transcription factor, is a key regulator of secondary wall synthesis in fibers of *Arabidopsis*. Plant Cell 18, 3158-3170.

Zhong, R., Lee, C., Zhou, J., Macarthy, R. L., and Ye, Z. H. (2008). A battery of transcription factors involved in the regulation of secondary cell wall biosynthesis in *Arabidopsis*. Plant Cell 20, 2763-2782.

Zhong R, Ye Z-H. (2010). The poplar PtrWNDs are transcriptional activators of secondary cell wall biosynthesis. Plant Signal. Behav. 5, 469-472.

Zhong, R., Lee, C., Macarthy, R. L., Reeves, C. K., Jones, E. G., and Ye, Z. H. (2011). Transcriptional activation of secondary wall biosynthesis by rice and maize NAC and MYB transcription factors. Plant Cell Physiol. 52:10, 1856-1871.

Zhong, R., and Ye, Z-H. (2014). Complexity of the transcriptional network controlling secondary wall biosynthesis. Plant Science 229, 193-207.

Zhou, J., Lee, C., Zhong, R., and Ye, Z. H. (2009). MYB58 and MYB63 are transcriptional activators of the lignin biosynthetic pathway during secondary cell wall formation in Arabidopsis. Plant Cell 21, 248–266.